

The genetic landscape and clonal evolution of breast cancer resistance to palbociclib plus fulvestrant in the PALOMA-3 trial

Authors: Ben O’Leary^{1,2}, Rosalind J Cutts¹, Yuan Liu³, Sarah Hrebien¹, Xin Huang³, Kerry Fenwick⁴, Fabrice André⁵, Sibylle Loibl⁶, Sherene Loi⁷, Isaac Garcia-Murillas¹, Massimo Cristofanilli⁸, Cynthia Huang Bartlett³, Nicholas C Turner^{1,2}

Affiliations: 1 Breast Cancer Now Research Centre, The Institute of Cancer Research, Fulham Rd, London, SW3 6JB. 2 Breast Unit, Royal Marsden Hospital, London, UK.

3 Pfizer, 235 E 42nd St, New York, NY, 10017, USA.

4 Tumour Profiling Unit, The Institute of Cancer Research, Fulham Rd, London, SW3 6JB.

5 Department of Medical Oncology, Institut Gustave Roussy, 94800 Villejuif, France.

6 German Breast Group, Martin Behaim-Strasse 12, 63263 Neu-Isenburg, Germany

7 Division of Research and Cancer Medicine, University of Melbourne, Peter MacCallum Cancer Centre, Melbourne, VIC 3000, Australia.

8 Robert H Lurie Comprehensive Cancer Centre, Feinberg School of Medicine, 675 N St. Clair, Chicago, IL, 60611, USA.

Running title: Genetic landscape of palbociclib resistant breast cancer

Corresponding author: Prof Nicholas Turner – Tel +442073528133, email nicholas.turner@icr.ac.uk

Word count: 7062 **Figures:** 5 **Supplementary figures:** 35 **Supplementary tables:** 8

Keywords: palbociclib, fulvestrant, circulating tumor DNA, *RB1*,

Conflict of interest disclosures: BO’L – Research funding (Inst): Pfizer. YL, XH, CHB – Employment: Pfizer, Stock ownership: Pfizer. FA – Travel, Accommodation, Expenses: Novartis, Roche,

GlaxoSmithKline, AstraZeneca, Research Funding (Inst): AstraZeneca, Novartis, Pfizer, Lilly, Roche.
SLoibl - Consulting or Advisory Role (Inst): Pfizer, Roche, Novartis, Seattle Genetics, Honoraria: Pfizer,
Roche, Research Funding (Inst): Pfizer, Roche, Celgene, Amgene, Novartis, Abbvie, AstraZeneca,
Seattle Genetics, Teva, Vifor Pharma. SLoi – Consulting or Advisory Role (Inst):
AstraZeneca/MedImmune, Seattle Genetics, Bristol-Myers Squibb, Pfizer, Novartis, Roche/Genentech,
Merck Sharp & Dohme, Research Funding (Inst): Roche/Genentech, Pfizer, Novartis, Merck, Puma
Biotechnology, Bristol-Myers Squibb. MC – Consulting or Advisory Role: Dompé Farmaceutici, Newomics,
Vortex Biosciences, Honoraria: Dompé Farmaceutici, Pfizer. NC - Consulting or Advisory Role: Roche,
Pfizer, Novartis, AstraZeneca Research Funding: Pfizer (Inst), Roche (Inst), AstraZeneca. The other
authors have no conflict of interest disclosures to make.

Funding: This research was funded by The Medical Research Council (MR/N002121/1), Breast Cancer
Now with support from the Mary-Jean Mitchell Green Foundation and Pfizer. ICR-CTSU receives program
grant funding from Cancer Research UK (grant C1491/A15955). We acknowledge National Institute for
Health Research funding to the Royal Marsden and Institute of Cancer Research Biomedical Research
Centre.

Abstract:

CDK4/6 inhibition with endocrine therapy is now a standard of care for advanced estrogen receptor positive breast cancer. Mechanisms of CDK4/6 inhibitor resistance have been described pre-clinically, with limited evidence from clinical samples. We conducted paired baseline and end of treatment circulating tumor DNA sequencing from 195 patients in the PALOMA-3 randomized phase III trial of palbociclib plus fulvestrant versus placebo plus fulvestrant. We show that clonal evolution occurs frequently during treatment, reflecting substantial sub-clonal complexity in breast cancer that has progressed after prior endocrine therapy. *RB1* mutations emerged only in the palbociclib plus fulvestrant arm and in a minority of patients (6/127, 4.7%, $p=0.041$). New driver mutations emerged in *PIK3CA* ($p=0.00069$) and *ESR1* after treatment in both arms, in particular *ESR1* Y537S ($p=0.0037$). Evolution of driver gene mutations was uncommon in patients progressing early on palbociclib plus fulvestrant but common in patients progressing later on treatment. These findings inform future treatment strategies to address resistance to palbociclib plus fulvestrant.

Statement of significance

Acquired mutations from fulvestrant are a major driver of resistance to fulvestrant and palbociclib combination therapy. *ESR1* Y537S mutation promotes resistance to fulvestrant. Clonal evolution results in frequent acquisition of driver mutations in patients progressing late on therapy, which suggests that early and late progression have distinct mechanisms of resistance.

Introduction

Selective cyclin dependent kinase 4 and 6 (CDK4 and CDK6) inhibitors have become the standard of care for advanced, estrogen receptor positive (ER+), HER2 negative metastatic breast cancer (1). Estrogen and oncogenic signaling increases cellular levels of the D type cyclins, particularly cyclin D1, activating CDK4 and CDK6 in a process modulated by the INK4A protein family, which includes p16, p21 and p27 (2). Activated CDK4/6 phosphorylates retinoblastoma (Rb), in turn partially activating the E2F transcription factors which promote S phase entry in a positive feedback loop involving cyclin E and CDK2 (3,4). Multiple phase III studies have now demonstrated that CDK4/6 inhibitors significantly prolong progression free survival in combination with endocrine therapy in ER positive breast cancer (5-8), identifying the CDK4/6-Rb axis as central to the biology of this subtype of breast cancer.

With CDK4/6 inhibitors now a standard of care, it is critical to identify the mechanisms of resistance to therapy and develop treatment strategies after clinical progression. A number of putative resistance mechanisms to CDK4/6 inhibition have been identified in preclinical models: *RB1* loss, cyclin E1 and cyclin E2 amplification (9), and *CDK6* amplification (10). Clinical evidence is limited, with a case report of *RB1* mutations in three patients treated with CDK4/6 inhibitors (11), but no systematic assessment of resistance mechanisms. Mutations in *RB1* are rare in primary breast cancer (12) but the prevalence of these in endocrine pre-treated and CDK4/6 inhibitor resistant breast cancer is unknown. Loss of function *RB1* mutations may render the tumor resistant to subsequent endocrine-based therapies or prevent benefit from continuing CDK4/6 inhibitors beyond progression, so identifying how frequently the tumor acquires *RB1* mutations is important in planning trials of post-CDK4/6 therapy. In addition, prior data has suggested that common genomic aberration such as *PIK3CA* mutations and *ESR1* mutations have limited value as a biomarker for CDK4/6 inhibitor treatment (13).

Here we provide a comprehensive assessment of the genetic aberrations of CDK4/6 inhibitor resistant disease using circulating tumor DNA analysis of paired baseline and end of treatment plasma samples from the PALOMA-3 study. The PALOMA-3 study was the first phase III trial of a CDK4/6 inhibitor in ER+, HER2- advanced breast cancer, randomizing both pre- and postmenopausal patients who had previously progressed on endocrine therapy to either palbociclib plus fulvestrant (P + F) or placebo plus fulvestrant (F), and demonstrating an improvement in median progression free survival from 4.6 to 11.2 months with the addition of palbociclib to fulvestrant (14), updated in (15). Analysis of

paired samples from this randomized study allows a dissection of which genetic events are acquired through therapy, specifically which component of the combination therapy may be driving selection of the mutations. Acquired mutations observed only in the palbociclib plus fulvestrant group likely promote resistance to the CDK4/6 inhibitor, while acquired mutations at equal frequency in both groups likely promote resistance to fulvestrant and, in general to endocrine therapy.

We demonstrate that *RB1* mutations arise following treatment with CDK4/6 inhibition, but that these mutations are likely subclonal and of relatively low prevalence, suggesting, in contrast to previous work, that they are not a major mechanism of resistance. Relatively frequent acquisition of new *PIK3CA* and *ESR1* mutations, in particular the *ESR1* Y537S mutation, in both treatment arms, implicate these changes in the development of parallel mechanisms of resistance to the elements of combination treatment and suggest new avenues for therapy.

Results

Exome sequencing of plasma DNA reveals clonal evolution on palbociclib plus fulvestrant

From the 521 patients who were enrolled in the PALOMA-3 study there were 459 patients with a baseline (day 1 of treatment) plasma sample available, 287 of these having a matched end of treatment (EOT) (Supplementary figure 1). The patients with paired samples from this group had similar palbociclib benefit compared to the overall PALOMA-3 study population (Supplementary figure 2). Of patients without available matched end of treatment samples (n = 172), 94 had not progressed (94/172, 54.6%) compared to 74 in the matched set (74/287, 25.8%). We first identified paired day 1 and EOT samples for plasma DNA exome sequencing to achieve comprehensive assessment of progression genetic events on palbociclib plus fulvestrant (Figure 1A). To identify paired plasma samples with sufficient tumor purity for exome sequencing, we developed a novel copy number and purity targeted sequencing strategy using a targeted amplicon panel that included approximately 1000 single nucleotide polymorphisms (SNPs) in regions commonly lost in breast cancer (See Materials and Methods, Supplementary figure 3) and combined this with digital PCR data for *PIK3CA* and *ESR1* mutations (13). Using this approach we identified 16 patients treated with palbociclib plus fulvestrant who had high tumor DNA purity in plasma (>10% tumor purity) at day 1 and EOT, with adequate material for exome library preparation (Supplementary table 1). Of these, 9/16 (56.3%) had a *PIK3CA* mutation and 6/16 (37.5%) an *ESR1* mutation in day 1 ctDNA. Five patients had matched germline DNA, and a further 3 additional unmatched germline DNA samples were also sequenced to expand the panel of germlines for filtering sequencing noise. As only 6 patients from the fulvestrant plus placebo arm had matched samples meeting the quality control criteria these were not sequenced.

Plasma DNA underwent exome sequencing to a median depth of 164X (range 139 – 212), with germline DNA sequenced to a median depth of 47X (range 34 – 58) (Supplementary table 2). Two day 1 samples had evidence of contamination and these pairs were excluded from comparative, paired analyses. The number of non-synonymous variants detectable in the day 1 samples varied considerably between patients (range 19 – 254, Supplementary figure 4). Analysis of the mutational signatures across all samples revealed the most prevalent were signatures 1 (age) and 3 (homologous recombination deficiency), consistent with existing data on breast cancer (16) (Supplementary table 3). Day 1 exome sequencing data additionally revealed genetic markers

potentially relevant to the development of endocrine resistance beyond *ESR1* mutations - mutations in the *NOTCH* family receptors *NOTCH2*, *NOTCH3* and *NOTCH4* in 4/14 (28.6%) patients, and *NF1* mutations in 2/14 patients (14.3%, Supplementary table 4). Genomic instability indices were broadly stable between day 1 and end of treatment for most patients, although as seen with mutation burden there was considerable variation between patients (Supplementary figure 5).

Clonal evolution and selection on palbociclib plus fulvestrant was clearly evident between day 1 and EOT plasma in 85.7% 12/14 patients (Figure 1, Supplementary figure 6). Patient 390 had two *RB1* truncating mutations, p.Q257X and p.N519fs, that were only detected at end of treatment (Figure 1B). Clonality analysis with PyClone (17) suggested these *RB1* mutations were in a resistant subclone, or potentially separate subclones with parallel evolution leading to phenotypic convergence, with a further treatment-sensitive sub-clone evident characterized by a *RUNXT1* mutation that regressed on treatment (Figure 1C). Mutation counts per subclone as determined by the PyClone model were 155 (cluster 1), 64 (cluster 2) and 51 (cluster 3). The mutations in the resistant sub clones were predominantly consistent with the APOBEC mutation signature (Figure 1D, Supplementary table 3). The *RB1* mutations were validated by digital PCR and confirmed to be absent at the start of treatment (Figure 1E).

A second patient, 253, during treatment with palbociclib plus fulvestrant exhibited marked selection of a subclone featuring an activating mutation in the tyrosine kinase domain of *FGFR2* p.K569E, not detectable in the day1 sample (Figure 1F). Mutations counts per subclone as determined by the PyClone model were 51 (cluster 1), 49 (cluster 2), 54 (cluster 3) and 20 (cluster 4). The newly dominant resistant sub clone, with an additional *ESR1* mutant Q75E daughter clone, replaced the day 1 *ESR1* D538G mutant clone that was negatively selected by treatment (Figure 1G). As Q75E is not a recognized cause of resistance to aromatase inhibitors and is positioned outside the ligand binding domain of *ESR1*, these findings in this case suggest changes in the dominant *ESR1* mutation between day 1 and EOT may reflect sub-clonal selection potentially unrelated to functional consequences of the *ESR1* mutation, with different *ESR1* mutations marking individual clones rather than potentially emergence of the resistant clone. As seen with the resistant sub clone in patient 390, the newly dominant *FGFR2* mutant sub clone in patient 253 also had a substantial proportion of mutations consistent with the APOBEC signature, with the minor daughter sub clone mutations dominated by the mismatch repair signature (Figure 1H, Supplementary table 3). Selection of the

FGFR2 mutation was validated by digital PCR (Figure 1I). In three further patients there was possible evidence of selection of emergent mutations in antigen presentation pathways (Supplementary table 4).

These findings demonstrate that clonal evolution is frequent in breast cancer on palbociclib plus fulvestrant, with evidence that the genomic plasticity of emergent subclones can be driven by different mutational processes from the bulk disease that is dominant at the start of treatment.

Patients acquire new driver mutations in both treatment arms

Paired exome sequencing findings were used to develop a targeted sequencing panel for error corrected ctDNA sequencing of all available paired plasma samples, with DNA from each sample input into two separate library preparations and sequenced on two sequencing platforms with different fundamental chemistry, then compared together for final analysis to reduce both PCR error and sequencing error (see Materials and Methods). The targeted panel included all the coding exons of *RB1*, *CDK4*, *CDK6*, *CDKN1A*, *CDKN2B*, *NF1*, exons 5-8 of *TP53*, and known mutation hotspots in *PIK3CA*, *ESR1*, *ERBB2*, *FGFR1*, *FGFR2*, *FGFR3*, *AKT1*, *KRAS*, *NRAS* and *HRAS*. *RB1* was included on the basis of the pre-existing literature, with *FGFR1/2/3* and *NF1* added following the exome sequencing. In addition to the 14 patients with paired exome sequencing, libraries were generated from 206 patients at both day 1 and EOT for targeted sequencing (Supplementary figure 1, Supplementary figure 7). These underwent sequencing to median coverage of 2187X and 3251X for day 1 and EOT samples respectively on an Ion Proton, and to median coverage of 10637X and 8947X for day 1 and EOT samples on an Illumina HiSeq 2500, yielding 184 patients with paired sequencing data from both platforms meeting quality requirements (Materials and Methods, Supplementary figure 1). Combined with the paired exome sequencing this yielded 195 patients with paired ctDNA sequencing data (3 patients being included in both sets, Supplementary figure 1) to investigate selection on treatment with palbociclib plus fulvestrant (n=127) or fulvestrant and placebo (n=68).

Initially considering both treatment groups together, overall there were more mutations detected at end of treatment than at day 1, with 183 variant calls made in 105 patients at day 1 versus 243 variant calls in 119 patients at end of treatment (Figure 2A). Sixty patients had at least one newly

detectable/acquired mutation at the end of treatment (60/195, 30.8%). The acquisition of mutations at end of treatment did not appear to reflect low day 1 tumor content, as there were similar proportions of detected day 1 mutations in both patients with and without acquired mutations (35/60, 58.3% versus 70/135, 51.9% respectively). Additionally there was no significant difference in the proportion of patients with >10% tumor purity at baseline (20.8% for patients with an acquired mutation, 31.0% for those without, $p = 0.21$, Fisher's exact test), calculated using the SNP panel on a subset of $n = 163$ day 1 samples. There were similar proportions of patients in both treatment groups who acquired at least one new mutation, 39/127 (30.7%) in the palbociclib plus fulvestrant arm and 21/68 (30.9%) in the placebo plus fulvestrant arm.

Six patients acquired detectable *RB1* mutations at end of treatment ($p = 0.041$, McNemar's test with continuity correction), all of these patients having received palbociclib plus fulvestrant. Two of these 6 patients had 2 *RB1* aberrations, one patient having been previously identified from the exome sequencing, suggesting polyclonal resistant sub clones (Figure 1C, Figure 2B). The Q257X mutation identified in sample 418 was also validated with ddPCR (Figure 2B). In the 6 patients who acquired *RB1* aberrations, all 8 variants were either a gain of a stop codon or a frameshift deletion, highly likely to result in abrogated Rb function. Four of the 6 patients who developed an *RB1* mutation also featured a *PIK3CA* mutation at a much higher allele fraction, suggesting that the *RB1* mutations could reflect sub clones (Supplementary figure 8). Considering the two orthogonal sequencing approaches, amplicon and exome capture, similar end of treatment *RB1* mutation frequencies were identified in both at end of treatment in the palbociclib plus fulvestrant arm (exome sequencing 7.1%, 1/14, amplicon sequencing 3.9%, 5/127). These observations support the emergence of *RB1* aberrations being acquired or selected under pressure from palbociclib, but only in a minority of patients (6/127, 4.7%). Although we did not identify any *RB1* mutations at day 1 this is chance result, we identified 2 patients (in the fulvestrant plus placebo arm) *RB1* mutations in a wider set of 331 day 1 samples that included patients without EOT samples.

Besides the emergence of *RB1* mutations on palbociclib, analysis of variants through treatment revealed different patterns across different genes, but a similar pattern between treatment groups (Figure 2C). For *TP53* there was predominantly persistence/maintenance of variants present at day 1 (Figure 2A, Figure 2C), consistent with variants in these genes commonly representing truncal

changes. One patient with a day 1 *TP53* mutation acquired 8 newly detectable variants in *TP53* at EOT (Supplementary figure 9).

Selection of PIK3CA mutations on treatment

For *PIK3CA*, considering both treatment arms, 39 variants in 37 patients (37/195, 19.0%) were identified in the day 1 samples (Figure 2A), consistent with previous findings (13) and indicating low levels of polyclonality. Almost all *PIK3CA* mutations present at day 1 were maintained after treatment (37/39, 95.7%), consistent with the majority of these being clonal/truncal mutations (Figure 2C). At end of treatment, 55 *PIK3CA* variants in 52 patients from both treatment groups (52/195, 26.7%) were detected, an increase compared to day 1 (Figure 2A, $p = 0.00069$, McNemar's test). There was acquisition of *PIK3CA* mutations in 8.2% patients overall (16/195, one of these acquiring 2 separate mutations and another patient acquired an additional *PIK3CA* variant (Figure 2C). The acquired *PIK3CA* mutations were validated with ddPCR for H1047R, H1047L, E545K and E542K (the most common, accounting for 16/18 acquired variants) with 100% (16/16) of these validating and showing close agreement with the sequencing allele fraction estimation ($r = 0.97$, Supplementary figure 10). Considering specific *PIK3CA* mutations, there was some limited evidence for positive selection of E542K ($p = 0.041$, McNemar's test with continuity correction, $q = 0.41$, Bonferroni correction, Supplementary figure 11). Using digital PCR to test day 1 samples, a minority of the acquired *PIK3CA* mutations had the 'acquired' mutation detectable at day 1 by digital PCR (6/18, 33.3%, Supplementary figure 12), with most of these at very low allele frequency below the limit of detection by ctDNA sequencing, providing evidence in some patients for outgrowth of a minor pre-existing *PIK3CA* mutant sub-clone. The increased proportion of *PIK3CA* mutant patients at the end of treatment remained statistically significant in an analysis that included the digital PCR data at day 1 ($p = 0.016$, McNemar's test). The proportion of patients acquiring newly detectable *PIK3CA* mutations did not appear to differ between treatment groups (Figure 2C, Supplementary figure 13, Supplementary figure 14). These data are consistent with a proportion of initially *PIK3CA* wild type tumors either positively selecting very low prevalence *PIK3CA* mutant sub clones, or newly acquiring them on treatment with fulvestrant.

Selection of ESR1 Y537S on treatment

ESR1 mutations were observed in patients 25.1% of patients at the start of treatment (49/195, 25.1%, Figure 2A), with a similar overall number of patients with an *ESR1* mutation at the end of treatment (61/195, 31.3%, $p = 0.07$ McNemar's test). However, 6.7% (13/195) patients had an *ESR1* mutation detected at baseline and did not have an *ESR1* mutation detected at progression, and similarly 12.8% (25/195) patients without an *ESR1* mutation detected at baseline had a newly acquired one at progression (Supplementary figure 14). Assessment of *ESR1* mutation status at baseline by digital PCR showed good overall agreement with the sequencing results (Supplementary figure 15).

Considering individual *ESR1* mutations, there was strong evidence for positive selection specifically of *ESR1* Y537S through treatment in both treatment groups ($p = 0.0037$, McNemar's test, $q = 0.047$, Bonferroni correction Figure 3A). All of the acquired Y537S mutations were validated in the end of treatment samples by repeat testing with digital PCR (17/17, Figure 3B). Considering the samples with a Y537S call in either time point, there was a minority of the acquired *ESR1* Y537S mutations that had the 'acquired' mutation detectable at day 1 by digital PCR (3/17, 17.6%, Figure 3C), providing evidence in some patients for outgrowth of a minor pre-existing *ESR1* Y537S mutant subclone. The increased proportion of *ESR1* Y537S mutant patients at the end of treatment remained statistically significant in an analysis that included the digital PCR data at day 1 and end of treatment ($p = 0.0019$, McNemar's test). An exploratory analysis of progression free survival comparing patients with a Y537S mutation at day 1 to those who acquired Y537S by end of treatment showed a trend to significance despite the small numbers (log rank $p = 0.011$, Supplementary figure 16). There were no clear differences in acquisition of specific *ESR1* mutations between treatment arms (Supplementary figure 17). Taken together, these data are consistent with *ESR1* Y537S promoting resistance to fulvestrant in the clinic.

Variants in further genes were acquired on treatment including hot-spot activating mutations in *ERBB2* (1.5%, 3/195), *KRAS* (0.5%, 1/195), *FGFR2* (1.0%, 2/195), with no obvious difference in selection between treatment groups (Figure 2C).

Clonal evolution of mutations with treatment

We next contrasted the clonal changes observed in different genes across both treatment arms, separately considering the course of individual clones, and of patients with different combinations of sub-clones (Figure 4A, Figure 4B). Genes with strong patterns of acquisition of new variants such as *RB1* and *PIK3CA* tended to lose relatively few clones on treatment (Figure 4C, Figure 4D). In contrast, *ESR1* mutations showed substantial variation through treatment, with frequent loss and gain of different mutations through treatment (Figure 4E, Figure 4F, Supplementary figure 14), and high levels of *ESR1* polyclonality (13). Patients commonly had a different combination of *ESR1* mutations detectable at EOT compared to day 1 (Figure 4F, Supplementary figure 14), and only 35.6% *ESR1* variants detected at any time point were detected at both and thus maintained on treatment (42/118). This pattern of polyclonal flux observed in *ESR1* mutations, supports the observation that individual *ESR1* mutations mark individual tumor sub-clones (Figure 1), demonstrating the frequent clonal selection pressure provided by treatment.

Copy number profiles remain predominantly consistent through treatment.

We next assessed copy number variation in plasma. Exome copy number profiles (n = 14) were largely consistent between day 1 and EOT on palbociclib plus fulvestrant (Supplementary figure 18, Supplementary figure 19), contrasting with the clonal evolution observed in single nucleotide variants (Figure 1). Loss of 13q, encompassing the *RB1* locus, was lost in 6/14 (42.9%) patients at day 1 and 5/16 (31%) patients at end of treatment, with the majority of these being present in the day 1 (4/5, 80%, Supplementary figure 20). There was no change in these findings with incremental reduction in the bin size, to investigate for large intra-genic deletions in *RB1*.

To expand copy number profile assessment beyond the exome sequencing, we assessed a larger set of matched pairs of day 1 and end of treatment samples from both treatment groups using the targeted sequencing panel that assessed loss of *RB1*, *PTEN* and *CDKN2A*, tumor purity and assessment of copy number in 12 genes commonly gained in breast cancer (Materials and Methods). In total, 324 samples were sequenced to assess copy number with median 1329X coverage, comprising 163 day 1 samples and 154 paired EOT samples (Supplementary figure 21, Supplementary figure 22).

As assessing copy-number in plasma DNA, and in particular copy number loss, is highly dependent on having sufficient tumor purity only the subset of samples with at least 20% tumor purity were used for assessment of losses. Of the day 1 samples, 37 had estimated $\geq 20\%$ purity, with 51 EOT samples having $\geq 20\%$ purity yielding 17 patients for paired analysis (Supplementary figure 23). There was an association between number of sites of disease and tumor content $>10\%$ ($p = 0.039$, Cochran-Armitage test). Loss of *RB1* was identified in 6/37 patients (16.2%) in day 1 samples and 14/51 patients (27.4 %) with end of treatment samples ($p = 0.30$, Fisher's exact test). Among these losses it was also possible to identify sub-genic deletions with our approach (Supplementary figure 22, Supplementary table 5). In EOT samples we identified 3.8% (2/51) sub-genic deletions, one of these also having a paired day 1 sample with the loss, suggesting these deletions pre-existed and were not acquired during treatment. In the 17 samples with paired $>20\%$ purity there was no evidence for selection of *RB1* loss on treatment (Supplementary figure 24, $p = 0.25$, McNemar's test), although this analysis was limited by sample size. Consistent copy number though treatment was also observed for *PTEN* and *CDKN2A* (Supplementary figure 24).

Copy number gain data at day 1 and end of treatment was assessed in those samples with $>10\%$ tumor purity and were largely consistent with the spectrum seen in primary breast cancer, with amplifications identified in *CCND1*, *MYC* and *FGFR1*, without evidence for selection or loss at end of treatment in the 43 samples with paired purity $>10\%$ (Supplementary figure 25). Two patients acquired *FGFR2* amplification at end of treatment (Supplementary figure 25). There were no patients with acquired *CCNE1* or *CCNE2* amplification at end of treatment.

Selection of genetic variants occurs late on palbociclib plus fulvestrant

To investigate clinical factors that associated with selection of mutations on treatment, we explored the relationship between time of treatment (PFS) and acquisition a new mutation at EOT (Materials and Methods) in both patients on palbociclib plus fulvestrant (Figure 5) and placebo plus fulvestrant (Supplementary figure 26). The presence of any acquired mutation at the end of treatment was associated with longer PFS compared to patients that did not acquire a mutation (Figure 5A, median 14.3 months acquired vs 5.5 months not acquired, log rank $p = 0.0018$, Supplementary figure 27, Supplementary figure 28), suggesting that new mutations were more likely to arise in patients who

had been on treatment longer. This trend was also seen separately for acquired *ESR1* mutations (Supplementary figure 29, median PFS 13.7 acquired versus 7.4 months not acquired, log rank $p = 0.032$) and *PIK3CA* mutations (Supplementary figure 30, median 12.7 acquired versus 9.2 months not-acquired, log rank $p = 0.34$), mutations in these two genes comprising the majority of the acquired mutations (Figure 5B). There were too few acquired *RB1* mutations to meaningfully assess a relationship with PFS (Supplementary figure 31). Assessment of baseline clinic-pathological characteristics with patients who had acquired a mutation revealed some evidence of an association with the presence of bone metastases ($p = 0.013$, $q = 0.15$, Supplementary table 6).

Discussion

CDK4/6 inhibitors in combination with endocrine therapy now represent the standard of care for advanced hormone-receptor positive breast cancer, but little is known about mechanisms of resistance to these treatments. Here we study the evolution of genetic mechanisms of resistance to palbociclib plus fulvestrant in these breast cancers and show that clonal evolution is frequent in response to therapy. Three main changes in driver genes are identified. Acquired mutations in *RB1* occur relatively infrequently, and are often sub-clonal, detected in the plasma of 5% of patients after palbociclib plus fulvestrant (Figure 2A-C). Acquired driver mutations in growth factor receptors and signal transduction pathways are frequently detected in patients treated with palbociclib plus fulvestrant, occurring in 39/127 (30.7%) of patients in total (Figure 2C, Figure 5D), dominated by 6% of these patients acquiring *PIK3CA* mutations, with 9% more patients having at least 1 *ESR1* mutation by end of treatment compared to day 1 (Figure 5D). Evolution of *ESR1* mutations is observed, with selection of *ESR1* Y537S as the variant most likely promoting resistance to fulvestrant in the combination (Figure 3A, Figure 4E). Conversely, as acquisition or selection of the mutations examined in our panel was seen predominantly in patients with longer treatment duration. This suggests that patients with tumors intrinsically resistant to treatment less frequently acquire mutations, presumably due to the lack of selective pressure of treatment, and that other mechanisms of resistance may dominate in early progression.

Preclinical work has identified *RB1* mutations(9,11) as a mechanism of resistance to CDK4/6 inhibition, consistent with the literature that functional Rb is required for the efficacy of CDK4/6 inhibitors (18). Of these potential mechanisms of resistance only mutations in *RB1* have been identified in the clinic although their prevalence in a treated population is unknown (11). Condorelli and colleagues have recently reported 3 patients with *RB1* mutations following treatment with CDK4/6 inhibition, 2 of these receiving palbociclib with fulvestrant in the setting of previous endocrine treatment, and the other ribociclib and letrozole as first line for advanced disease (11). With the advantages of analyzing an unbiased registration study, our study confirms apparent positive selection of *RB1* aberrations on palbociclib plus fulvestrant, but demonstrates they are only evident in a minority of patients (Figure 2A). In these patients we identify polyclonal *RB1* aberrations, suggestive of phenotypic convergence under selective pressure, such as is seen with *ESR1* mutations in response to endocrine therapy (13,19). Intriguingly, *RB1* mutations were only selected in

tumors wild-type for *ESR1* mutations (Figure 2D). Although we are unable to exclude a chance finding, this does possibly suggest that *RB1* mutations could be selected when fulvestrant efficacy is not compromised by *ESR1* mutation, suggesting divergent routes to resistance. Our findings of relatively uncommon *RB1* mutations is important in suggesting that subsequent lines of endocrine based therapy have the potential to be active on progression, concurring with currently available post-progression clinical data(15).

With the exception of *RB1* mutations, there was no evident difference in acquired mutation profiles between the fulvestrant and palbociclib versus fulvestrant and placebo groups (Figure 2C). This observation within the context of a randomized trial suggests that resistance to fulvestrant is a major genetic driver of resistance to combination therapy, possibly with tumors able to adapt to CDK4/6 inhibition without ER signaling suppressed. *ESR1* mutations are an important mechanism of resistance to aromatase inhibitors, with mutations in the ligand binding domain, particularly helix 12, resulting in a constitutively active protein (20,21). Nevertheless, the detection of multiple resistant sub clones at baseline did not predict palbociclib activity in PALOMA-3 (13). Our data suggests a significant proportion of *ESR1* mutations present at day 1 are lost on palbociclib plus fulvestrant, at least in part reflecting the high level of clonal evolution on therapy with loss of *ESR1* mutations reflecting loss of the sensitive sub clone (Figure 1C, 1G), with others emerging during subsequent fulvestrant treatment at the same rate and pattern in both treatment groups (Figure 2C). We find evidence for positive selection of Y537S at end of treatment (Figure 3A, Figure 3D, Figure 4E), this being the ligand binding domain mutation identified in pre-clinical studies as the most resistant to fulvestrant (22). This suggests separate, parallel evolution of mechanisms of resistance to the combination of palbociclib plus fulvestrant.

Further acquired driver mutations were observed in growth factor receptors and signal transduction pathways (Figure 5D). *PIK3CA* mutations are important founding variants in ER positive primary breast cancers (12) and remain clonally dominant in most metastatic breast cancers (23). We now identify that 6% of patients with no detectable *PIK3CA* mutations at day 1 acquire, or positively select, newly evident *PIK3CA* mutations at the end of treatment with palbociclib plus fulvestrant (Figure 2C, 4A, Figure 4C, Figure 4D), in particular E542K in this study (Supplementary figure 11). The prevalence of emergent *PIK3CA* mutations did not appear to differ between treatment groups (Supplementary figure 13), favoring the hypothesis that these are principally effecting fulvestrant

resistance (24). Through exome sequencing we identify a role for APOBEC in driving clonal diversity and resistance to palbociclib plus fulvestrant (Figure 1D, 1H, Supplementary table 3). We note E542K is a potential APOBEC site, with the dominance of E542K potentially providing further evidence to support APOBEC mutagenesis in promoting genetic diversity in advanced ER positive breast cancer(25,26).

Our study also has potentially important findings in relation to the existing pre-clinical literature on mechanisms of resistance to CDK4/6 inhibitors. Prior pre-clinical work identified acquired amplification of *CCNE1*(9) or *CDK6*(10), in palbociclib and abemaciclib resistant models respectively. We find no evidence that acquired *CCNE1*, *CDK4* or *CDK6* amplification are relevant in the clinic, although we do note that circulating tumor DNA analysis is limited in analyzing copy number due to the challenge of low tumor purity. We partly address this limitation by adopting a novel targeted sequencing approach to allow concurrent assessment of purity and copy number, restricting copy number analysis for gain to those tumors with at least 10% tumor purity, and loss to those with at least 20% tumor purity (Supplementary figures 21 -25). Our plasma tumor purity observations are comparable to the third of patients having >10% tumor content in the large breast cancer set reported in Adalsteinsson et al (27), with the slightly higher rates of observed purity in our study (42% of day 1 samples, 68/163, and 53% of end of treatment samples, 82/154) perhaps due to be explained by all the samples being processed under the strict protocol mandated in the study. However, we emphasize that ctDNA analysis would be unlikely to detect many sub-clonal amplifications or losses. In addition, we find no evidence for gatekeeper mutations in *CDK4* or *CDK6*, and can effectively exclude this from being a common mechanism of resistance (Figure 2A).

Our study has a number of limitations. Making comparisons between longitudinal time points in circulating tumor DNA is difficult due to variations in tumor content - inability to identify mutations may be a result of absence of tumor DNA in plasma, or presence at a low level that falls into the sequencing noise. We mitigate this concern by conducting secondary analyses - analyzing baseline plasma with digital PCR for newly emergent mutations, and performing a subset analysis of patients with known day 1 tumor content. The problem of purity is particularly challenging for assessing genomic loss, compounded for comparative analyses where confidence is required in the tumor content at more than a single time point. This may limit the investigation of *RB1* loss, and we suggest that tissue based analysis will be required for a definitive analysis of copy number on progression.

Although we analyzed 14 patients by paired exome sequencing, for discovery and to design our targeted panel, we cannot address whether there are rare acquired events not interrogated by our targeted panel. Additionally, we have interrogated relatively few end of treatment plasma samples from patients with over 2 years treatment duration, and so we are unable to address whether very late progression may have a different pattern of acquired mutations. Finally, we use the term 'acquired' in this manuscript to reflect a mutation detectable at EOT that was not detectable at day 1. It is very challenging to assess whether these mutations may have pre-existed in the tumor prior to treatment in a minor and undetectable subclone. Investigating this exhaustively for Y537S with very high sensitivity digital PCR we do detect at very low level some of the 'acquired' and 'lost mutations at day 1 and end of treatment respectively, but show that these are balanced between the two time points and do not significantly affect the comparative result (Figure 3D).

Our study has important clinical implications for future therapeutic approaches in breast cancer. Resistance to fulvestrant is identified as a major driver of resistance to the combination of palbociclib plus fulvestrant. A number of potent oral selective estrogen receptor downregulators (SERDs) are in clinical development, and our findings suggest that more potent targeting of the estrogen receptor has potential to improve on fulvestrant in combination with palbociclib. Oral SERDs should specifically address their clinical activity against *ESR1* Y537S. A number of targetable kinase mutations are enriched on palbociclib plus fulvestrant, with an approximate doubling of the number of detectable hot-spot activating *ERBB2* mutations, activating *FGFR* mutations and high level acquired *FGFR2* amplification, all of which invite precision medicine-guided therapeutic approaches after progression. Mutations in *PIK3CA* are selected through fulvestrant therapy, suggesting a greater role for PI3 kinase inhibitors after therapy as well as the potential for triple combination therapy (ER, CDK4/6, PI3 kinase) to prevent the outgrowth of resistant clones driven by acquired *PIK3CA* mutations.

Our work demonstrates the value of interrogating large registration trials with paired ctDNA analysis, demonstrating how ongoing clonal evolution in breast cancer drivers undermines palbociclib plus fulvestrant therapy, highlighting a potential role for APOBEC mutagenesis in promoting clonal evolution, and identifies rational therapeutic strategies that could improve efficacy of CDK4/6 inhibition.

Materials and methods

PALOMA-3 Study design

The PALOMA-3 trial was a phase III, double-blind randomized controlled trial comparing palbociclib plus fulvestrant to placebo plus fulvestrant in patients with ER+/HER2- advanced breast cancer. The trial recruited 521 patients randomized in a 2:1 ratio to receive oral palbociclib 125 mg daily, 3 weeks on, 1 week off, or matched placebo. All patients received fulvestrant 500mg every 4 weeks. Pre-menopausal women received goserelin in addition. Patients were eligible if they had either progressed on endocrine treatment for advanced disease or progressed during or within 12 months following adjuvant endocrine therapy.

Plasma collection and processing

Blood samples were collected at day 1 of treatment and end of treatment in EDTA blood collection tubes. These were centrifuged within 30 minutes at 1500-2000g before separation of the plasma and storage at -80C and transfer to a central laboratory. Prior to extraction plasma was centrifuged again at 3000g for 10 minutes and the supernatant used for extraction. DNA extraction was performed using the Circulating Nucleic Acid kit (Cat No./ID: 55114) from Qiagen® (Venlo, Netherlands). DNA was quantified using a Taqman-based digital PCR assay against *RPPH1* from LifeTech® (California, USA, Cat no. 4403326). Buffy coat were available was extracted using the Qiagen Qiacube according to the manufacturer's instructions.

Digital PCR

Digital PCR experiments were performed with Taqman probes in 20ul reactions partitioned into 20,000 micelles in an oil and water emulsion using the Bio-Rad® AutoDG® system before undergoing PCR in a G Storm thermocycler. Prior to use, cycling conditions for each Taqman assay was optimized using a thermal gradient and G-blocks from Integrated DNA Technologies (Iowa, USA). Droplets were read on a Bio-Rad® QX200 and concentrations calculated by fitting a Poisson model to the data using Bio-Rad® QuantaSoft version 1.4.0.99. Day 1 DNA samples were screened for *ESR1* mutations S463P (c.1387T>C), Y537N (c.1609T>A) E380Q (c.1138G>C), L536R (c.1607T>G),

Y537C (c.1610A>G), D538G (c.1613A>G) and *PIK3CA* mutations E542K (c.1624 G > A), E545K (c.1633 G > A), H1047R (c.3140 A > G) and H1047L (c.3140 A > T) as previously described(13). For the purposes of exome sequencing, end of treatment samples were tested for a mutation with digital PCR only if a mutation was found in the matched day 1 sample to estimate purity. For purity estimates from digital PCR allele fractions mutations were assumed to be heterozygous with a copy number of 2.

Exome sequencing

Matched day 1 and end of treatment samples with adequate material (minimum 13ng to preserve library complexity) and purity (10%) were selected for exome sequencing. Hybrid capture libraries were prepared using Agilent SureSelect V6 with paired end sequencing performed on an Illumina HiSeq 2500 to a target depth of 150X for plasma and 50X for germline. Reads were aligned to the hg19 reference using BWA v0.7.12 (28) and duplicates removed with Picard (v2.8.2) according to GATK best practices (28). Copy number was assessed using cnvkit v0.8.4 (29) and purity with ASCAT 2 (30). Variant calling between pairs was performed with MuTECT v1.1.7 (31), MuTECT2 (GATK v3.7), VarDict v1.5.0 (32) and between samples and the panel of germlines using MuTect2 and GATK. Variants were only considered if they had coverage of 40X and were identified by 2 callers. Clonality analysis was performed with PyClone (0.13.0)(17), the mutational signature analysis with the R package deconstructSigs (33) and the chromosomal instability indices as described in Andor et al(34). For samples without matched germline DNA, PyClone was used to identify and screen germline SNPs from paired analysis. For samples without matched germline DNA putative SNPs were removed from analysis either using a variant allele fraction (VAF) cut off < 0.4 or by comparing VAF in both EOT and day 1 samples. Copy number profiles were compared using GISTIC (35). Additional diagrams and fish plots were produced using clonevol (36). Sequencing data are publically available at the Sequencing Read Archive, using the accession number SRP157645.

Targeted copy number and purity panel

A 1729 amplicon custom panel was designed using the Ampliseq designer software (Thermo Fisher Scientific, Waltham, USA) to allow combined copy number and purity assessment. For purity assessment the panel included approximately 100 SNPs with population prevalence over 20% in 8 chromosomal regions that commonly exhibit loss of heterozygosity in breast cancer: 16q24.3, 17p12, 8p23.2, 11q23.3, 22q13.31, 1p36.13, 6q27, 3p21.31. Assessment of tumor purity was validated down to 10% by comparison with validated digital PCR assay allele fraction (Supplementary table 7). For robust assessment of loss a similar approach was used to include *RB1*, *CDKN2A* (p16) and *PTEN* with 119, 134, and 128 SNPs for each, respectively. For copy number assessment approximately 20 amplicons were sited in 11 genes commonly amplified in breast cancer and 19 reference genes identified from TCGA(12) and METABRIC(37) data as being relatively copy number invariant. Libraries were constructed with 1-3ng input using the IonTorrent Library kit v2.0 (Thermo Fisher Scientific, Waltham, USA) and sequenced to a target depth of 1000-2000X on the Ion Proton using P1 chips. Reads were aligned using Torrent Suite software. Loss of heterozygosity was estimated using a bespoke pipeline that used a threshold of 5% for the presence of a β allele based on variance seen in germline material with a minimum of 15 informative SNPs (Supplementary figure 32, Supplementary table 8) using an approach adopted from previous CLONET analyses (38,39). A minimum of 4 amplicons was used. Purity was estimated by assuming a single diploid clone with loss of heterozygosity, with this approach yielding similar estimates of purity to digital PCR (Supplementary table 7) and CLONET(40) (Supplementary figure 33), with reported profiles in the validated set matching the expected distribution from the TCGA (Supplementary figure 34). Copy number was assessed using the OncoCNV (v6.8) (41) package with calls based on normalized logR values obtained using thresholds of 0.24 for gain and -0.18 for loss. These thresholds were established using 3 standard deviations from the mean, derived from sequenced germline samples using the purity panel. To account for inter-gene variability within the panel an additional z test with an α of 0.05 was performed against the local logR for all the samples. Copy number estimates were adjusted for purity where purity exceeded the minimum threshold of 10%. Primers capturing *CCNE2* were only included for 226/324 samples, and so *CCNE2* was not assessable in the other 98 samples. *RB1* loss was defined as either evidence of heterozygous loss (normalized logR < -0.18 with or without evidence of LOH) or probable homozygous loss where the adjusted copy number was <1.

Targeted gene panel sequencing

The AmpliSeq designer (Thermo Fisher Scientific, Waltham, USA) was used to create a 305 amplicon custom panel with amplicons covering the coding exons of *RB1*, *CDK4*, *CDK6*, *CDKN1A*, *CDKN1B*, *NF1*, exons 5 – 8 of *TP53* and mutational hotspots in *ERBB2*, *PIK3CA*, *AKT1*, *ESR1*, *FGFR1*, *FGFR2* and *FGFR3*. Two libraries were constructed for each sample with 1.5 – 5ng of DNA per primer pool at each time point with the initial multiplex PCR of 22-24 cycles depending on input. One set of libraries were taken through the conventional IonTorrent Library kit v2.0 protocol, while the matched set was cleaned with AMPure XP (Beckmann Coulter, Brea, USA) beads following FuPa digestion and the library prep completed using the KAPA Hyper Prep kit with dual-index adaptors without further PCR. The IonTorrent libraries were then sequenced to a target depth of 2,000X on a Proton with P1 chips. The custom libraries were sequenced on an Illumina HiSeq 2500 to target coverage of 15,000X. Sequencing reads were aligned and BAM files generated for the IonTorrent libraries using the Torrent Suite software and with BWA for the Illumina libraries. Sequencing artefact was removed with iDES(42) and manual curation with variants called from pileup only if present in both datasets above an allele fraction of 0.3% for hotspots, stopgains and frameshifts and 0.5% for all other calls, with a minimum of 5 alternative reads. VarDict was used to call indels under the same constraints on both platforms and torrent caller was used for IonTorrent libraries and Mutect2 for Illumina libraries. This approach was validated using dilutions of a blend of circulating tumor DNA (Supplementary figure 35).

Statistical analyses

Kaplan Meier survival analyses for progression free survival were performed with the log rank test using a Cox proportional hazards model to obtain hazard ratios and 95% confidence intervals. Comparison of frequency of particular genomic aberrations in unpaired day 1 samples versus end of treatment was done using Fisher's exact test. Analysis of paired data between day 1 and end of treatment was performed using McNemar's test with a continuity correction where required. Unless stated otherwise all p values were two-sided with an α of 0.05. Statistical analyses were conducted using R version 3.4.3. To address potential under-sampling at the day 1 time point, for the survival analysis comparing patients with and without an acquired mutation mutations were only included as acquired if the variant calls in the Ion Torrent and Illumina libraries passed an additional statistical

test. The proportions of alternative and reference reads between day 1 and end of treatment were compared using Fisher's exact test, with only those calls with $p < 0.05$ in both libraries being included in the survival analysis. Of 60 patients with acquired mutations, 53/60 met these criteria and were included in the survival analysis. Survival analyses were conducted using the latest data cut off from the trial (October 2015) in which the median PFS was 4.6 months for fulvestrant plus placebo and 11.2 months for palbociclib plus fulvestrant(15).

Acknowledgments: We thank the patients, families and trial staff who took part in the PALOMA-3 trial. We thank Francesca Demichelis and Alessandro Romanel for their help performing the CLONET validation analyses, Irene Chong for assistance with *MYC* amplification validation by digital PCR and Erle Holgersen for advice regarding the circos plots.

Figure legends

Figure 1. Paired circulating tumor DNA (ctDNA) exome sequencing reveals frequent clonal selection on fulvestrant plus palbociclib

A – Day 1 and end of treatment plasma samples from the PALOMA-3 trial were screened using droplet digital PCR and a targeted SNP sequencing approach to identify patients from the palbociclib plus fulvestrant arm who had paired plasma samples of sufficient tumor purity (>10%) for plasma exome sequencing.

B – Paired ctDNA exome sequencing in patient 390 analyzed for clonal composition. A newly emergent *RB1*-mutant clone is detected at EOT, harboring two inactivating *RB1* mutations.

C – Inferred phylogenetic tree of breast cancer from patient 390 derived from ctDNA. Yellow - truncal mutations present in all cancer cells; Purple - subclone present at day 1 that subsequently regressed on treatment; Gray - a newly emergent resistant clone characterized by two *RB1* mutations, arising separately to the purple sub clone.

D – Representation of mutational signatures identified in each individual sub clone for patient 390. The raw data are shown in Supplementary table 3.

E – Digital PCR validation of the two *RB1* mutations Q257X and N519fs identified in the treatment-resistant sub clone from patient 390. Results for day 1 and EOT are shown, Y axis mutant probe amplitude and X axis wild type probe amplitude.

F – Paired ctDNA exome sequencing in patient 253 analyzed for clonal composition. A new *FGFR2* mutant clone undetectable at day 1 is detected at EOT.

G – Inferred phylogenetic tree of breast cancer from patient 253 derived from ctDNA. Yellow - truncal mutations present in all cancer cells; Purple - subclone characterized by an *ESR1* D538G mutation present at day 1 that subsequently regressed on treatment; Orange - newly emergent resistant clone characterized by an *FGFR2* kinase domain mutation, arising separately from the purple sub clone; Gray – a sub clone arising from the *FGFR2*-mutant sub clone characterized by a Q75E *ESR1* mutation.

H – Representation of mutational signatures identified in each individual clone from patient 253. The raw data are shown in Supplementary table 3.

I – Digital PCR validation of the *FGFR2* mutation from patient 253 showing results for plasma at day 1 and EOT.

EOT – end of treatment, HR – homologous recombination, MMR – mismatch repair, ctDNA – circulating tumor DNA

Figure 2. Genetic landscape of breast cancer driver genes in paired plasma samples on PALOMA-3 with frequent selection of mutations on treatment

A – Paired ctDNA sequencing results with frequency of observed variants in genes included in the targeted driver gene panel (SNVs and indels). Results are shown for both day 1 and end of treatment in 195 patients with matched data from day 1 and EOT. P values McNemar's test with continuity correction.

B – *RB1* mutations identified at EOT in patients treated with palbociclib plus fulvestrant (6/127). No *RB1* mutations were identified in the EOT plasma samples from patients treated with placebo and fulvestrant (n = 68). The digital PCR plot shows orthogonal validation of Q257X in the EOT sample from patient 418.

C – End of treatment (EOT) ctDNA sequencing results from 195 patients with paired samples, split by treatment, and whether the mutation status changed on treatment between day 1 and EOT. The cohort of 195 patients is formed from both the targeted sequencing cohort (n = 184) and exome sequencing cohort (n = 14, with n = 3 in both sets, see Supplementary figure 1). The pattern of mutation acquisition is similar across both treatment arms.

SNV – single nucleotide variant, indel – insertion or deletion, EOT – end of treatment, ctDNA – circulating tumor DNA. Mixed – patients with different variants in the same gene at day 1 and EOT.

Figure 3. Positive selection of *ESR1* Y537S on fulvestrant based treatment

A – Percentages of patients at baseline and end of treatment with specific *ESR1* mutations observed in paired ctDNA sequencing data (n = 195, treatment groups combined). Data includes both fulvestrant plus placebo and fulvestrant plus palbociclib groups together. P values calculated from McNemar's test with continuity correction, and q value after Bonferroni correction for multiple comparisons.

B – Validation of acquired *ESR1* Y537S end of treatment mutations with digital PCR (17/17). Allele fraction is plotted for each technique.

C – Concordance between sequencing and digital PCR for allele fraction in patients with an *ESR1* Y537S mutation in ctDNA sequencing at either day 1 or end of treatment. Blue - concordant calls present in both sequencing and digital PCR. Orange - present only in digital PCR.

ctDNA – circulating tumor DNA

Figure 4. Clonal evolution of breast cancer driver genes through treatment

A – Individual variants for each gene in the treatment groups combined (n=195), split by variants maintained between day 1 and end of treatment, lost over the course of treatment, or acquired during treatment. A number of patients had polyclonal variants in a single gene, particularly *ESR1*. The majority of *TP53* acquired variations are accounted for by a single patient acquiring 8 separate new variants at EOT (see also Supplementary figure 9).

B – Cartoon with data from patient 237 illustrating subclonal selection on treatment. A clonal *PIK3CA* mutation and an *ESR1*-mutant sub clone are detectable at day 1. Over the course of treatment the *ESR1*-mutant subclone present at day 1 is lost, with acquisition of a new *ERBB2*-mutant sub clone.

C – Sankey diagram to illustrate changes in individual *PIK3CA* mutations through treatment in both treatment groups combined. Polyclonal mutations from a single patient are displayed separately. Only two *PIK3CA* mutations detected at day 1 are undetectable at EOT, one from a patient with the other polyclonal mutation detected at EOT.

D – Clonal state diagram to illustrate changes in *PIK3CA* polyclonality through treatment, with each individual patient represented once at day1 and EOT. Inner track demonstrates clonal states, representing different combinations of *PIK3CA* mutations indicated by segments of the circle. The middle tracks show individual mutations in the clonal states. The outer track shows the number of patients with that specific combination of mutations at day 1 (green bar) and end of treatment (purple bar). The central arrows show changes between day1 and EOT. The plot incorporates data from both treatment arms (n = 195).

E – Sankey diagram to illustrate changes in individual *ESR1* mutations through treatment in both treatment groups combined.

F – Clonal state diagram to illustrate changes in *ESR1* polyclonality through treatment, with each individual patient represented once at day1 and EOT, legend see D.

EOT – end of treatment

Figure 5. New driver mutations are selected late on treatment with palbociclib plus fulvestrant

A – Swimmers plot of patients with paired sequencing data who received palbociclib plus fulvestrant (n = 127) comparing PFS between patients with any acquired driver mutation at end of treatment (n = 35) versus patients that did not acquire a new driver mutation (n = 92). P value calculated using log rank.

B – Genetic landscape of breast cancer progressing after palbociclib plus fulvestrant treatment. Each box shows the percentage of patients with a mutation identified at EOT (gray) and the subset of these patients who have newly acquired a mutation by EOT (yellow) for each gene. Patients with the same gene detected mutant and day 1 and EOT, but with a different pattern of mutations in the gene, are not counted as being acquired.

PFS – progression free survival, HR – hazard ratio, CI – Confidence interval, EOT – end of treatment

References

1. Turner NC, Neven P, Loibl S, Andre F. Advances in the treatment of advanced oestrogen-receptor-positive breast cancer. *The Lancet* **2016**;389(10087):2403-14 doi 10.1016/S0140-6736(16)32419-9.
2. Sherr CJ, Roberts JM. CDK inhibitors: positive and negative regulators of G1-phase progression. *Genes & Development* **1999**;13(12):1501-12.
3. Goodrich DW, Wang NP, Qian Y-W, Lee EYHP, Lee W-H. The retinoblastoma gene product regulates progression through the G1 phase of the cell cycle. *Cell* **1991**;67(2):293-302 doi [http://dx.doi.org/10.1016/0092-8674\(91\)90181-W](http://dx.doi.org/10.1016/0092-8674(91)90181-W).
4. Harbour JW, Luo RX, Santi AD, Postigo AA, Dean DC. Cdk Phosphorylation Triggers Sequential Intramolecular Interactions that Progressively Block Rb Functions as Cells Move through G1. *Cell* **1999**;98(6):859-69 doi [http://dx.doi.org/10.1016/S0092-8674\(00\)81519-6](http://dx.doi.org/10.1016/S0092-8674(00)81519-6).
5. Sledge GW, Toi M, Neven P, Sohn J, Inoue K, Pivot X, *et al.* MONARCH 2: Abemaciclib in Combination With Fulvestrant in Women With HR+/HER2- Advanced Breast Cancer Who Had Progressed While Receiving Endocrine Therapy. *Journal of Clinical Oncology* **2017**;JCO.2017.73.7585 doi 10.1200/JCO.2017.73.7585.
6. Goetz MP, Toi M, Campone M, Sohn J, Paluch-Shimon S, Huober J, *et al.* MONARCH 3: Abemaciclib As Initial Therapy for Advanced Breast Cancer. *Journal of Clinical Oncology* **2017**;35(32):3638-46 doi 10.1200/jco.2017.75.6155.
7. Finn RS, Martin M, Rugo HS, Jones S, Im S-A, Gelmon K, *et al.* Palbociclib and Letrozole in Advanced Breast Cancer. *New England Journal of Medicine* **2016**;375(20):1925-36 doi doi:10.1056/NEJMoa1607303.
8. Hortobagyi GN, Stemmer SM, Burris HA, Yap Y-S, Sonke GS, Paluch-Shimon S, *et al.* Ribociclib as First-Line Therapy for HR-Positive, Advanced Breast Cancer. *New England Journal of Medicine* **2016**;0(0):null doi doi:10.1056/NEJMoa1609709.
9. Herrera-Abreu MT, Palafox M, Asghar U, Rivas MA, Cutts RJ, Garcia-Murillas I, *et al.* Early Adaptation and Acquired Resistance to CDK4/6 Inhibition in Estrogen Receptor-Positive Breast Cancer. *Cancer Res* **2016** doi 10.1158/0008-5472.can-15-0728.
10. Yang C, Li Z, Bhatt T, Dickler M, Giri D, Scaltriti M, *et al.* Acquired CDK6 amplification promotes breast cancer resistance to CDK4/6 inhibitors and loss of ER signaling and dependence. *Oncogene* **2017**;36(16):2255-64 doi 10.1038/onc.2016.379.
11. Condorelli R, Spring L, O'Shaughnessy J, Lacroix L, Bailleux C, Scott V, *et al.* Polyclonal RB1 mutations and acquired resistance to CDK 4/6 inhibitors in patients with metastatic breast cancer. *Annals of Oncology* **2017**:mdx784-mdx doi 10.1093/annonc/mdx784.
12. The Cancer Genome Atlas Network. Comprehensive molecular portraits of human breast tumours. *Nature* **2012**;490(7418):61-70 doi <http://www.nature.com/nature/journal/v490/n7418/abs/nature11412.html#supplementary-information>.
13. Fribbens C, O'Leary B, Kilburn L, Hrebien S, Garcia-Murillas I, Beaney M, *et al.* Plasma ESR1 Mutations and the Treatment of Estrogen Receptor-Positive Advanced Breast Cancer. *Journal of Clinical Oncology* **2016** doi 10.1200/jco.2016.67.3061.

14. Cristofanilli M, Turner NC, Bondarenko I, Ro J, Im S-A, Masuda N, *et al.* Fulvestrant plus palbociclib versus fulvestrant plus placebo for treatment of hormone-receptor-positive, HER2-negative metastatic breast cancer that progressed on previous endocrine therapy (PALOMA-3): final analysis of the multicentre, double-blind, phase 3 randomised controlled trial. *The Lancet Oncology* **2016** doi 10.1016/S1470-2045(15)00613-0.
15. Turner NC, Andre F, Cristofanilli M, Verma S, Iwata H, Loi S, *et al.* Abstract P4-22-06: Treatment postprogression in women with endocrine-resistant HR+/HER2-advanced breast cancer who received palbociclib plus fulvestrant in PALOMA-3. 2017. P4-22 p.
16. Nik-Zainal S, Morganella S. Mutational Signatures in Breast Cancer: The Problem at the DNA Level. *Clinical cancer research : an official journal of the American Association for Cancer Research* **2017**;23(11):2617-29 doi 10.1158/1078-0432.CCR-16-2810.
17. Roth A, Khattra J, Yap D, Wan A, Laks E, Biele J, *et al.* PyClone: statistical inference of clonal population structure in cancer. *Nature methods* **2014**;11:396 doi 10.1038/nmeth.2883
<https://www.nature.com/articles/nmeth.2883#supplementary-information>.
18. Finn R, Dering J, Conklin D, Kalous O, Cohen D, Desai A, *et al.* PD 0332991, a selective cyclin D kinase 4/6 inhibitor, preferentially inhibits proliferation of luminal estrogen receptor-positive human breast cancer cell lines in vitro. *Breast Cancer Research* **2009**;11(5):R77.
19. Chandarlapaty S, Chen D, He W, *et al.* Prevalence of *esr1* mutations in cell-free dna and outcomes in metastatic breast cancer: A secondary analysis of the bolero-2 clinical trial. *JAMA Oncology* **2016** doi 10.1001/jamaoncol.2016.1279.
20. Toy W, Shen Y, Won H, Green B, Sakr RA, Will M, *et al.* ESR1 ligand-binding domain mutations in hormone-resistant breast cancer. *Nat Genet* **2013**;45(12):1439-45 doi 10.1038/ng.2822
<http://www.nature.com/ng/journal/v45/n12/abs/ng.2822.html#supplementary-information>.
21. Jeselsohn R, Buchwalter G, De Angelis C, Brown M, Schiff R. ESR1 mutations-a mechanism for acquired endocrine resistance in breast cancer. *Nat Rev Clin Oncol* **2015**;12(10):573-83 doi 10.1038/nrclinonc.2015.117.
22. Toy W, Weir H, Razavi P, Lawson M, Goepfert AU, Mazzola AM, *et al.* Activating ESR1 Mutations Differentially Affect the Efficacy of ER Antagonists. *Cancer Discovery* **2017**;7(3):277-87 doi 10.1158/2159-8290.cd-15-1523.
23. Pereira B, Chin S-F, Rueda OM, Vollan H-KM, Provenzano E, Bardwell HA, *et al.* The somatic mutation profiles of 2,433 breast cancers refine their genomic and transcriptomic landscapes. *Nature communications* **2016**;7:11479 doi 10.1038/ncomms11479
<https://www.nature.com/articles/ncomms11479#supplementary-information>.
24. Mayer IA, Arteaga CL. PIK3CA Activating Mutations: A Discordant Role in Early Versus Advanced Hormone-Dependent Estrogen Receptor-Positive Breast Cancer? *Journal of Clinical Oncology* **2014**;32(27):2932-4 doi 10.1200/jco.2014.55.9591.
25. Lefebvre C, Bachelot T, Filleron T, Pedrero M, Campone M, Soria J-C, *et al.* Mutational Profile of Metastatic Breast Cancers: A Retrospective Analysis. *PLOS Medicine* **2016**;13(12):e1002201 doi 10.1371/journal.pmed.1002201.
26. Savas P, Teo ZL, Lefevre C, Flensburg C, Caramia F, Alsop K, *et al.* The Subclonal Architecture of Metastatic Breast Cancer: Results from a Prospective Community-Based Rapid Autopsy Program “CASCADE”. *PLOS Medicine* **2016**;13(12):e1002204 doi 10.1371/journal.pmed.1002204.

27. Adalsteinsson VA, Ha G, Freeman SS, Choudhury AD, Stover DG, Parsons HA, *et al.* Scalable whole-exome sequencing of cell-free DNA reveals high concordance with metastatic tumors. *Nature communications* **2017**;8(1):1324 doi 10.1038/s41467-017-00965-y.
28. Van der Auwera GA, Carneiro MO, Hartl C, Poplin R, Del Angel G, Levy-Moonshine A, *et al.* From FastQ data to high confidence variant calls: the Genome Analysis Toolkit best practices pipeline. *Current protocols in bioinformatics* **2013**;43:11.0.1-33 doi 10.1002/0471250953.bi1110s43.
29. Talevich E, Shain AH, Botton T, Bastian BC. CNVkit: Genome-Wide Copy Number Detection and Visualization from Targeted DNA Sequencing. *PLOS Computational Biology* **2016**;12(4):e1004873 doi 10.1371/journal.pcbi.1004873.
30. Van Loo P, Nordgard SH, Lingjærde OC, Russnes HG, Rye IH, Sun W, *et al.* Allele-specific copy number analysis of tumors. *Proceedings of the National Academy of Sciences* **2010**;107(39):16910-5.
31. Cibulskis K, Lawrence MS, Carter SL, Sivachenko A, Jaffe D, Sougnez C, *et al.* Sensitive detection of somatic point mutations in impure and heterogeneous cancer samples. *Nature Biotechnology* **2013**;31:213 doi 10.1038/nbt.2514
<https://www.nature.com/articles/nbt.2514#supplementary-information>.
32. Lai Z, Markovets A, Ahdesmaki M, Chapman B, Hofmann O, McEwen R, *et al.* VarDict: a novel and versatile variant caller for next-generation sequencing in cancer research. *Nucleic Acids Research* **2016**;44(11):e108-e doi 10.1093/nar/gkw227.
33. Rosenthal R, McGranahan N, Herrero J, Taylor BS, Swanton C. deconstructSigs: delineating mutational processes in single tumors distinguishes DNA repair deficiencies and patterns of carcinoma evolution. *Genome Biology* **2016**;17(1):31 doi 10.1186/s13059-016-0893-4.
34. Andor N, Graham TA, Jansen M, Xia LC, Aktipis CA, Petritsch C, *et al.* Pan-cancer analysis of the extent and consequences of intratumor heterogeneity. *Nature Medicine* **2015**;22:105 doi 10.1038/nm.3984
<https://www.nature.com/articles/nm.3984#supplementary-information>.
35. Mermel CH, Schumacher SE, Hill B, Meyerson ML, Beroukhim R, Getz G. GISTIC2.0 facilitates sensitive and confident localization of the targets of focal somatic copy-number alteration in human cancers. *Genome Biology* **2011**;12(4):R41 doi 10.1186/gb-2011-12-4-r41.
36. Dang HX, White BS, Foltz SM, Miller CA, Luo J, Fields RC, *et al.* ClonEvol: clonal ordering and visualization in cancer sequencing. *Annals of Oncology* **2017**;28(12):3076-82 doi 10.1093/annonc/mdx517.
37. Curtis C, Shah SP, Chin S-F, Turashvili G, Rueda OM, Dunning MJ, *et al.* The genomic and transcriptomic architecture of 2,000 breast tumours reveals novel subgroups. *Nature* **2012**;486(7403):346-52 doi <http://www.nature.com/nature/journal/v486/n7403/abs/nature10983.html#supplementary-information>.
38. Carreira S, Romanel A, Goodall J, Grist E, Ferraldeschi R, Miranda S, *et al.* Tumor clone dynamics in lethal prostate cancer. *Science Translational Medicine* **2014**;6(254):254ra125 doi 10.1126/scitranslmed.3009448.
39. Romanel A, Tandefelt DG, Conteduca V, Jayaram A, Casiraghi N, Wetterskog D, *et al.* Plasma AR and abiraterone-resistant prostate cancer. *Sci Transl Med* **2015**;7(312):312re10 doi 10.1126/scitranslmed.aac9511.
40. Prandi D, Baca S, Romanel A, Barbieri C, Mosquera J-M, Fontugne J, *et al.* Unraveling the clonal hierarchy of somatic genomic aberrations. *Genome Biology* **2014**;15(8):439.

41. Boeva V, Popova T, Lienard M, Toffoli S, Kamal M, Le Tourneau C, *et al.* Multi-factor data normalization enables the detection of copy number aberrations in amplicon sequencing data. *Bioinformatics* **2014**:btu436.
42. Newman AM, Lovejoy AF, Klass DM, Kurtz DM, Chabon JJ, Scherer F, *et al.* Integrated digital error suppression for improved detection of circulating tumor DNA. *Nat Biotech* **2016**;advance online publication doi 10.1038/nbt.3520
<http://www.nature.com/nbt/journal/vaop/ncurrent/abs/nbt.3520.html#supplementary-information>.

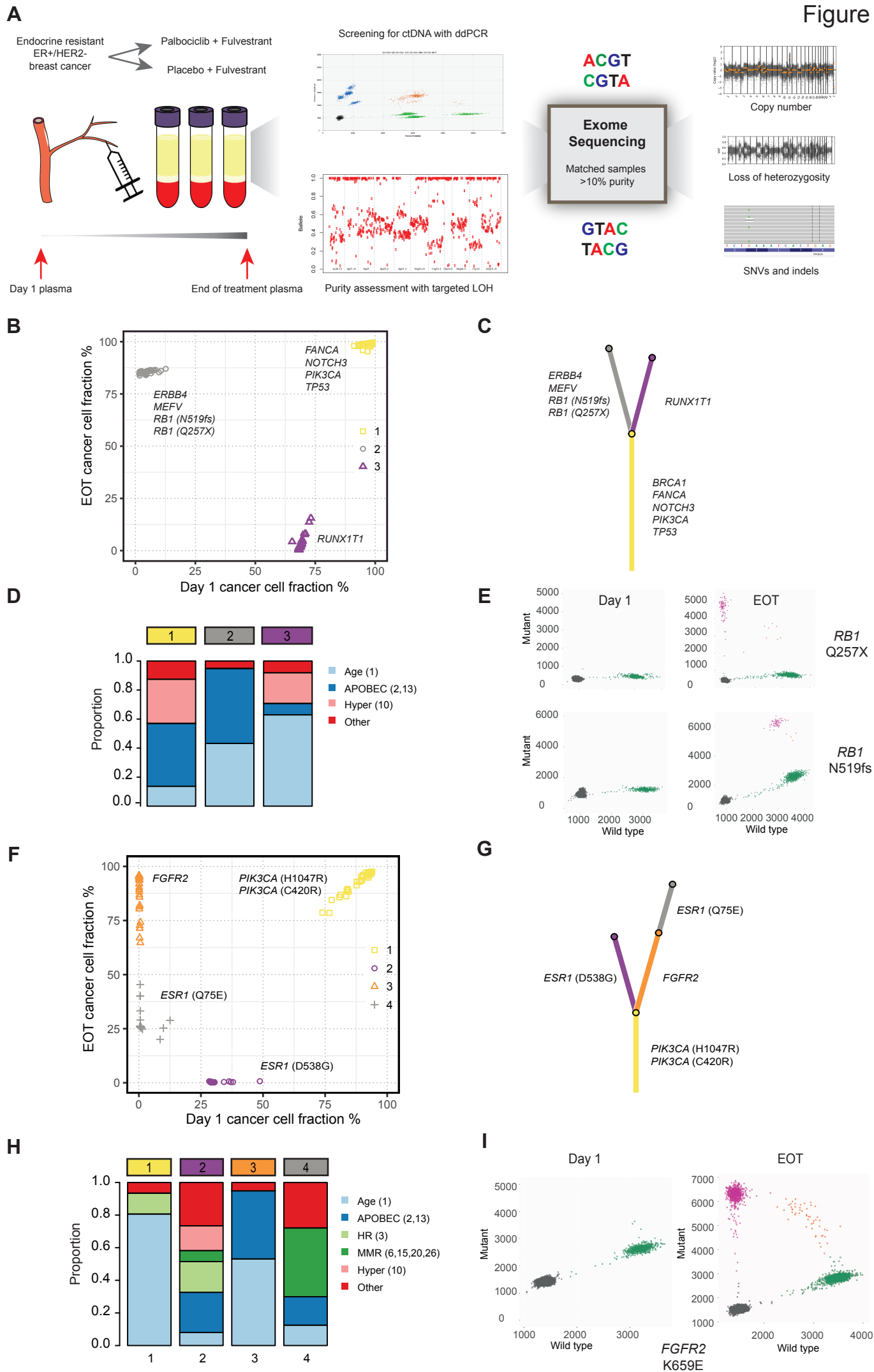


Figure 2

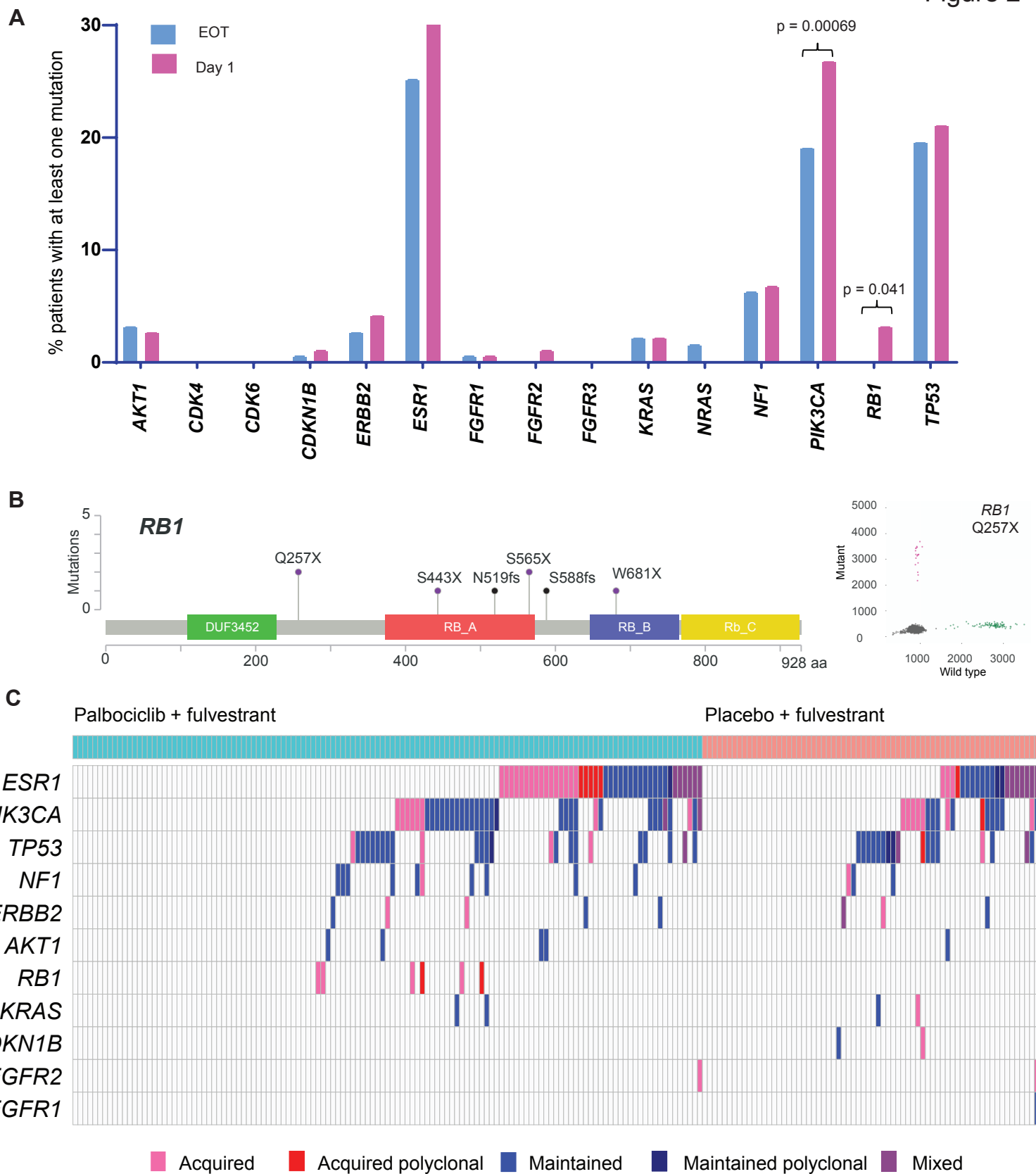
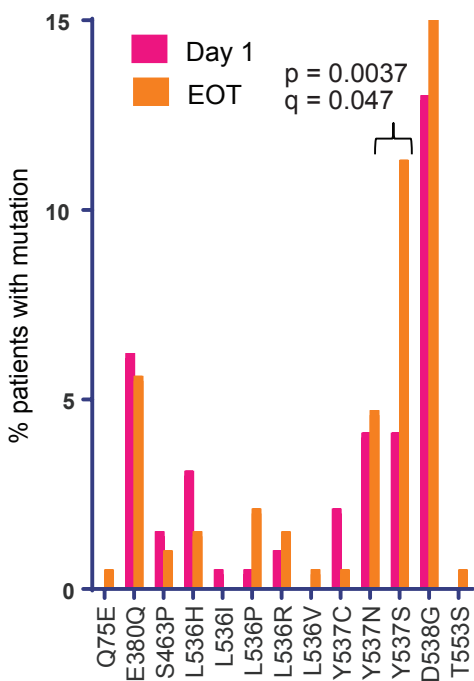
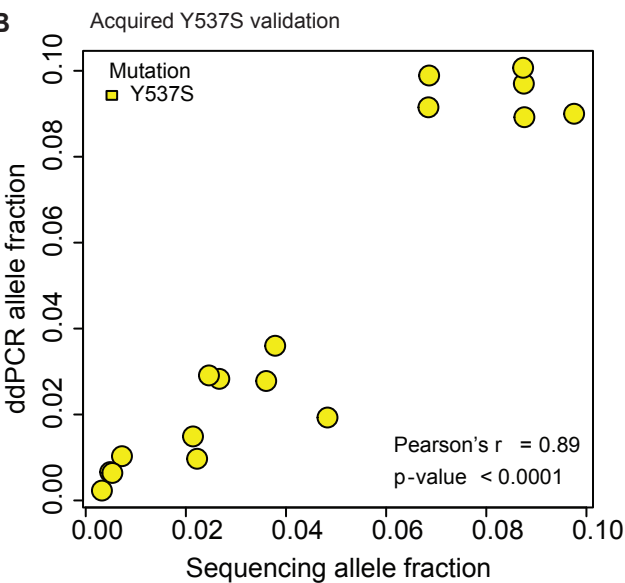


Figure 3

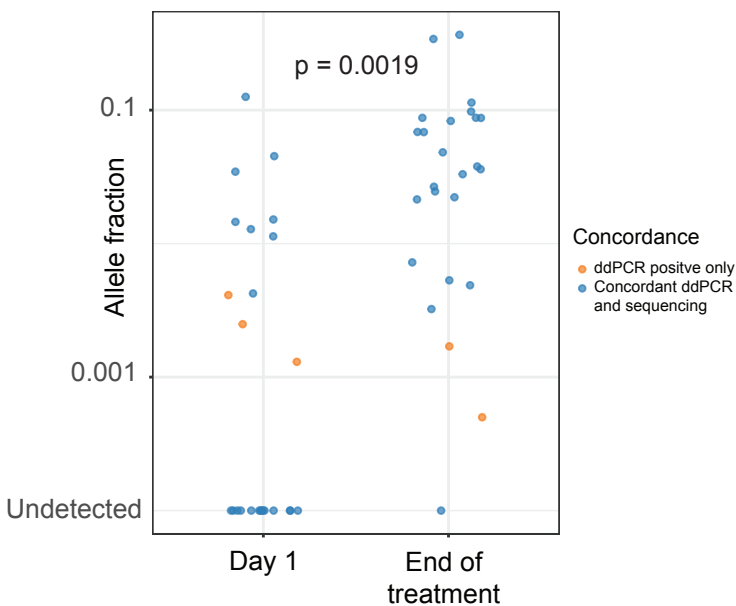
A



B



C



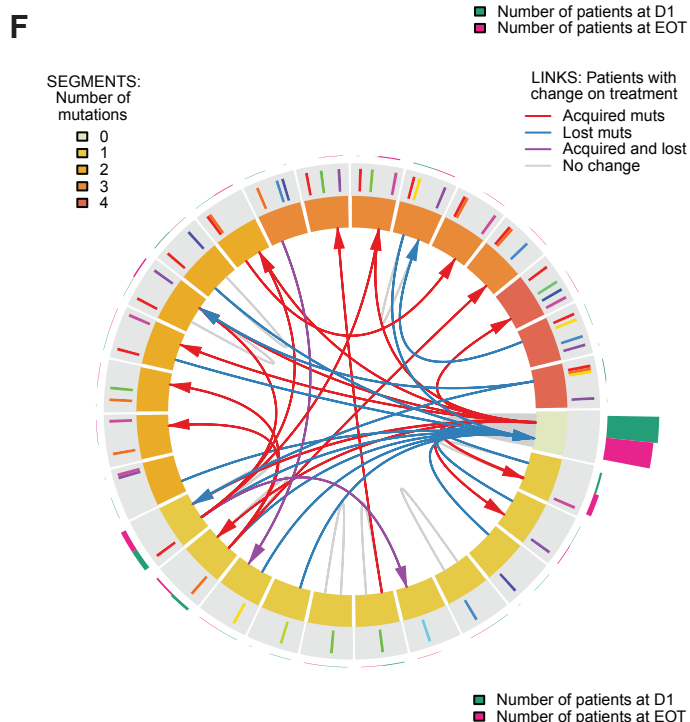
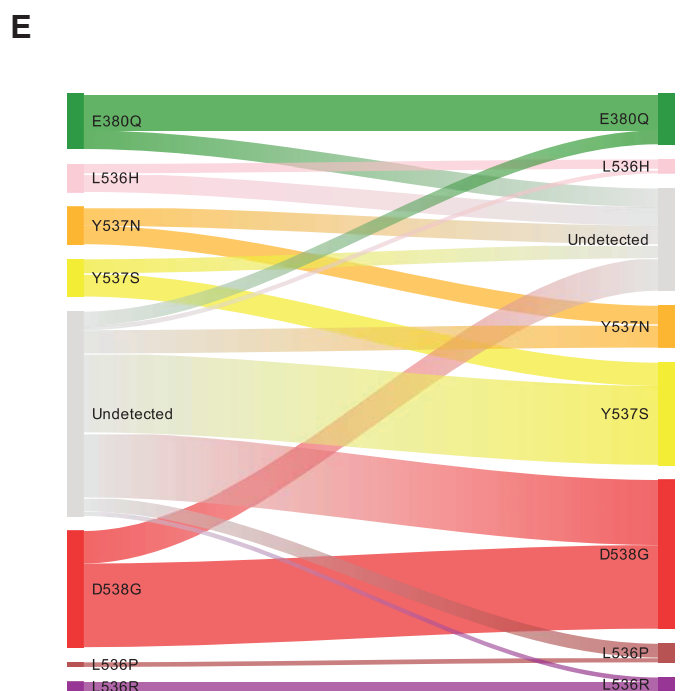
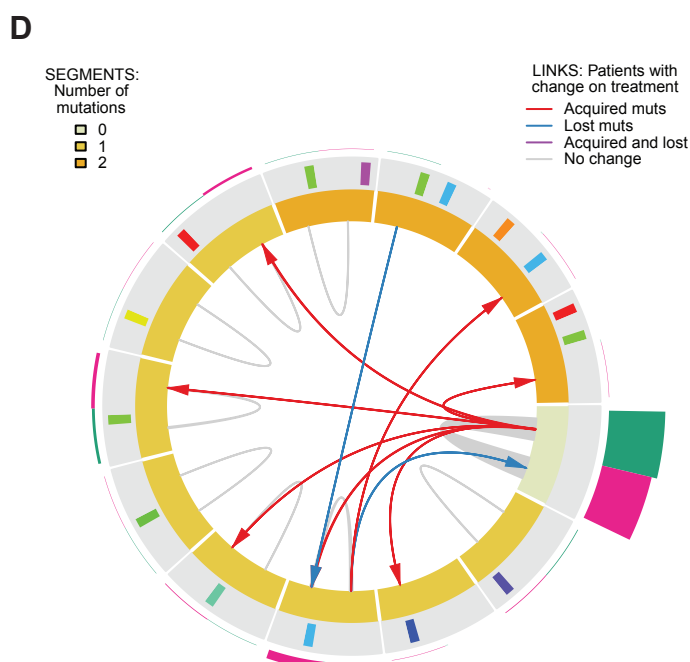
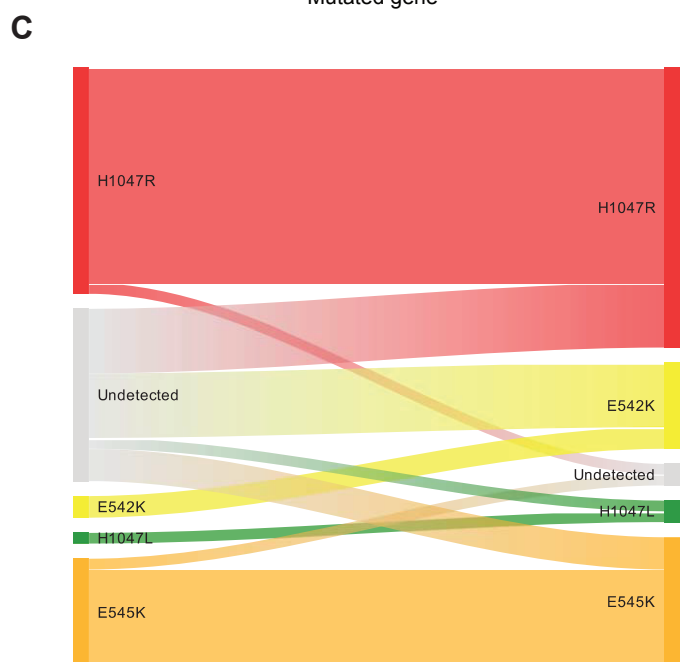
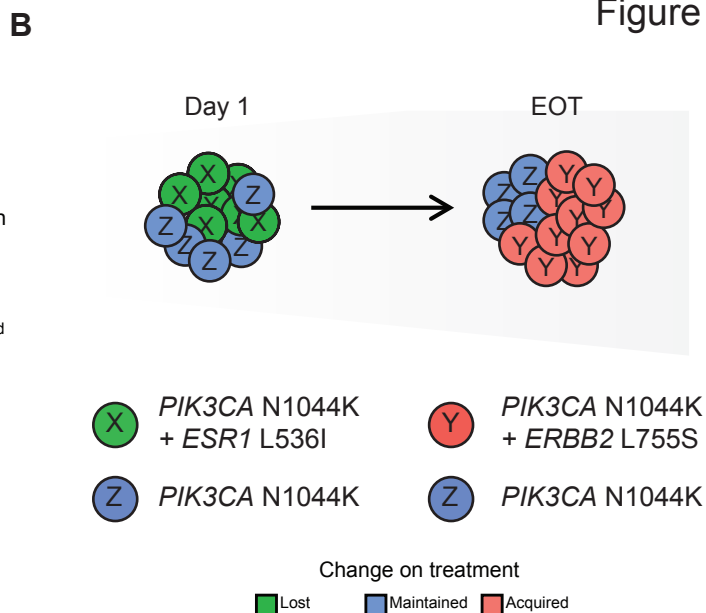
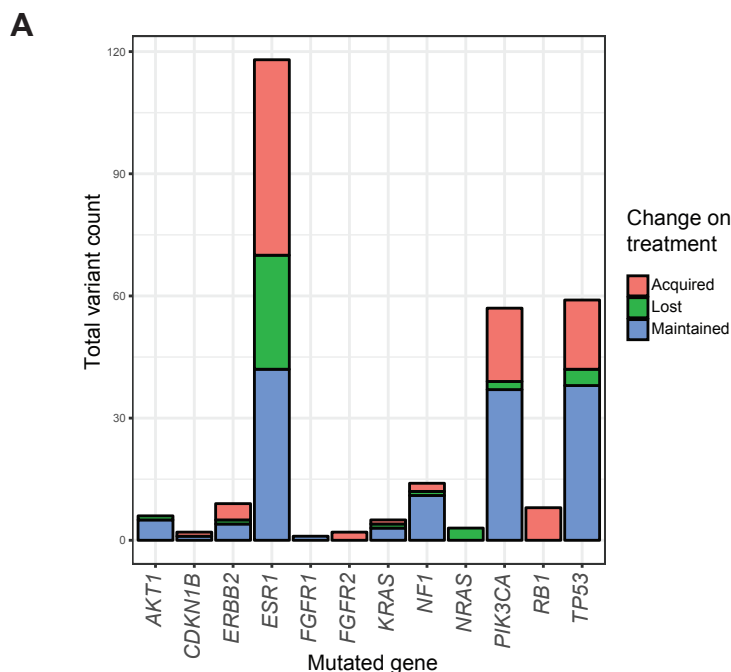
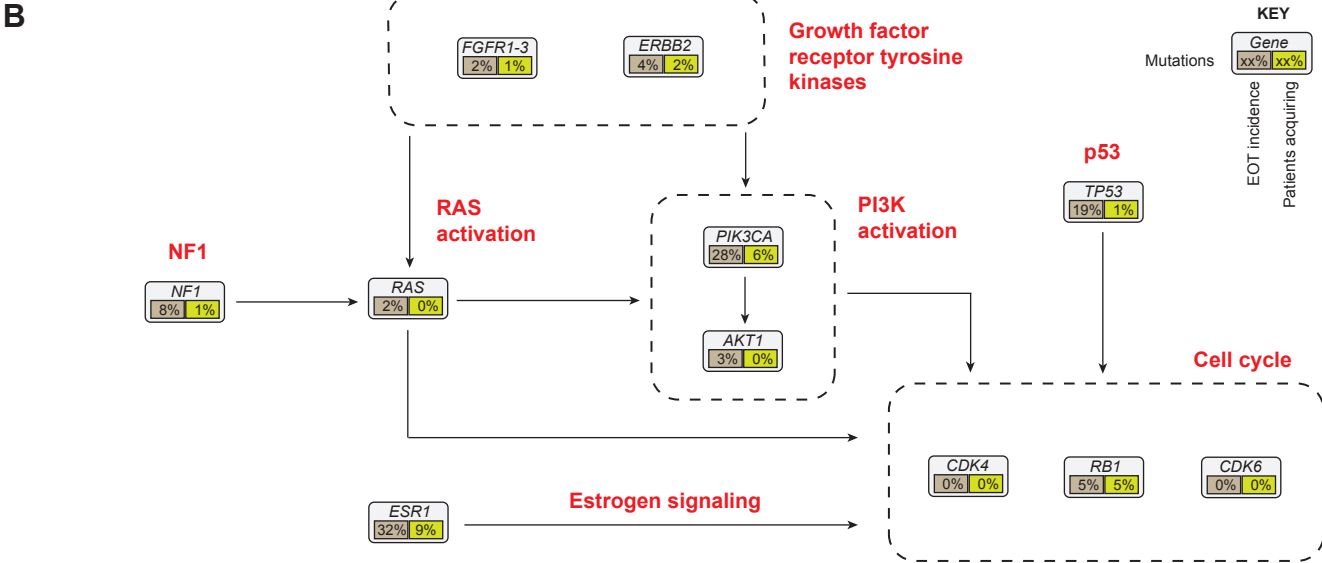
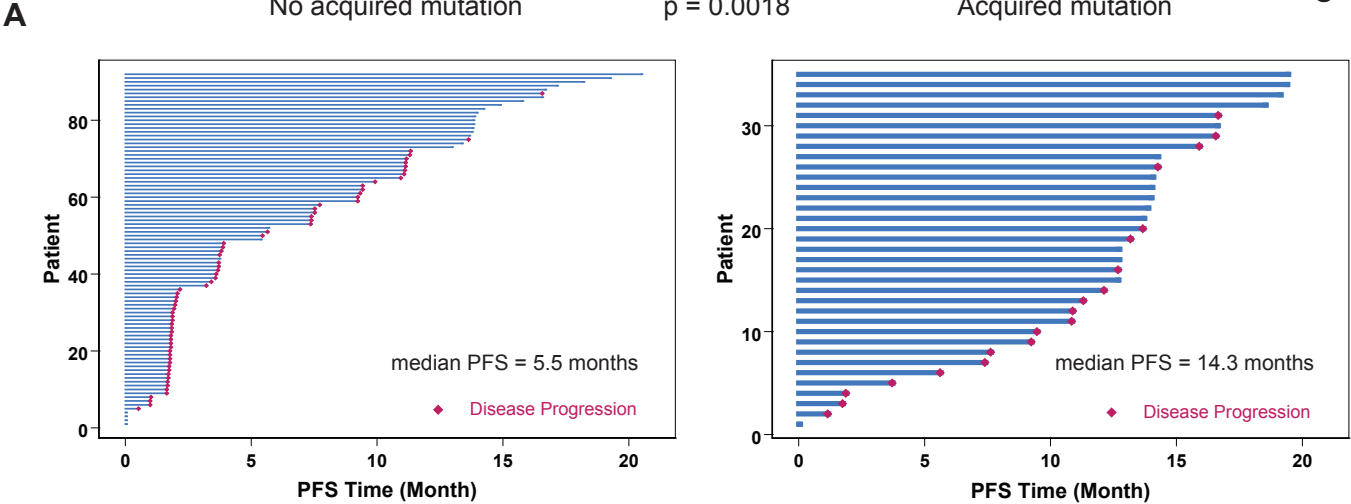
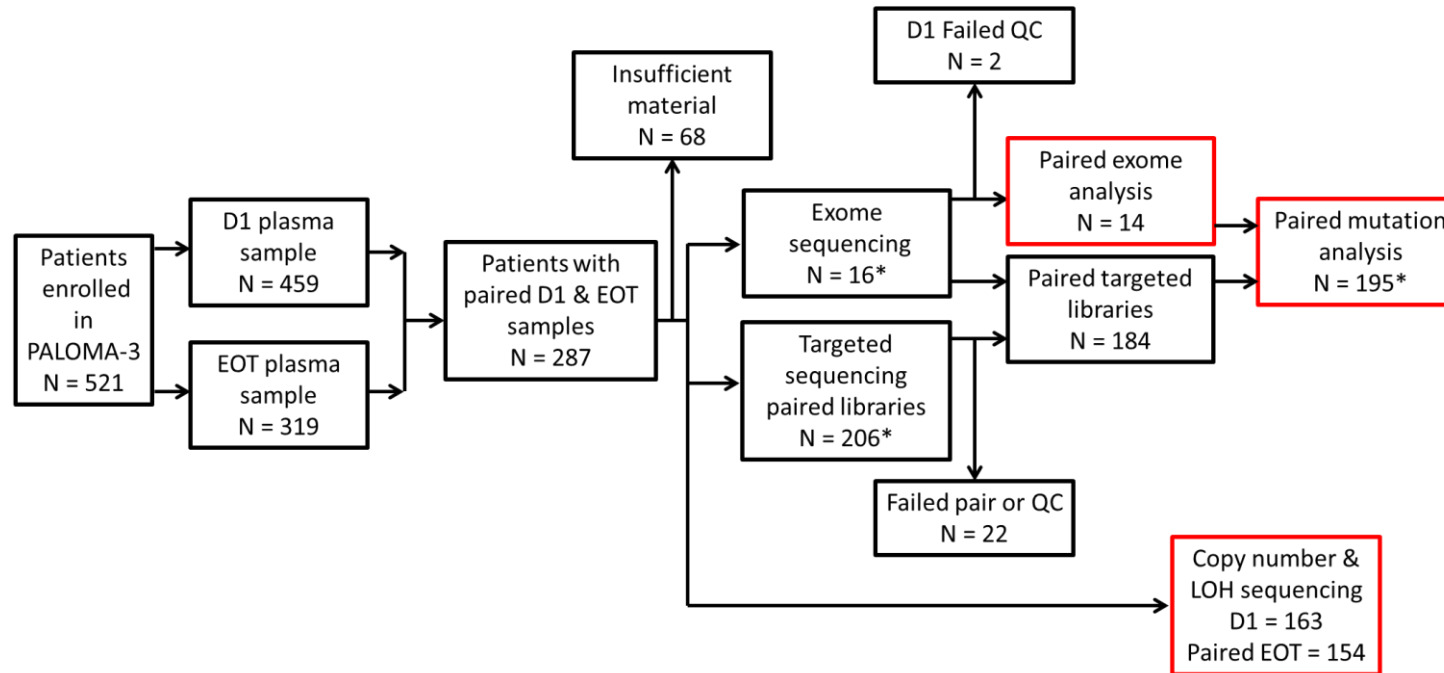


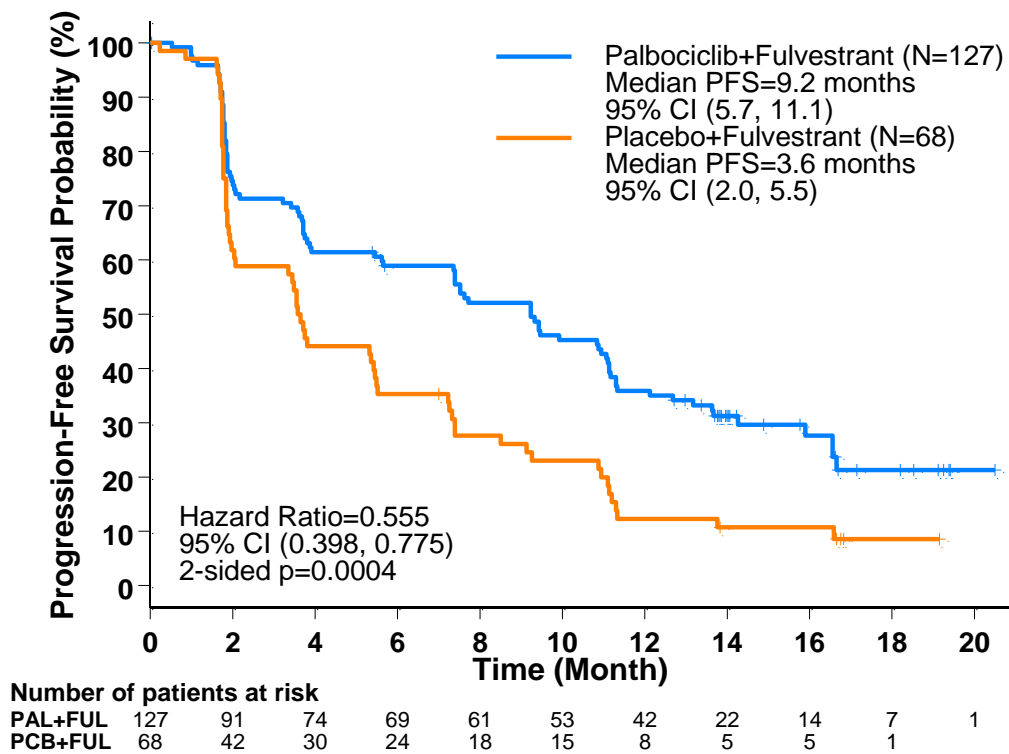
Figure 5



Supplementary figures



Supplementary figure 1. CONSORT diagram showing availability of patient plasma samples, and subsequent sequencing analyses. Presented analyses are in red. Paired mutation analysis included data from the targeted panel genes found in the exome sequencing cohort. D1 – day 1, EOT – End of treatment, QC – Quality control, LOH – Loss of heterozygosity. *Note 3 patients underwent both paired exome sequencing and targeted sequencing.



Supplementary figure 2. Kaplan Meier curve showing progression free survival (PFS) curves for the subset of 195 patients with data from paired plasma samples at day 1 and end of treatment. HR – hazard ratio, CI – confidence interval, p value is log rank, PAL – Palbociclib, FUL – Fulvestrant, PCB - Placebo

CNV reference	Chr	Amplicons
ADORA3	1	18
INSIG2	2	16
EFHB	3	17
EIF4E	4	17
SMAD5	5	19
TERT	5	19
TMEM248	7	17
HNRPK	9	19
HOGA1	10	16
FOLH1	11	19
OR8S1	12	17
ATP12A	13	20
RPPH1	14	16
TTC5	14	18
ANXA2	15	19
EFTUD2	17	19
AQP4-AS1	18	19
XRN2	20	16
SCAF4	21	19
Total		340

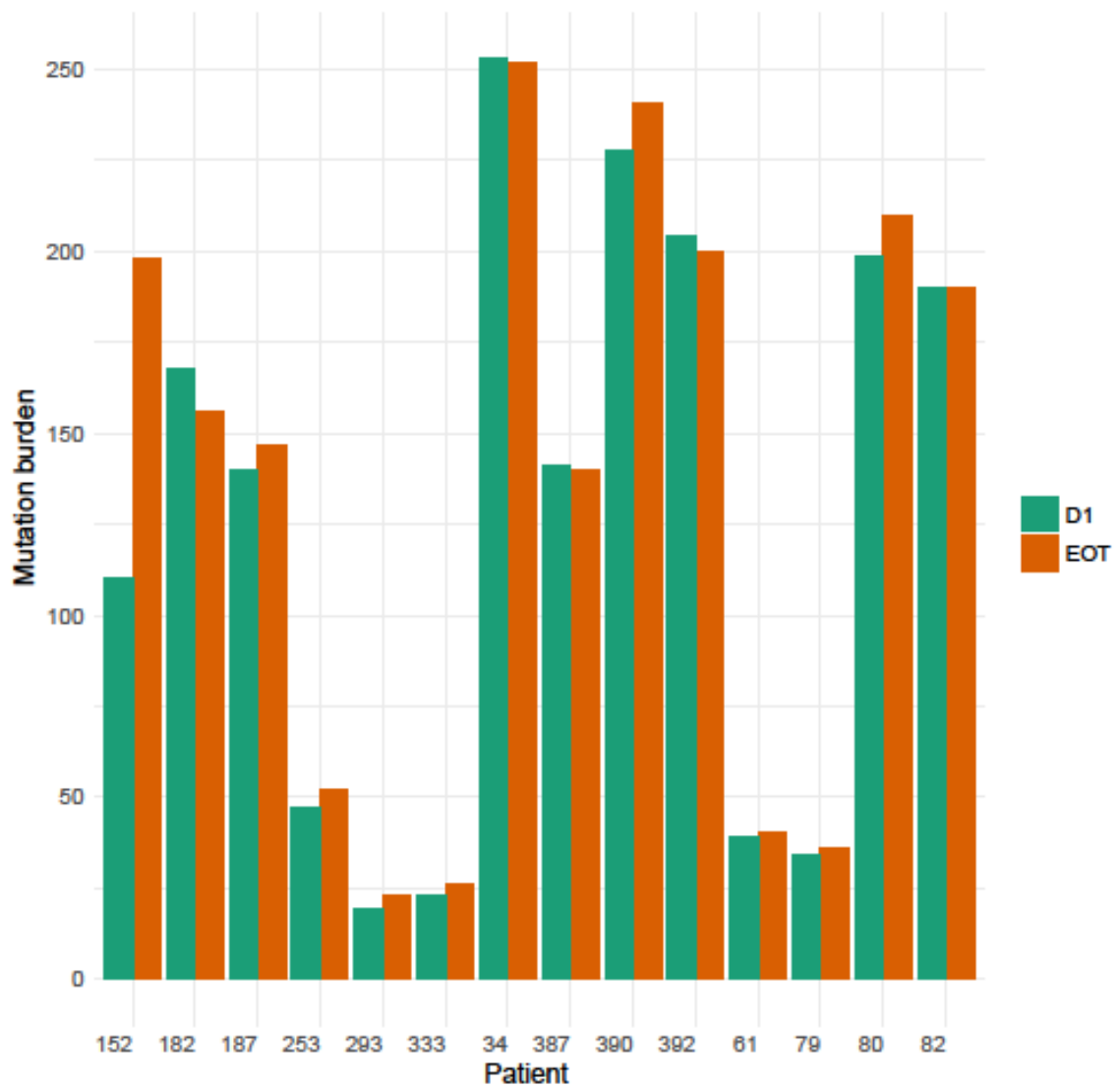
CNV target	Chr	Amplicons
<i>HER2</i>	17q12	22
<i>EGFR</i>	7p11	18
<i>FGFR1</i>	8p11	19
<i>FGFR2</i>	10q26	16
<i>PIK3CA</i>	3q26	20
<i>CDK4</i>	12q14	21
<i>CCND1</i>	11q13	17
<i>CCNE1</i>	19q12	23
<i>ESR1</i>	6q25	22
<i>MYC</i>	8q24	21
<i>MCL1</i>	1	16
Total		215

SNP regions	SNPs	Prevalence (%)
16q24.3	103	54
17p12	102	49
8p23.2	97	48
11q23.3	110	41
22q13.31	104	36
1p36.13	106	29
6q27	108	28
3p21.31	97	26
Total	827	

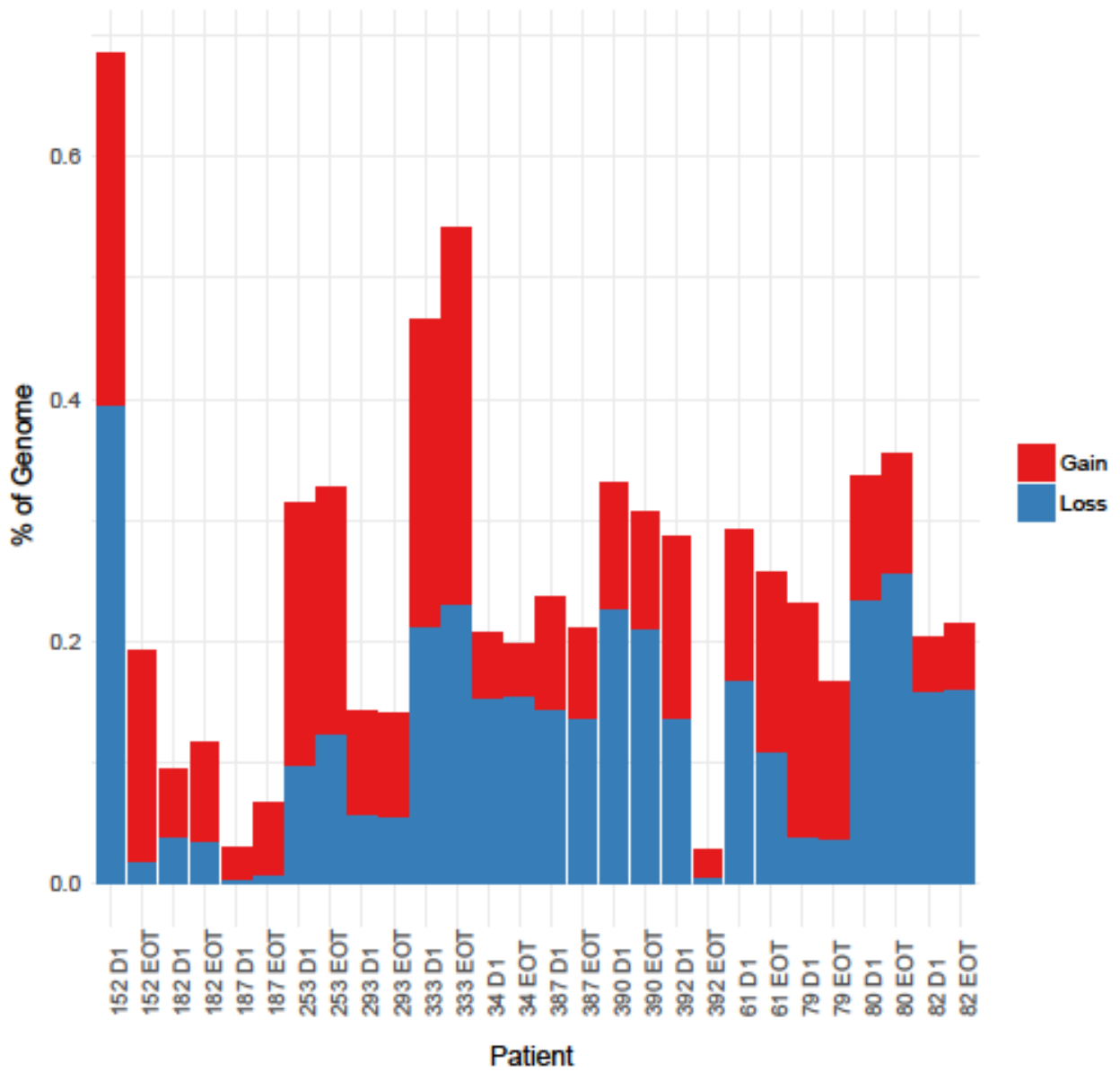
SNP genes	Chr	Amplicons
<i>RB1</i>	13	119
<i>CDKN2A</i>	9	134
<i>PTEN</i>	10	128
Total		381

Summary		Amplicons
CNV targets	11	215
CNV reference	19	340
SNP genes	3	381
SNP regions	8	827
Total		1763

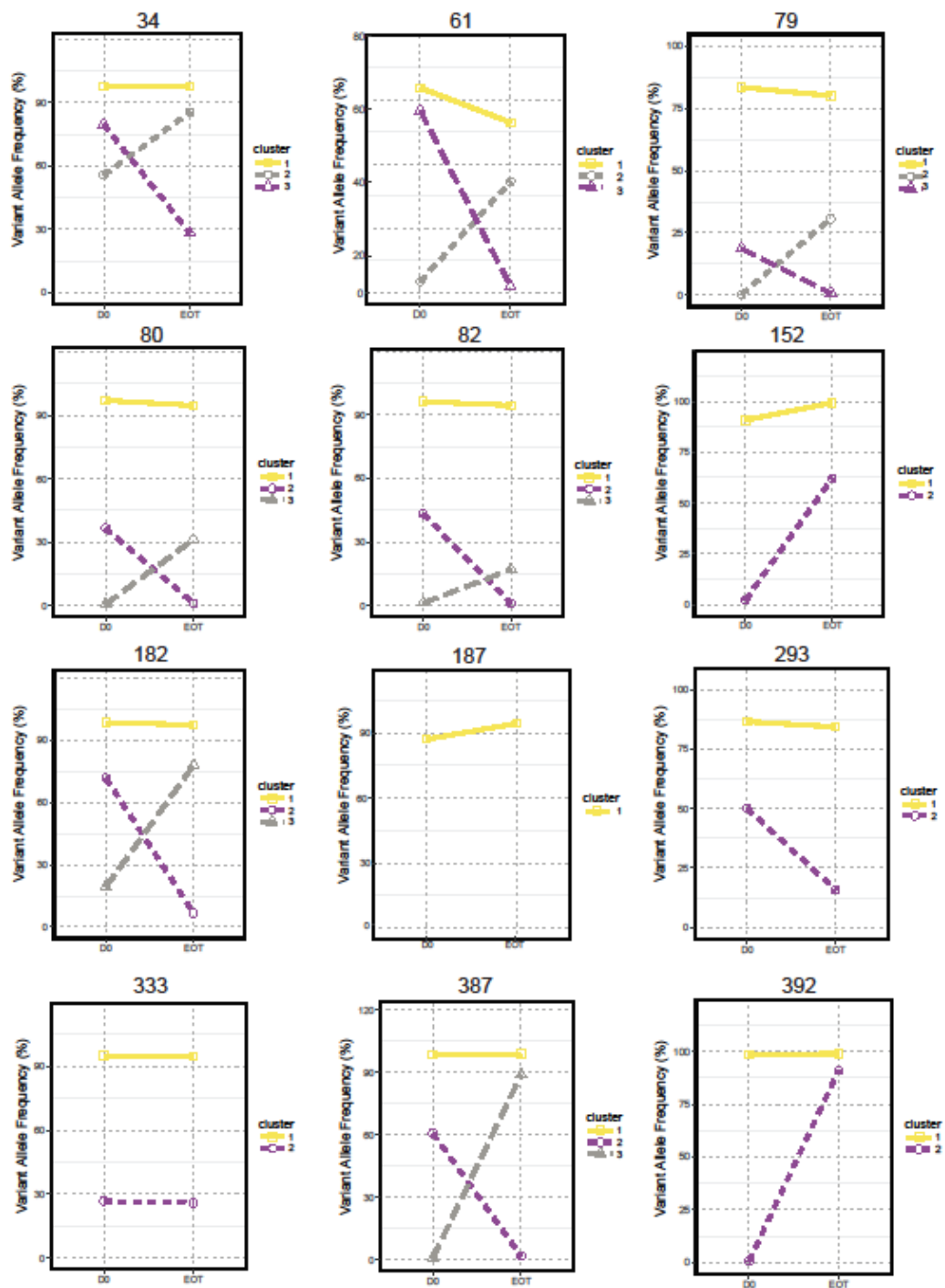
Supplementary figure 3. The genes and genomic regions of the purity panel. Blue – Reference genes. Red – Genes for assessment through normalized read count for loss or gain. Green – Genes to be assessed for loss through a combination of normalized read count and loss of heterozygosity, amplicons located such as to include single nucleotide polymorphisms with a population prevalence > 20%. Yellow – Chromosomal regions commonly lost in breast cancer to be assessed in the same manner as the genes in green.



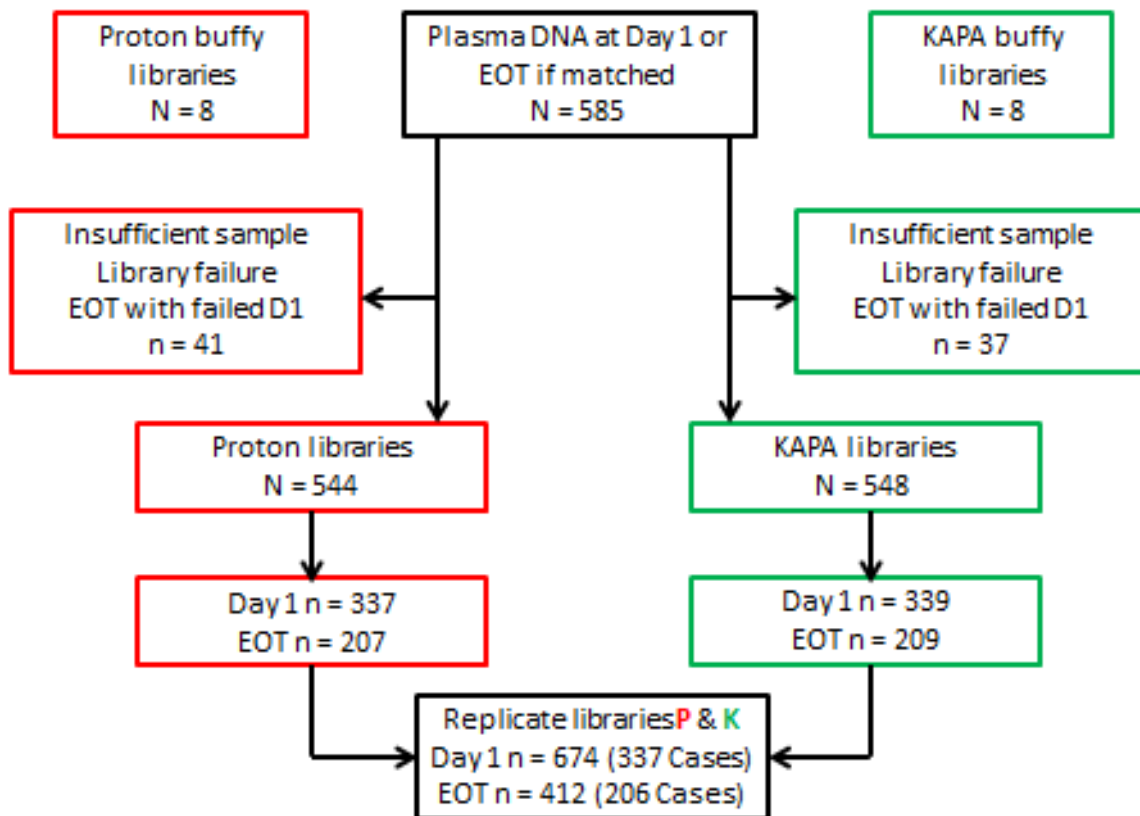
Supplementary figure 4. Mutation burden in circulating tumour DNA at day 1 and end of treatments for patients with paired exome sequencing. D1 – day 1, EOT – End of treatment.



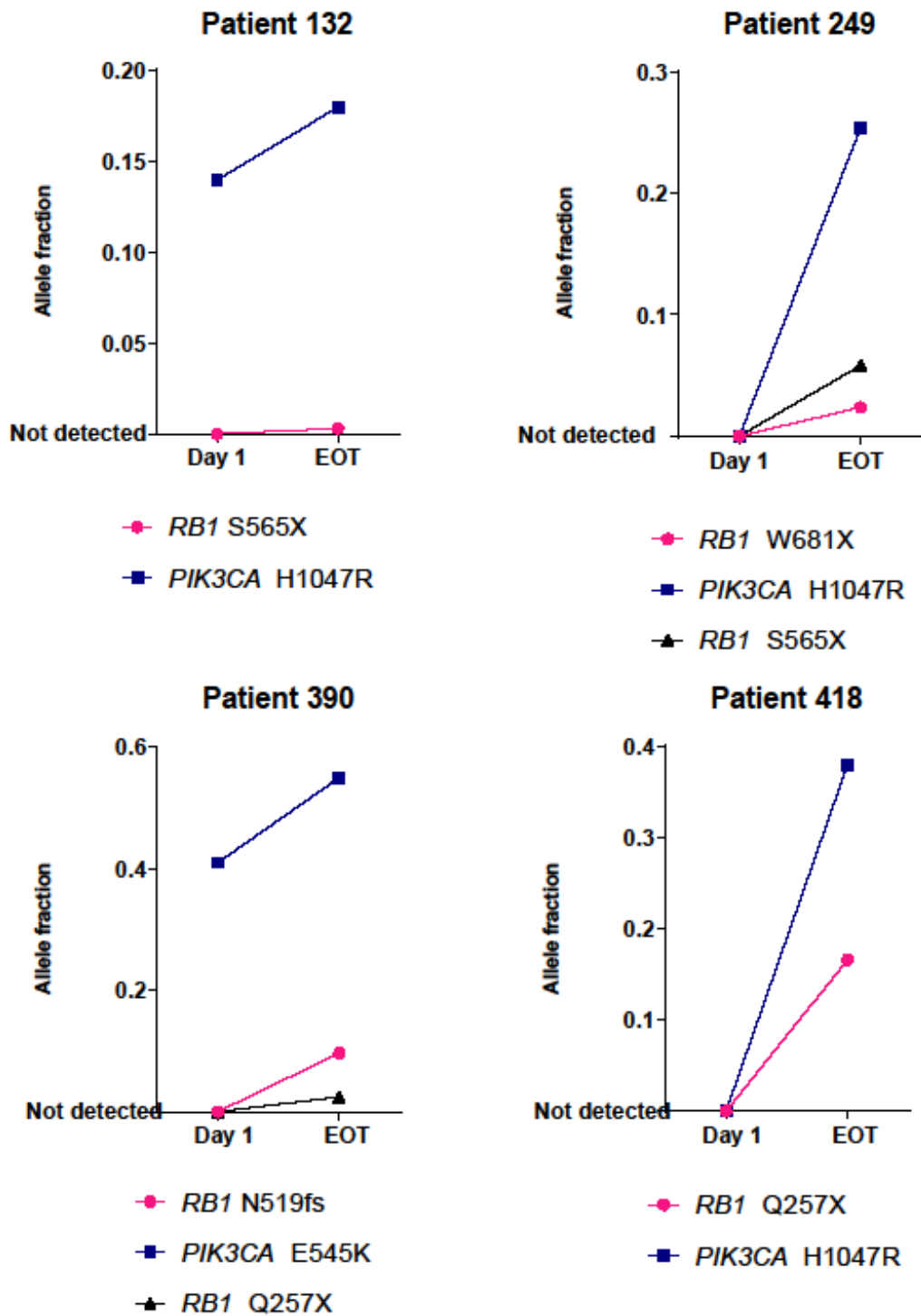
Supplementary figure 5. Percentage of metagenome affected by single copy gains/losses in patients with paired exome sequencing. D1 – day 1, EOT – End of treatment.



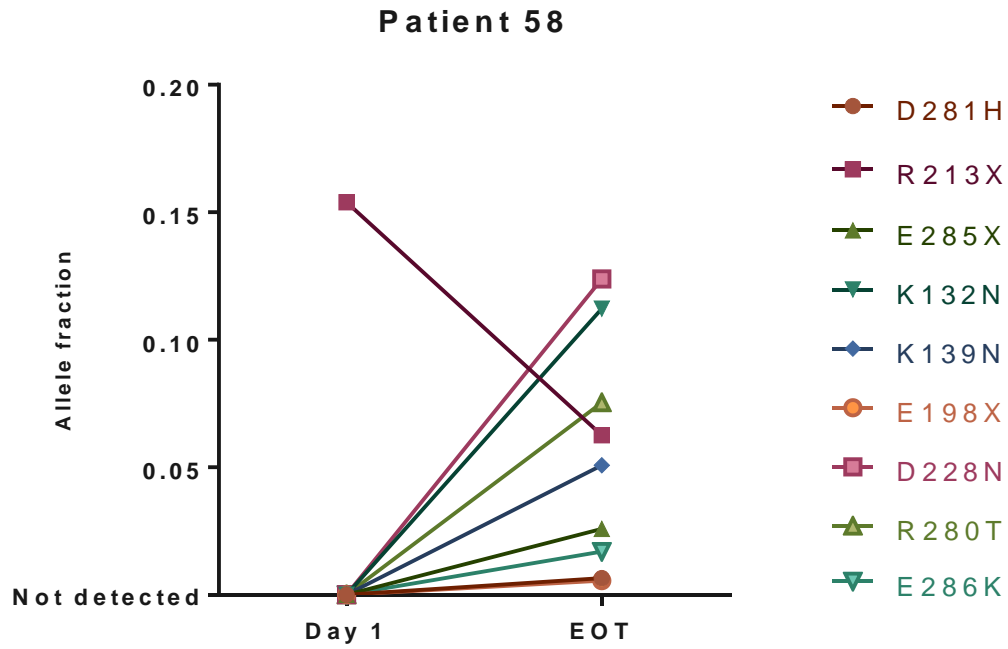
Supplementary figure 6. Clonal analysis of samples with paired exome sequencing data using PyClone. Lines show sub clonal fraction between baseline and end of treatment where separate clones have been identified.



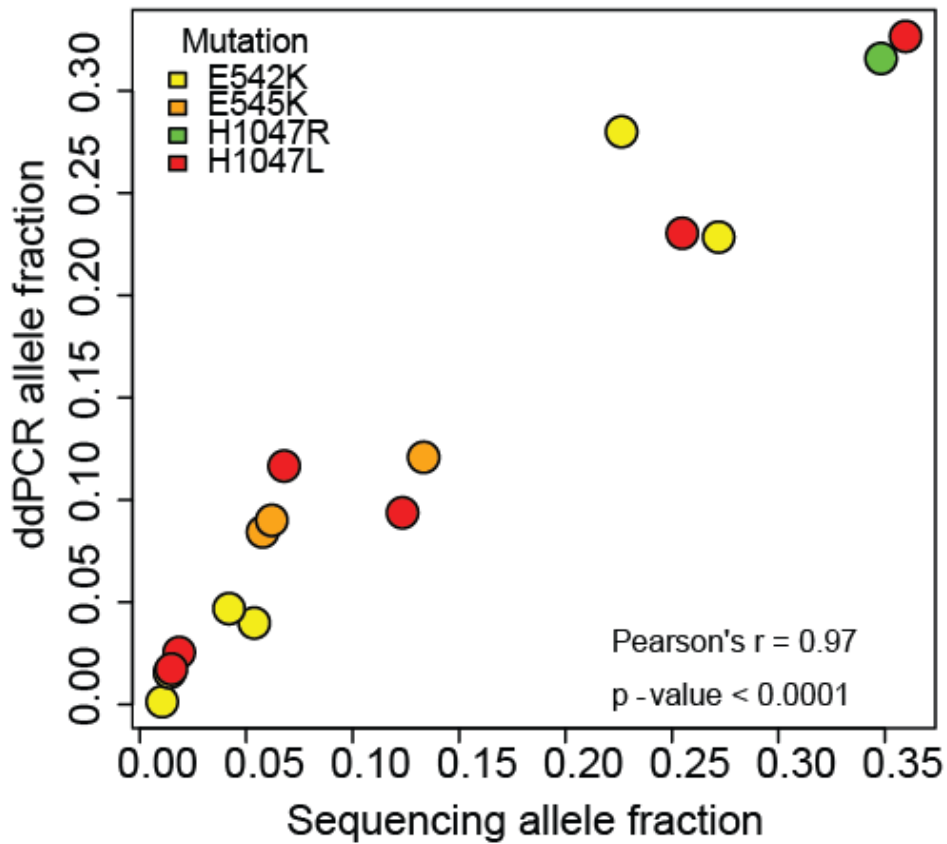
Supplementary figure 7. CONSORT diagram for sequencing of plasma DNA samples to reduce PCR and sequencing error. A total of 585 samples went into the library preparation workflow for both a Proton and a KAPA library. This yielded 206 patients with libraries for both sequencing platforms at both day 1 and end of treatment. Each DNA sample underwent two separate library preparations for each time point, such that one could be sequenced on a HiSeq2500, and one on the Proton, with a cross-comparison made to remove PCR and sequencing error. Only time points with both libraries passing QC were sequenced.



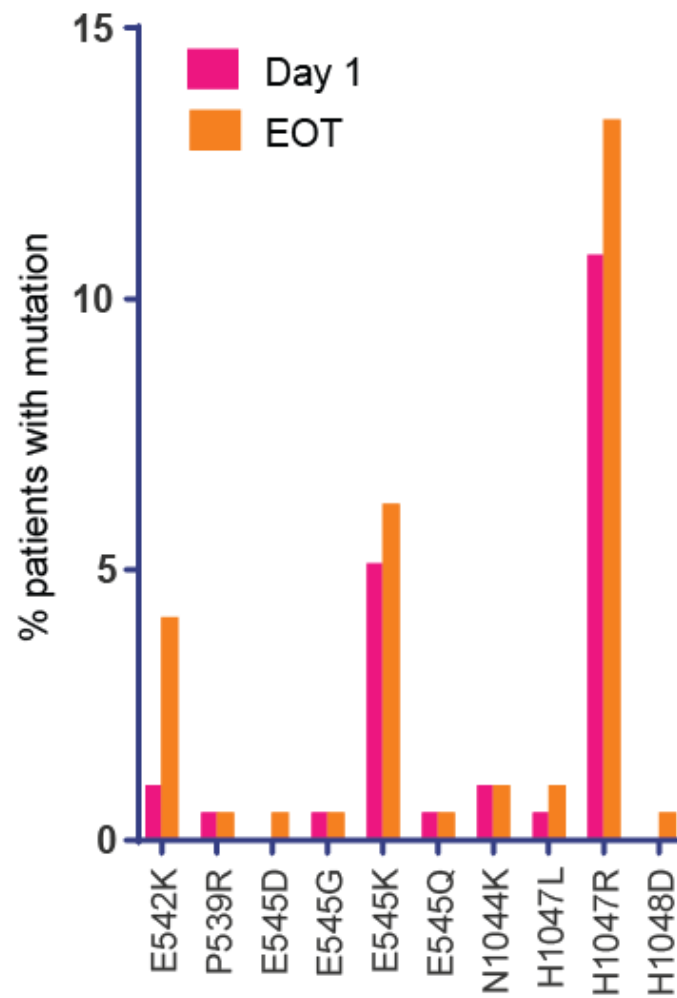
Supplementary figure 8. Allele fractions of emergent *RB1* mutations in the 4/6 samples also with a *PIK3CA* mutation, the consistently lower allele fraction of the *RB1* variants suggesting potentially sub clonal status.



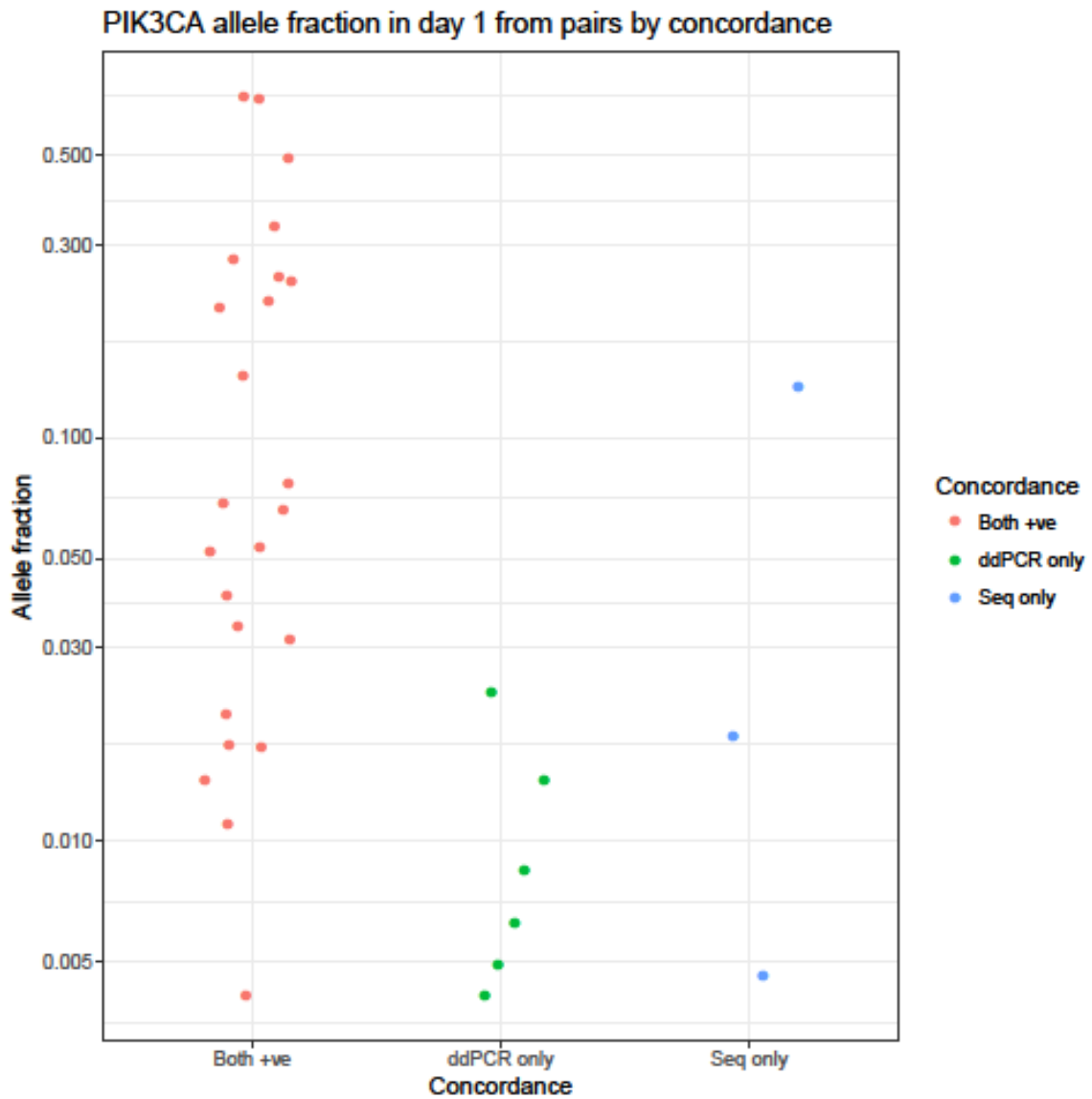
Supplementary figure 9. Allele fractions of multiple detected *TP53* variants in patient 58 between day 1 and end of treatment. Amino acid codes correspond to transcript NM_000546.



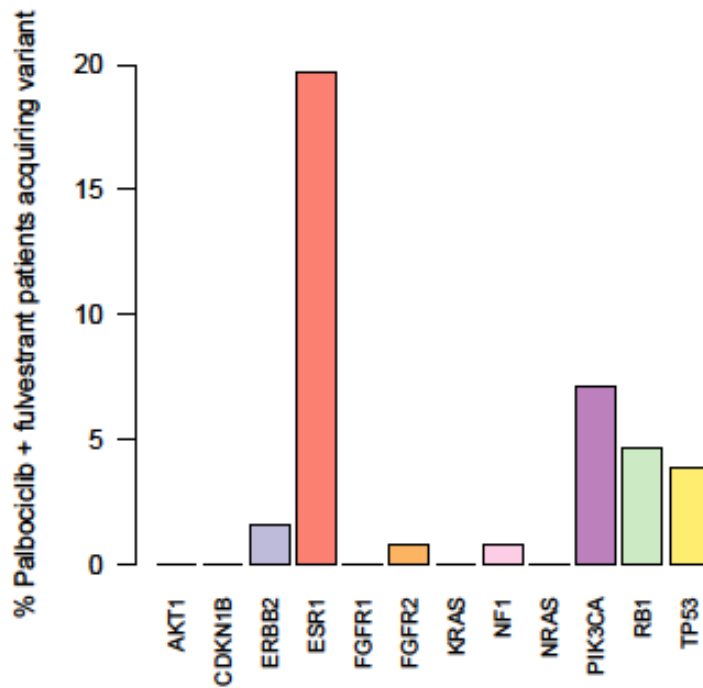
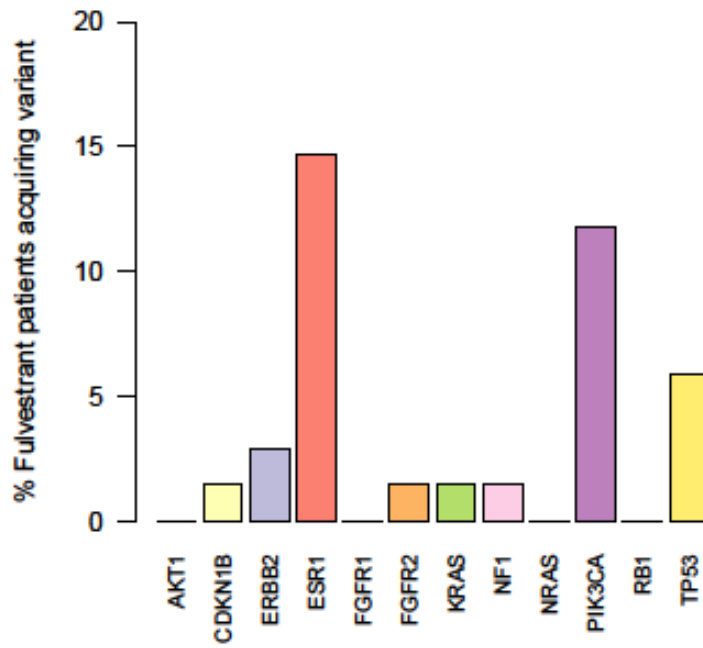
Supplementary figure 10. Validation of acquired mutation calls in *PIK3CA* from the paired ctDNA sequencing for H1047R, H1047L, E545K and E542K. 18 acquired mutations were identified in 17 patients from both treatment arms, one of these mutations in a patient who had a *PIK3CA* mutation at baseline and was found to have an additional one at the end of treatment. Of the 18 acquired mutations, 16 were H1047R, H1047L, E545K or E542K, all of these validating by ddPCR and showing close agreement with the sequencing allele fraction.



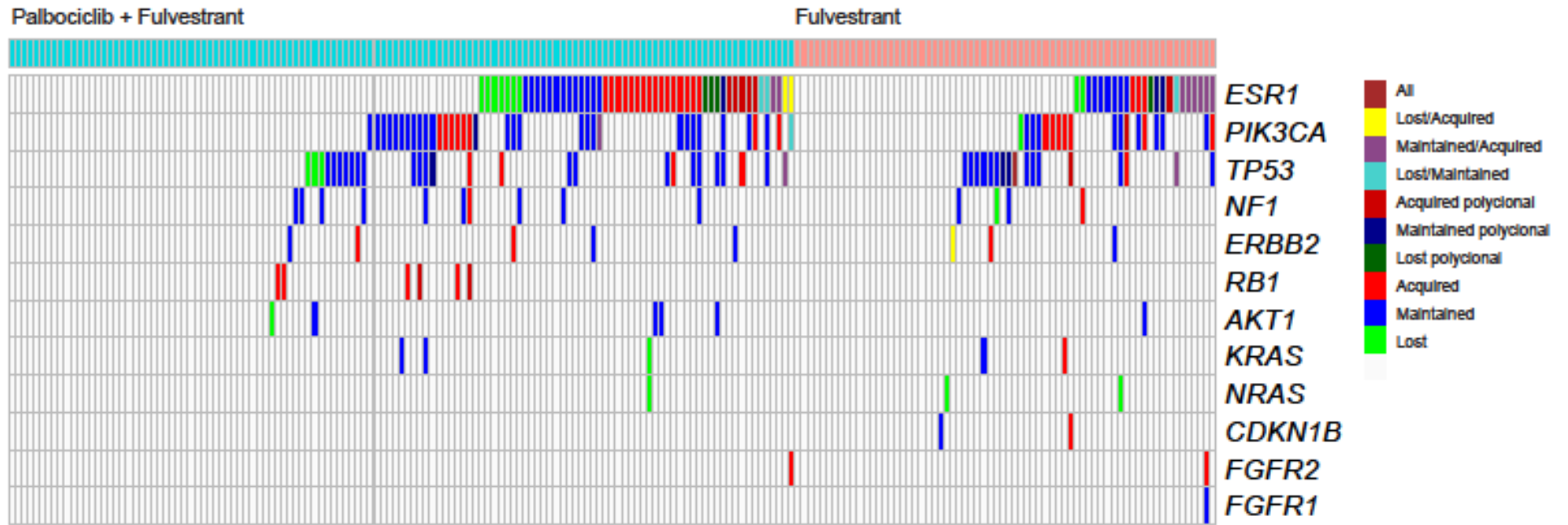
Supplementary figure 11. Difference in prevalence between specific *PIK3CA* mutations at day 1 and end of treatment in both treatment arms (n = 195). There was a significant increase in E542K ($p = 0.041$, McNemar's test with continuity correction) between day 1 and end of treatment, although this was not significant once a correction was made for multiple testing ($q = 0.41$, Bonferroni correction).



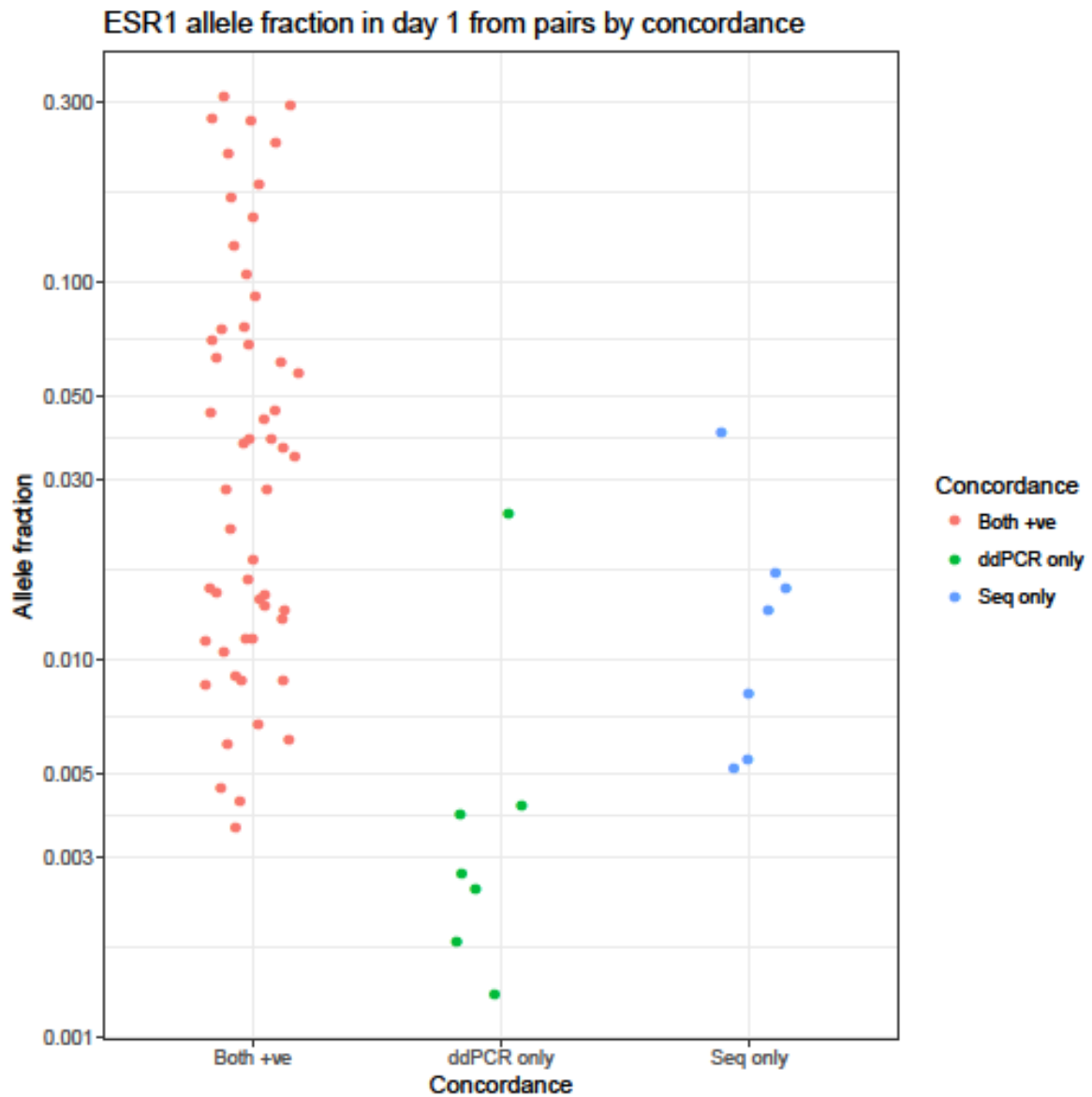
Supplementary figure 12. Concordance between baseline assessment of *PIK3CA* mutation between targeted sequencing and digital PCR. Comparison made for the *PIK3CA* mutations E542K, E545K, H1047R, H1047L. Excludes exome sequencing data. The 6 data points shown in green demonstrate mutation calls only made in the digital PCR data, representing 6/18 (33.3%) of mutations observed to be acquired in the paired sequencing.



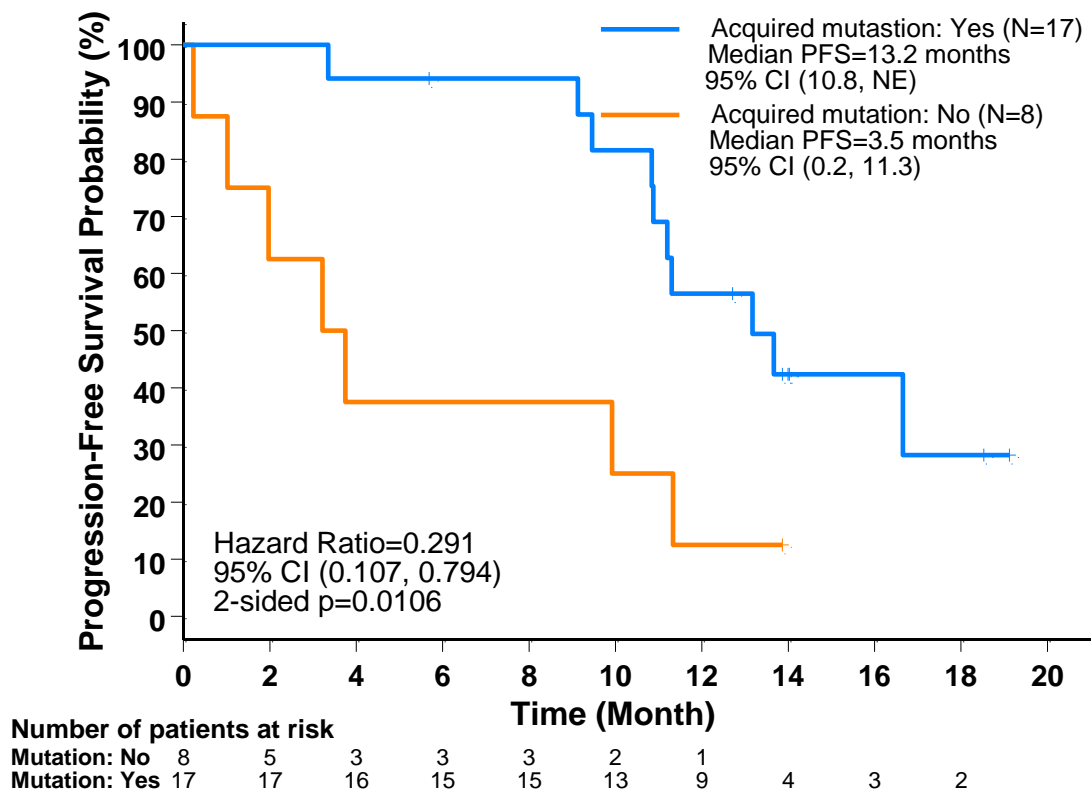
Supplementary figure 13. Percentage of patients acquiring a new mutation split between treatment arms. Upper panel – placebo + fulvestrant, lower panel – palbociclib +fulvestrant.



Supplementary figure 14. Mutations called in each patient by treatment. Squares per gene are colour coded to show the fate on treatment of subclones where more than one variant was identified at a single time point.

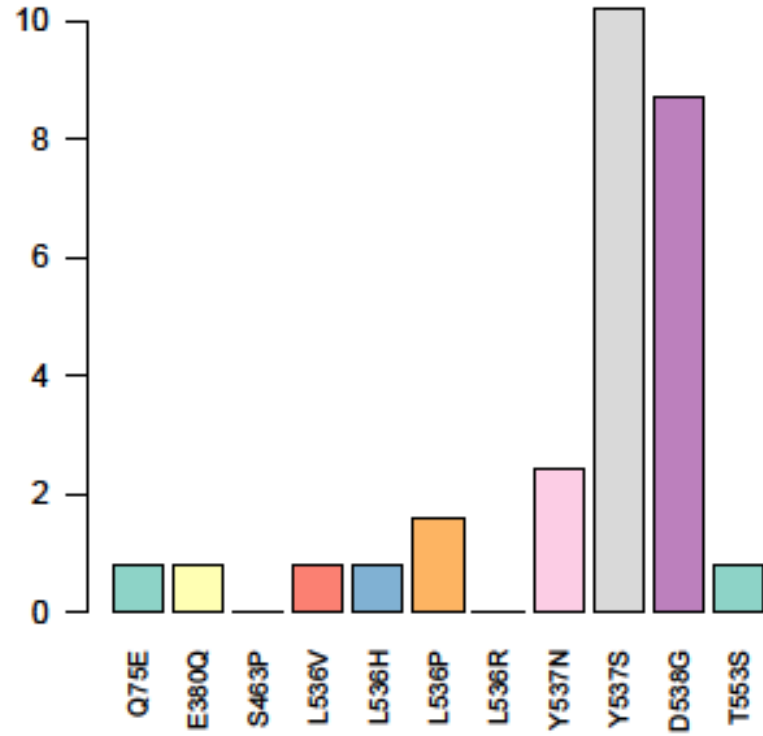


Supplementary figure 15. Concordance between baseline assessment of *ESR1* mutation between targeted sequencing and digital PCR. Comparison made for the *ESR1* mutations D538G, Y537S, Y537N, Y537C, L536R, S463P, E380Q. Excludes exome sequencing data.

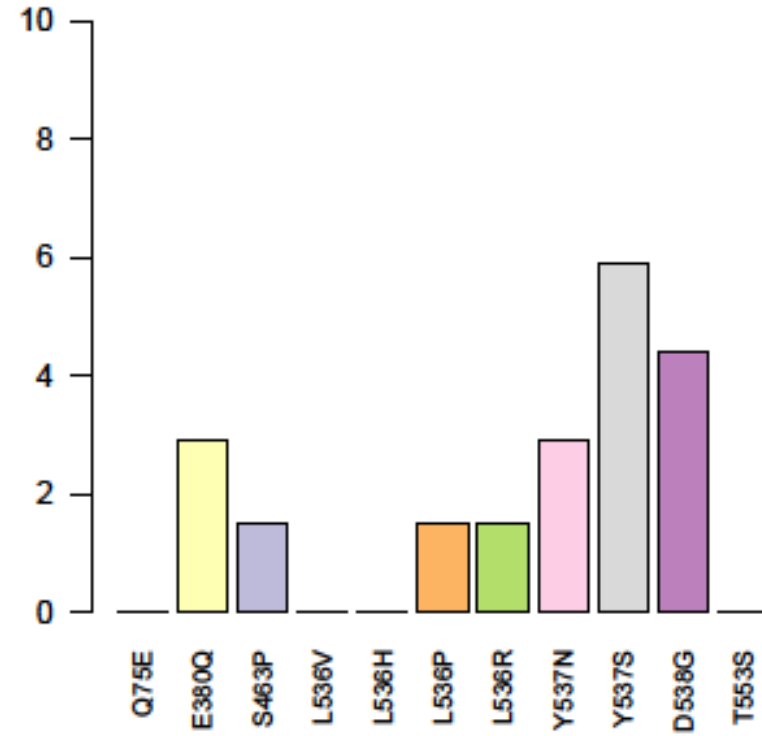


Supplementary figure 16. Kaplan Meier curve comparing the progression free survival in days between patients with a Y537S mutation at the start of treatment and patients without a Y537S mutation at the start of treatment who went on to acquire one by the end of treatment.

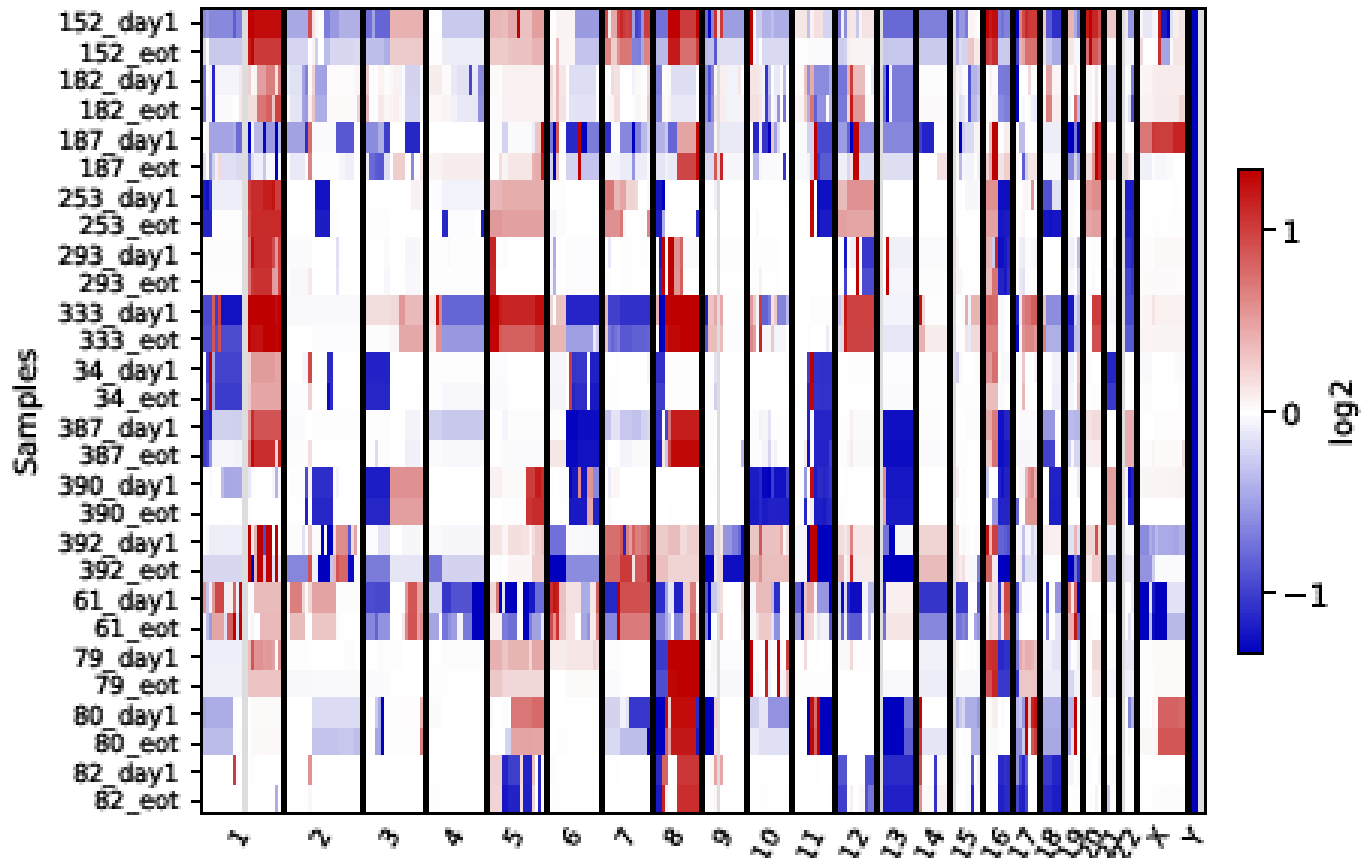
% Palbociclib + fulvestrant patients acquiring variant, n = 127



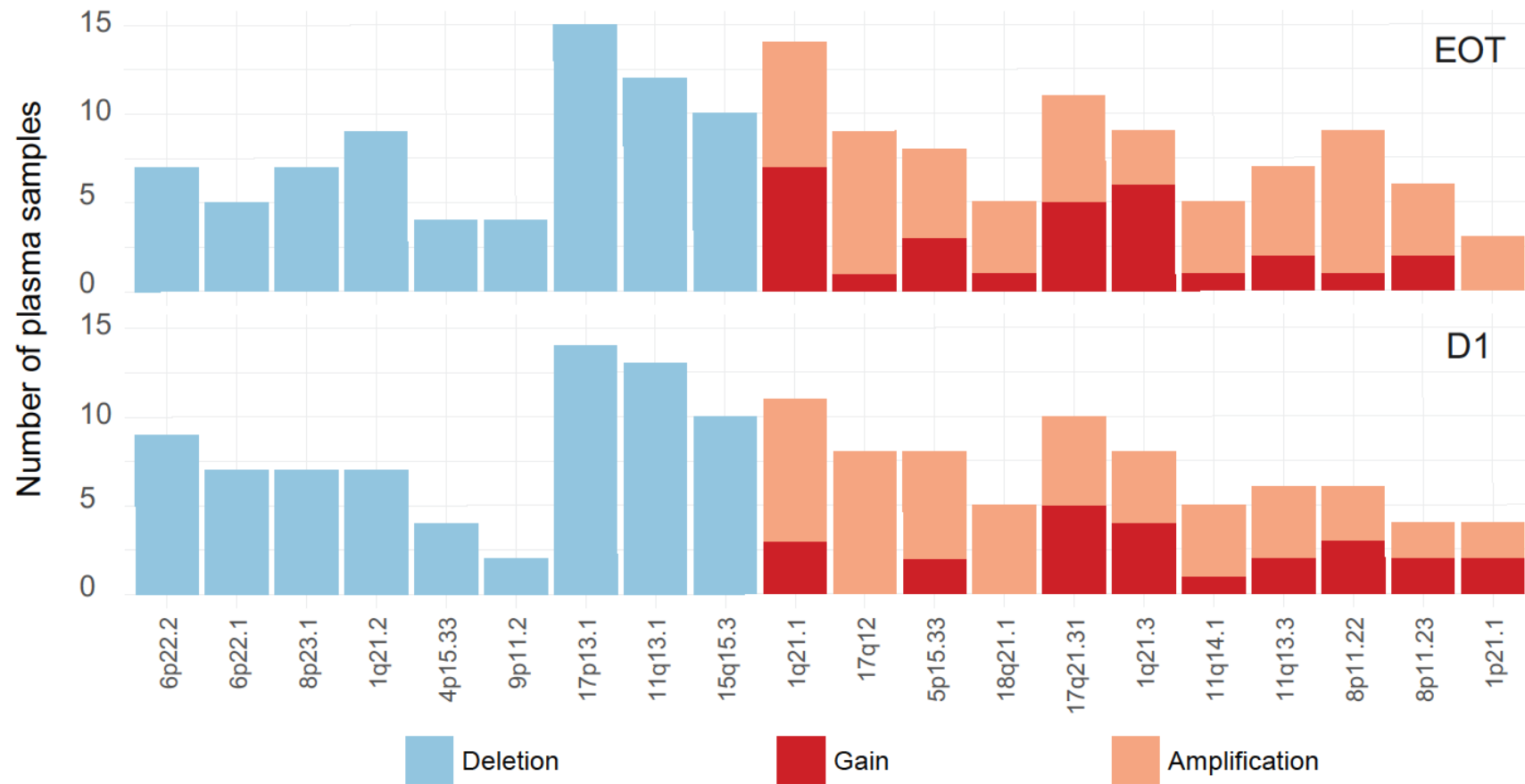
% Fulvestrant patients acquiring variant, n = 68



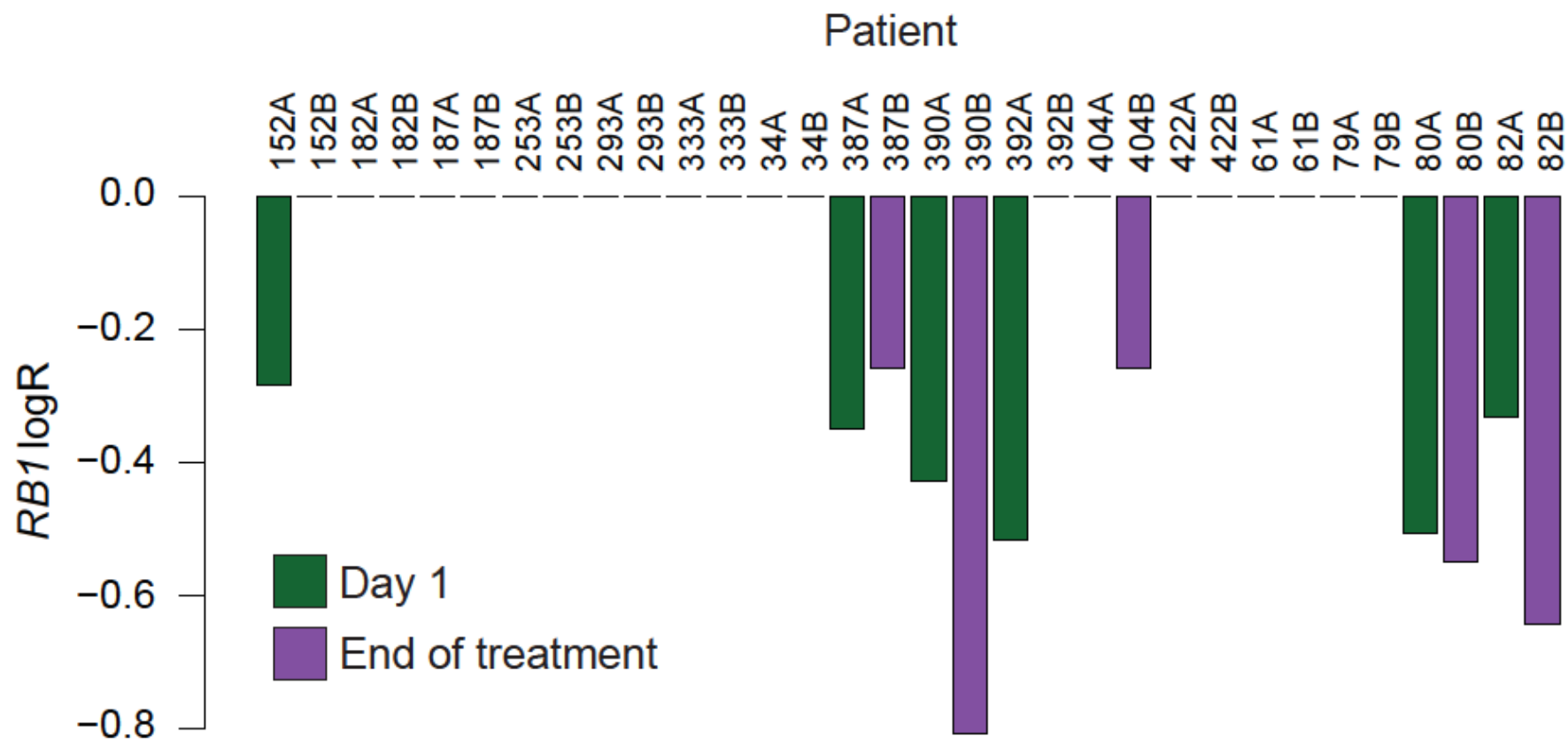
Supplementary figure 17. Percentages of specific *ESR1* mutations acquired in patients receiving palbociclib plus fulvestrant (n = 127) or placebo and fulvestrant (n = 68).



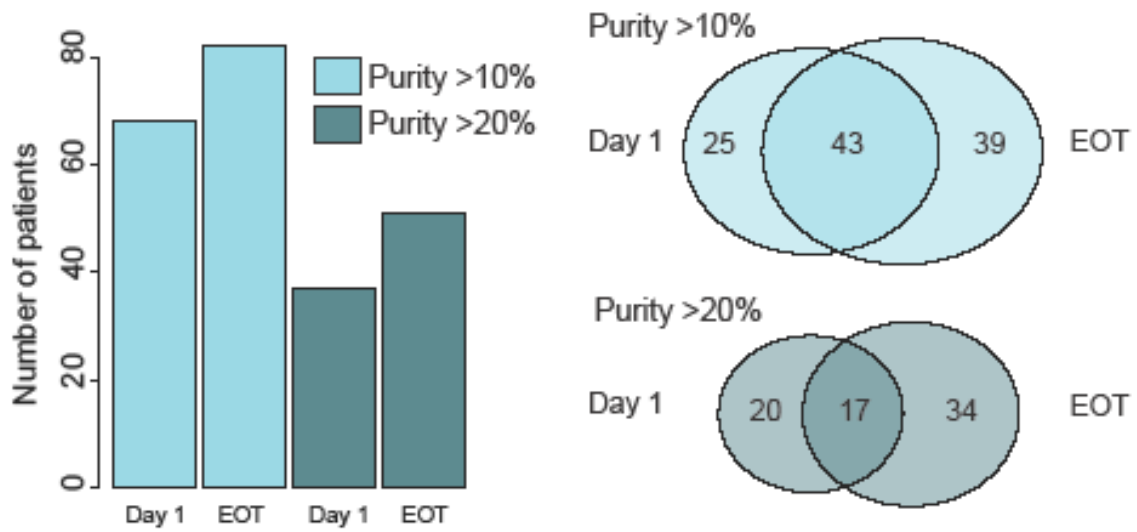
Supplementary figure 18. Copy number assessment comparison between day 1 and end of treatment (eot) from exome sequencing of plasma DNA for n = 14 patients receiving palbociclib plus fulvestrant showing stable copy number profiles adjusted for purity.



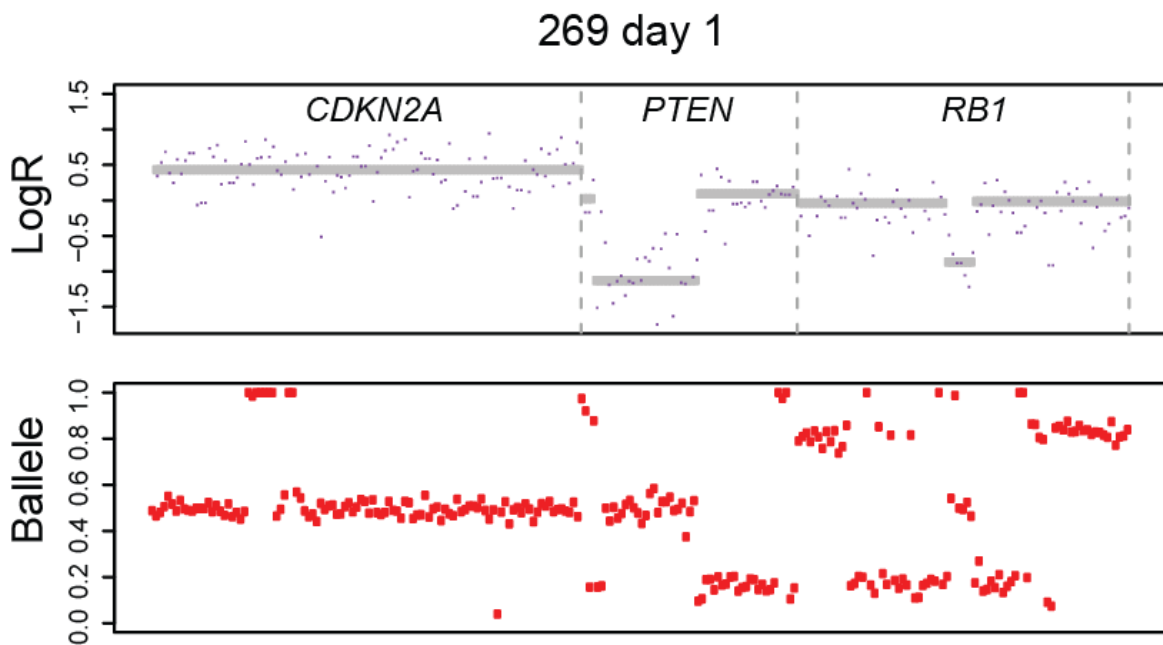
Supplementary figure 19. Regions significantly deviated from baseline in copy number data from the paired plasma exome samples (n = 14) compared between baseline and end of treatment using GISTIC.



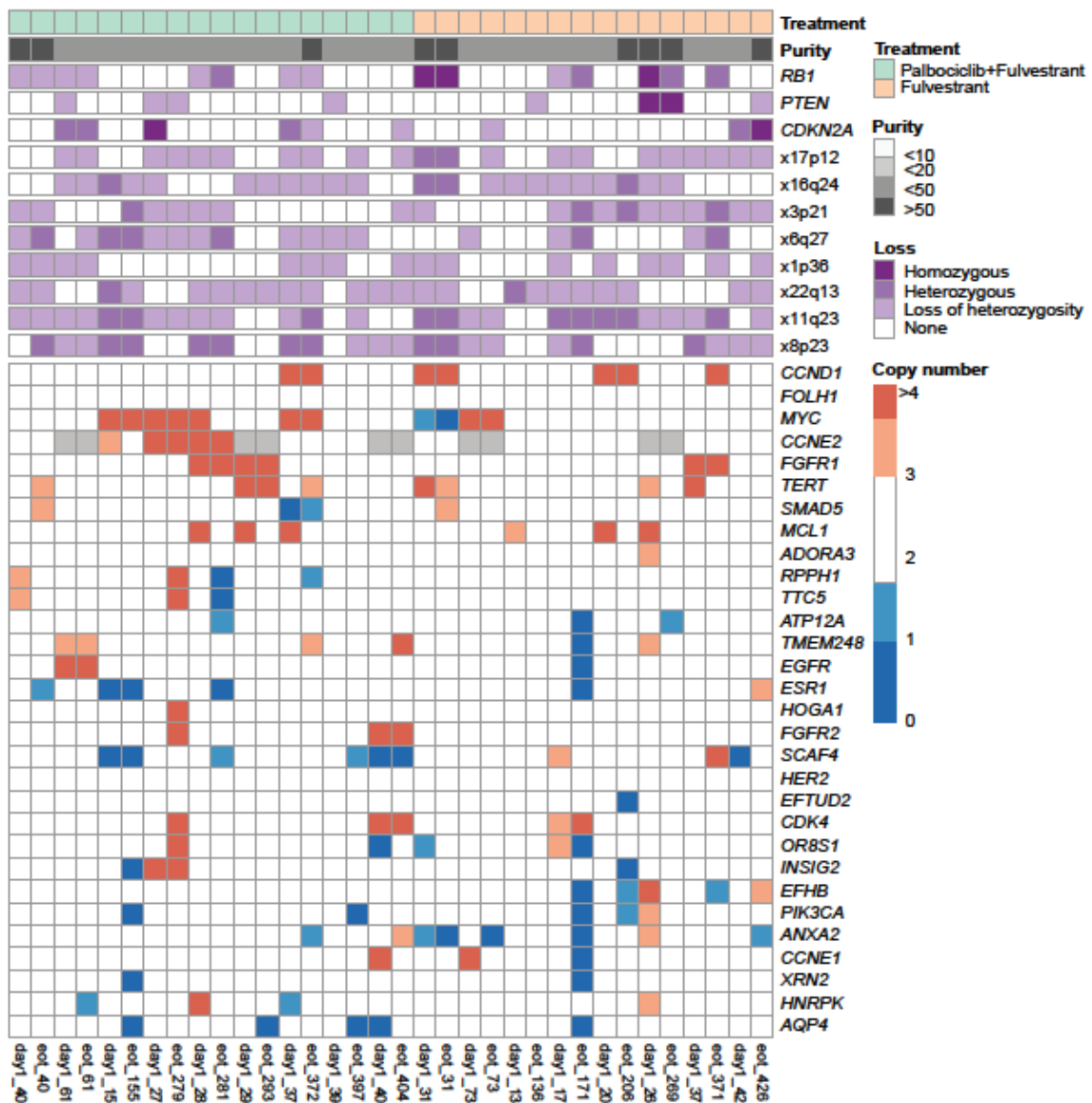
Supplementary figure 20. Copy number assessment comparison of *RB1* between day 1 and end of treatment (eot) from exome sequencing of plasma DNA for n = 14 patients receiving palbociclib plus fulvestrant. Differences seen in patients 152 and 392 are likely due to differentials in tumor purity between the time points (see Supplementary figure 17).



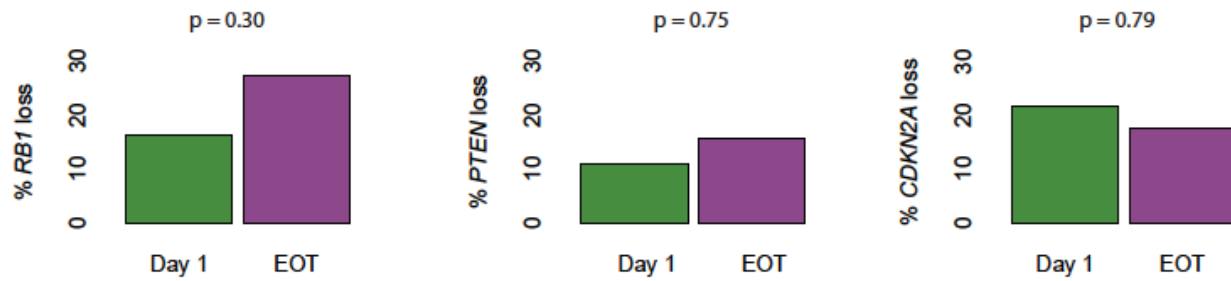
Supplementary figure 21. Number of patient samples at day 1 and end of treatment identified as having purity over 10% and over 20%, and overlap of assessable paired samples. EOT – End of treatment.



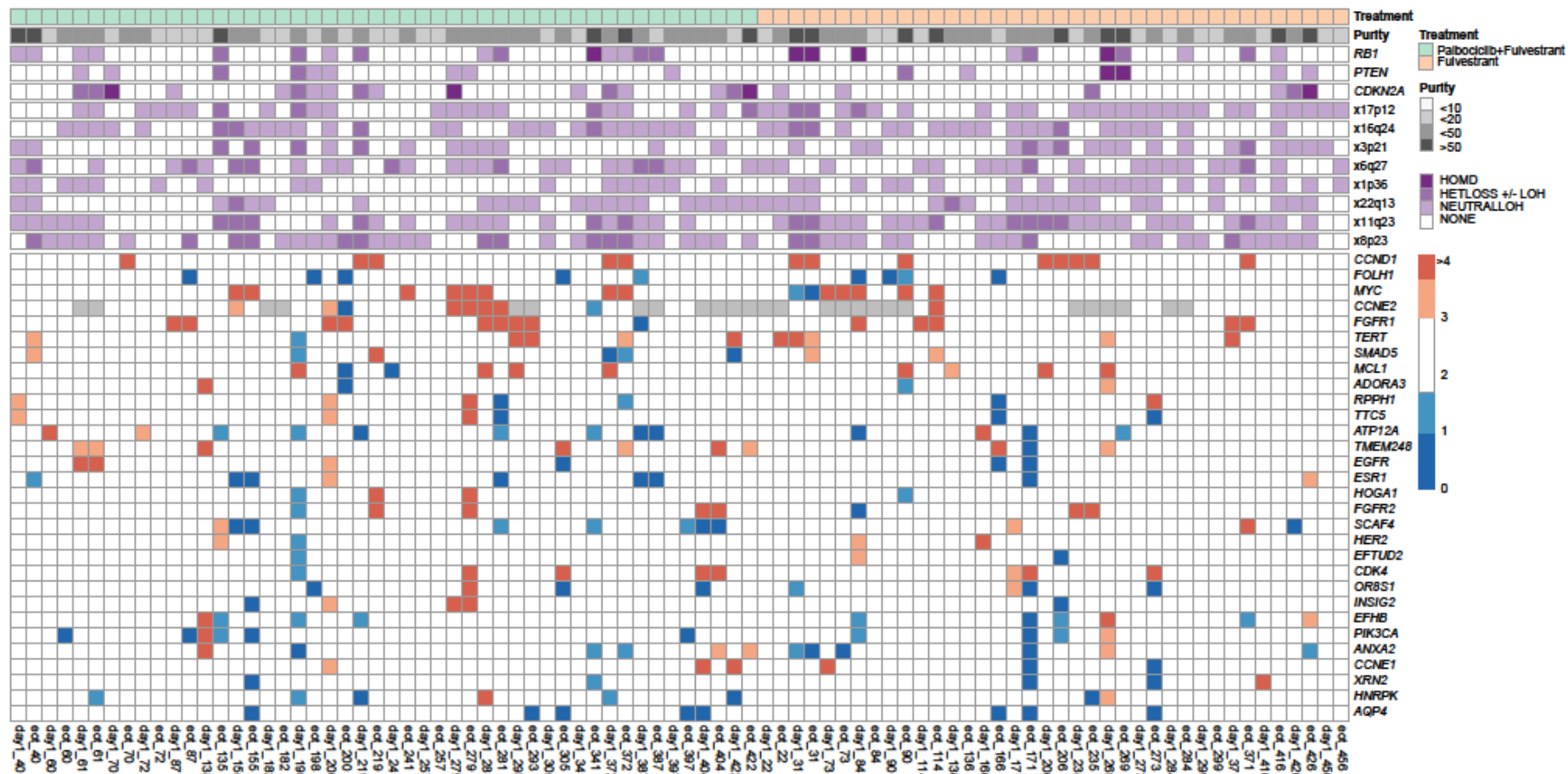
Supplementary figure 22. Example copy number analysis from patient 269 day 1 sample, *top* copy number LogR *bottom* B allele frequency. Homozygous loss of *PTEN* (exons 1-5) and *RB1* (intronic).



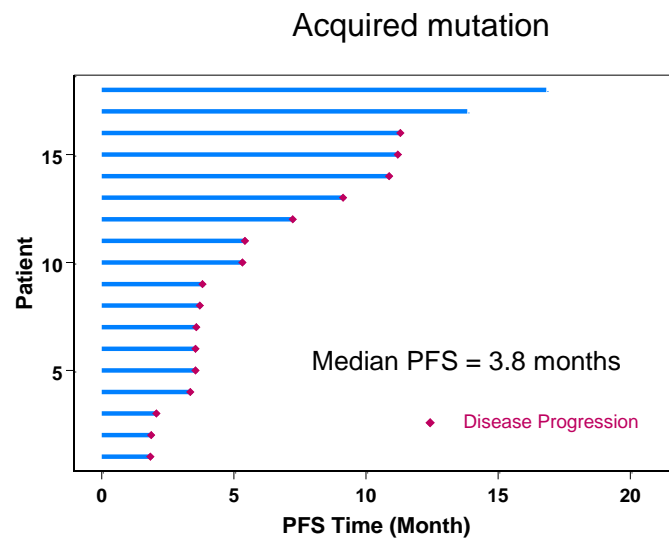
Supplementary figure 23. Heatmap shows copy number and purity assessments for all paired samples with purity > 20% at both time points, n = 17 pairs, separated by treatment n = 9 palbociclib plus fulvestrant and n = 8 placebo plus fulvestrant. Gray squares indicate where *CCNE2* was not assessable see Materials and Methods. Data for paired samples with purity > 10% is shown in Supplementary figure 24.



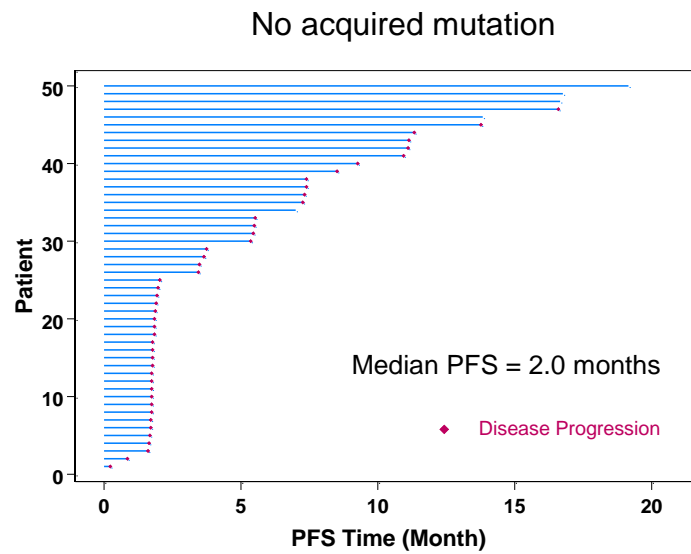
Supplementary figure 24. Bar charts show comparison of proportions of loss in *RB1*, *PTEN* and *CDKN2A* in unpaired day 1 (n = 37) and EOT (n = 51) samples with purity > 20% P values from Fisher's exact test. EOT – end of treatment. Loss of *PTEN* was observed in similar proportions of day 1 and end of treatment samples (4/37, 10.8% versus 8/51, 15.7%, p = 0.75 Fisher's exact test), similarly to loss of *CDKN2A* (day 1 8/37, 21.6%, end of treatment 9/51, 17.6%, p = 0.79, Fisher's exact test).



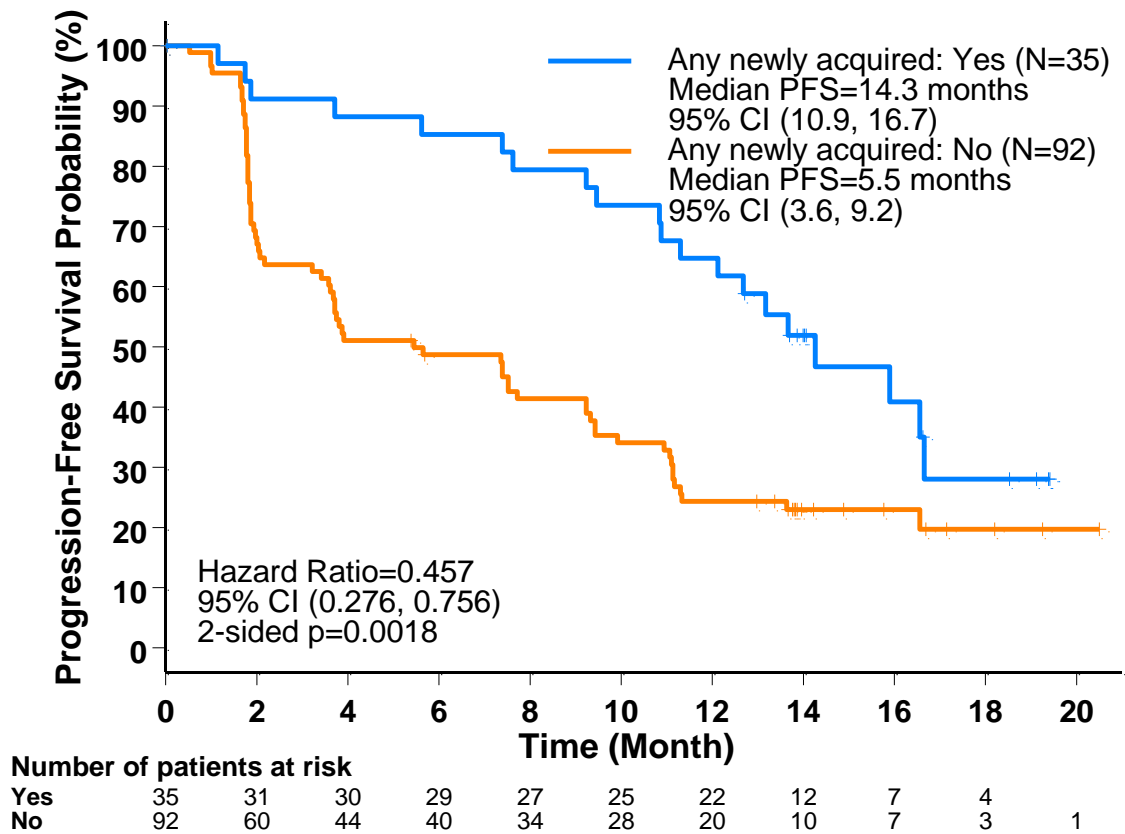
Supplementary figure 25. Comparison of copy number status in patients with paired day 1 and end of treatment (eot) samples with at least 10% tumor purity at both day 1 and end of treatment (n = 43 pairs). Gray squares in the lower panel indicate samples where *CCNE2* was not assessable. There was no difference in rates of loss of *RB1*, *PTEN* or *CDKN2A* between day 1 and end of treatment in the larger subset of samples of >10% tumor purity shown here.



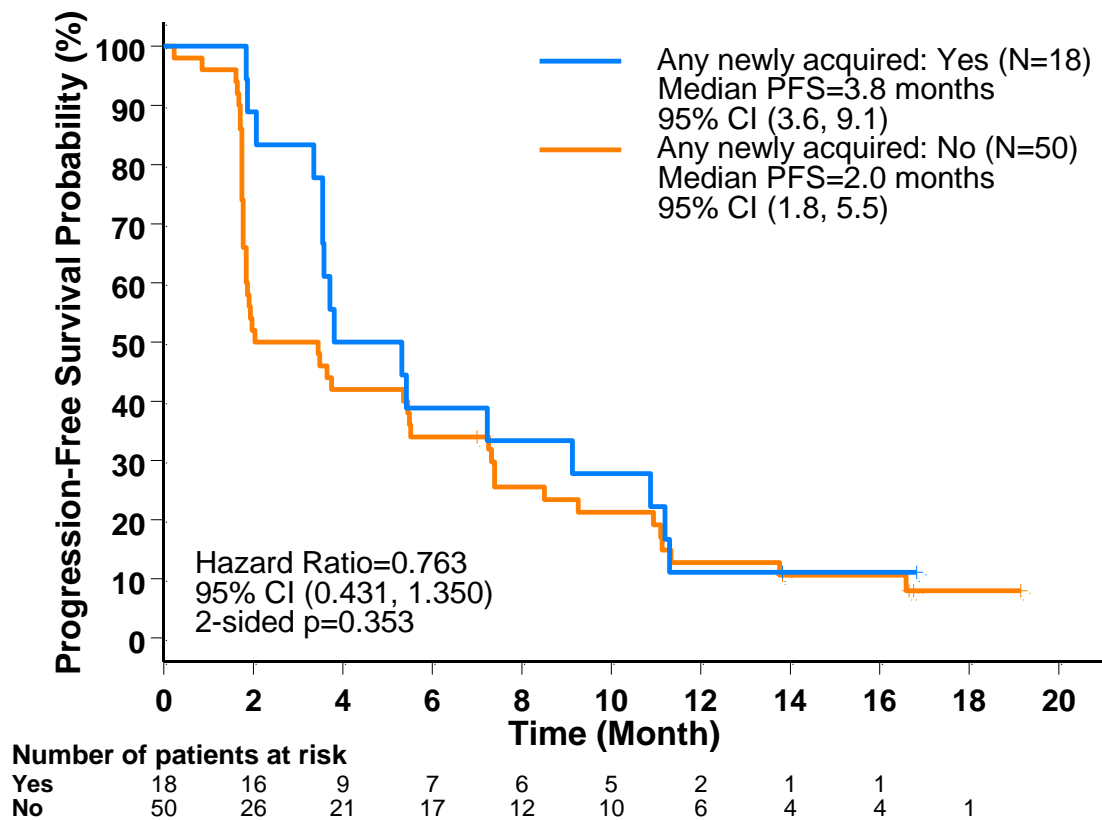
$p = 0.35$



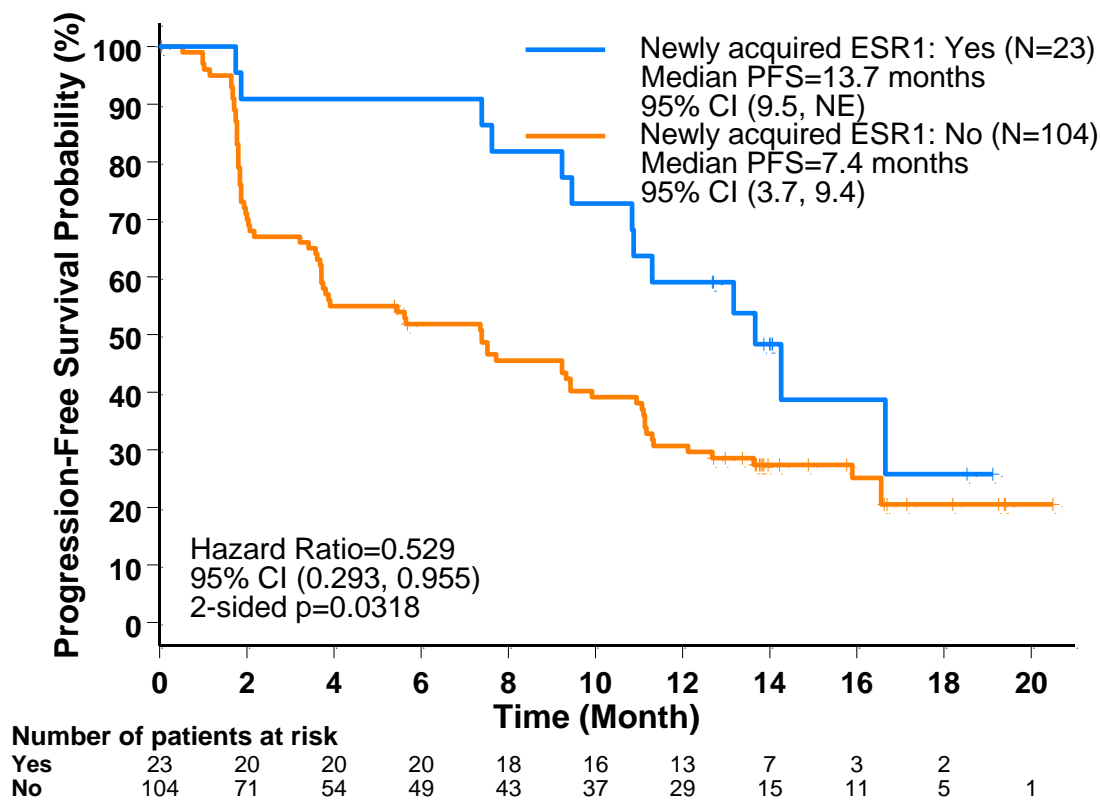
Supplementary figure 26. Swimmer plots of progression free survival in the placebo and fulvestrant arm comparing patients with (upper panel) and without (lower panel) newly acquired or selected mutations at the end of treatment. PFS – progression free survival, p value log rank.



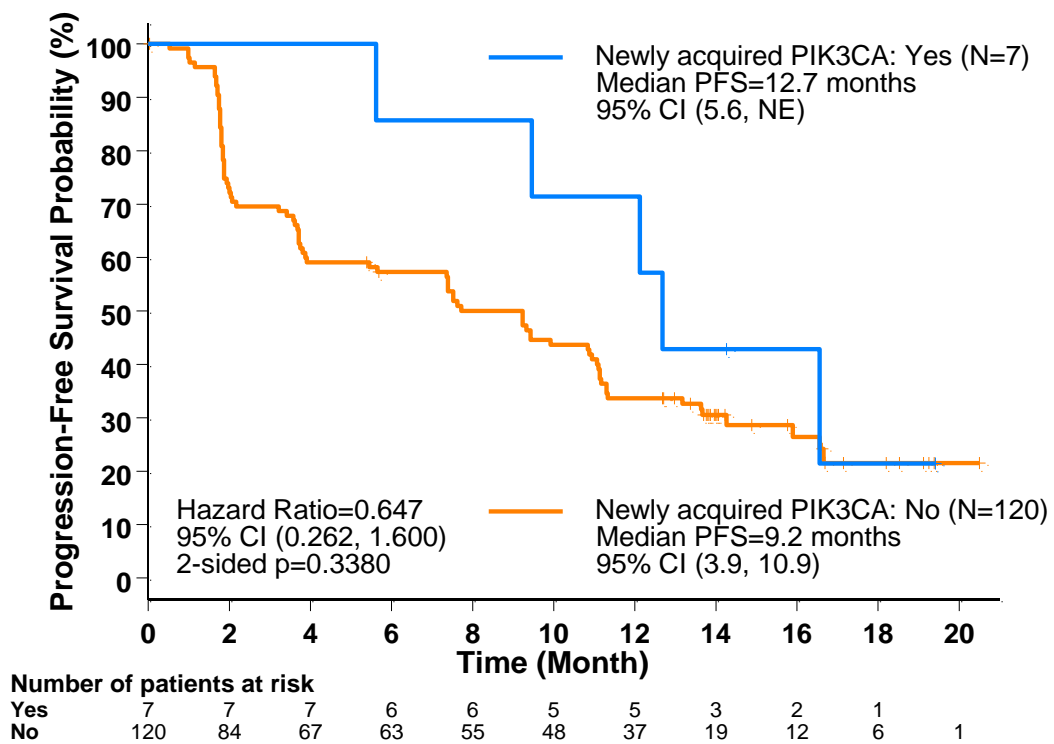
Supplementary figure 27. Kaplan Meier curves comparing progression free survival in the palbociclib plus fulvestrant arm between patients who acquired or selected at least 1 mutation and those who did not. PFS – progression free survival, CI – confidence interval.



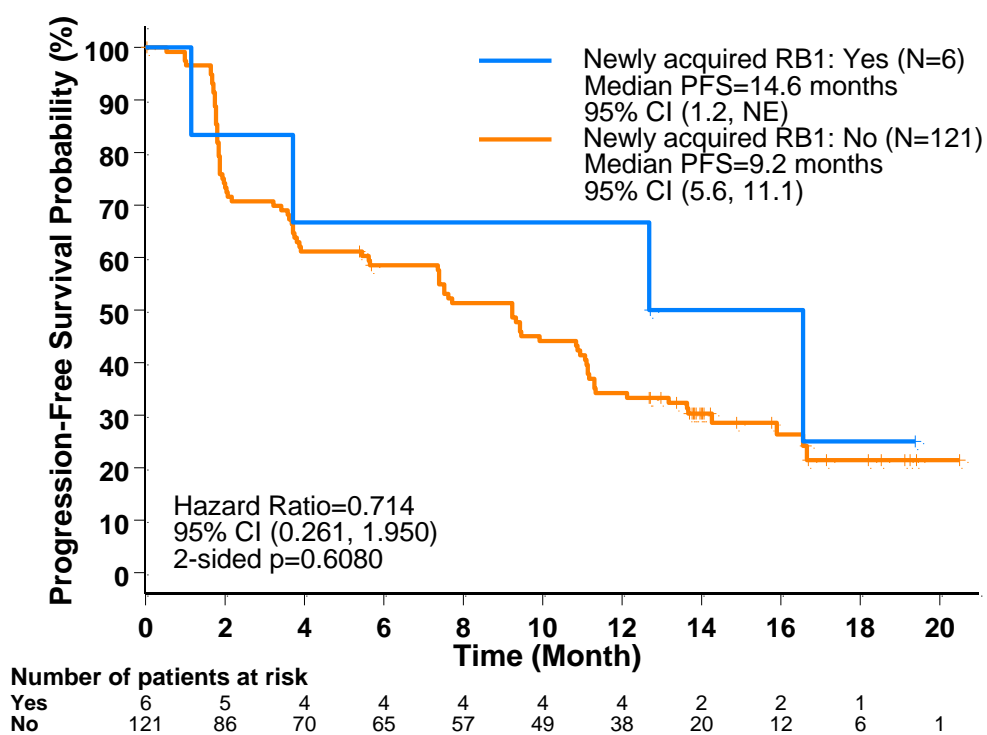
Supplementary figure 28. Kaplan Meier curves comparing progression free survival in the placebo plus fulvestrant arm between patients who acquired or selected at least 1 mutation and those who did not. PFS – progression free survival, CI – confidence interval.



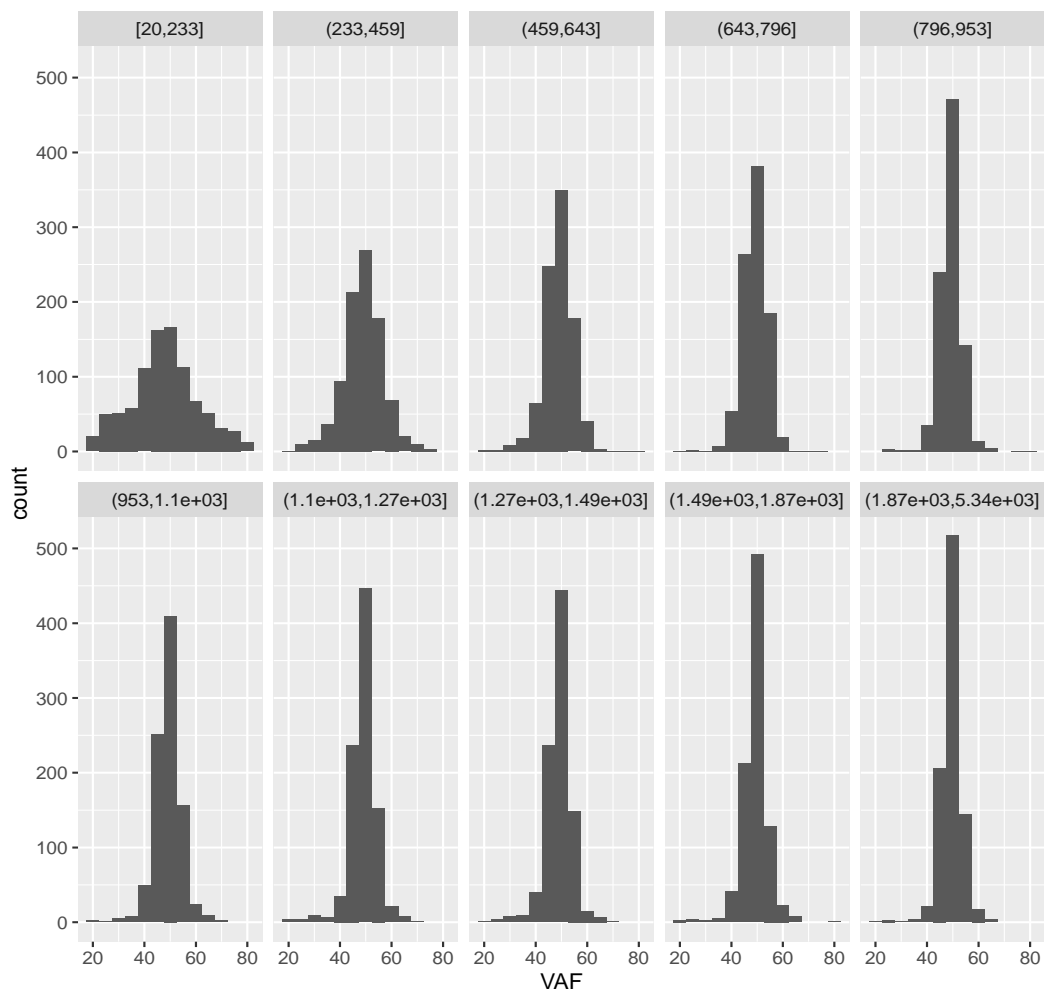
Supplementary figure 29. Kaplan Meier curves comparing progression free survival in the palbociclib plus fulvestrant arm between patients who acquired or selected an *ESR1* mutation and those who did not. PFS – progression free survival, NE – not estimable, CI – confidence interval.



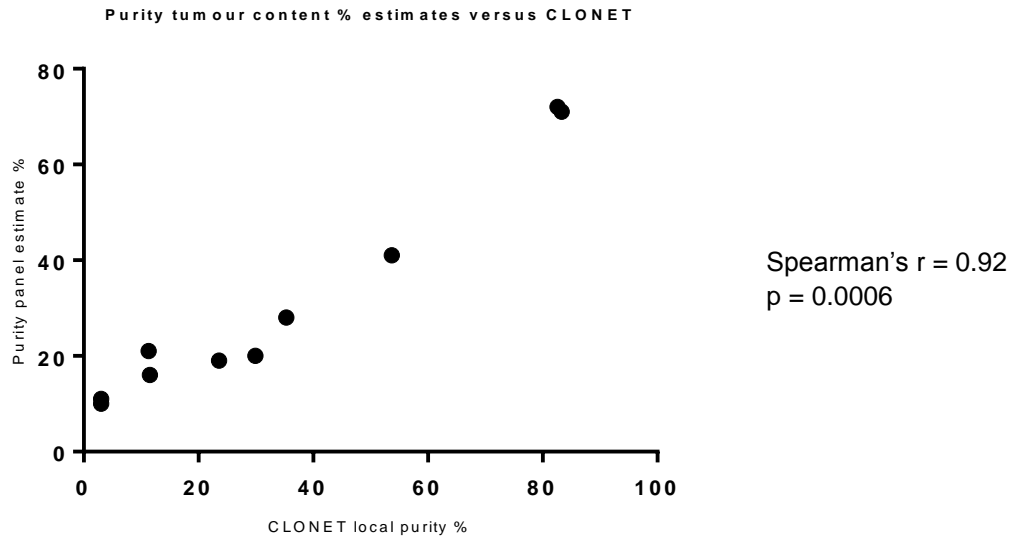
Supplementary figure 30. Kaplan Meier curves comparing progression free survival in the palbociclib plus fulvestrant arm between patients who acquired or selected a *PIK3CA* mutation and those who did not. PFS – progression free survival, NE – not estimable, CI – confidence interval.



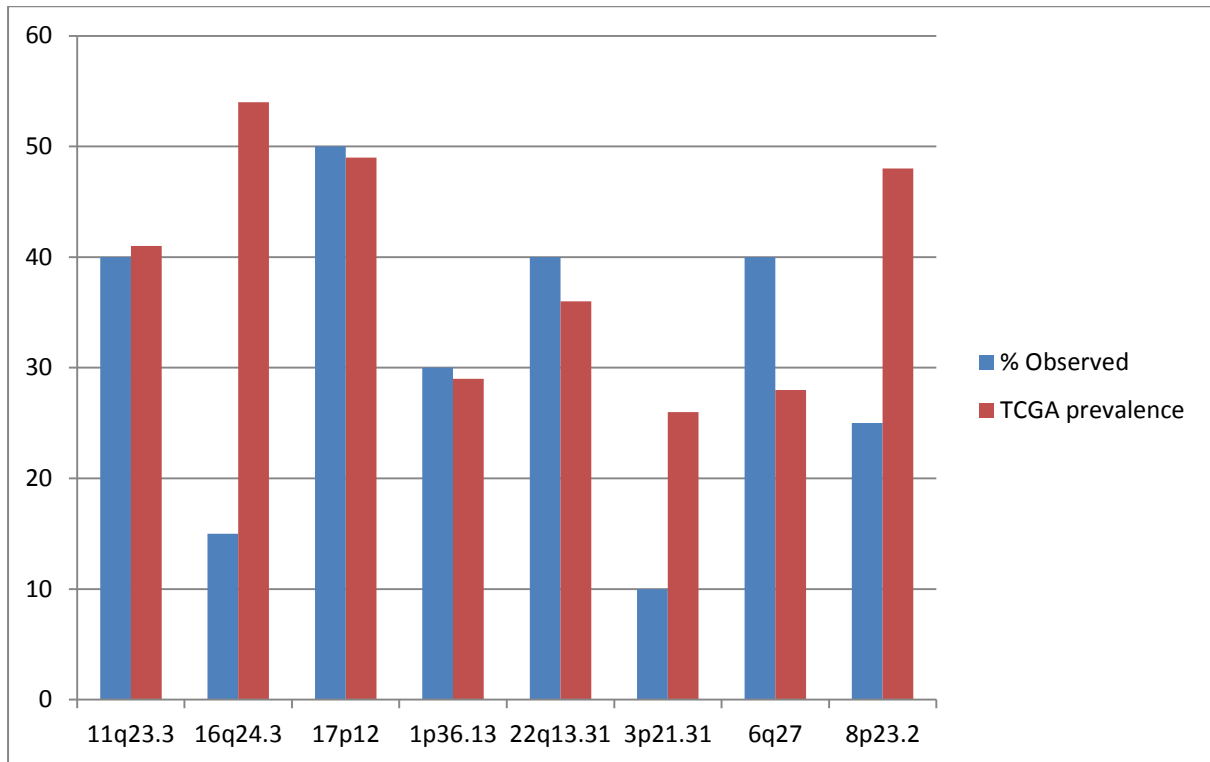
Supplementary figure 31. Kaplan Meier curve of progression free survival in the palbociclib plus fulvestrant arm comparing patients with acquired *RB1* mutation (n = 6) to those without (n = 121).



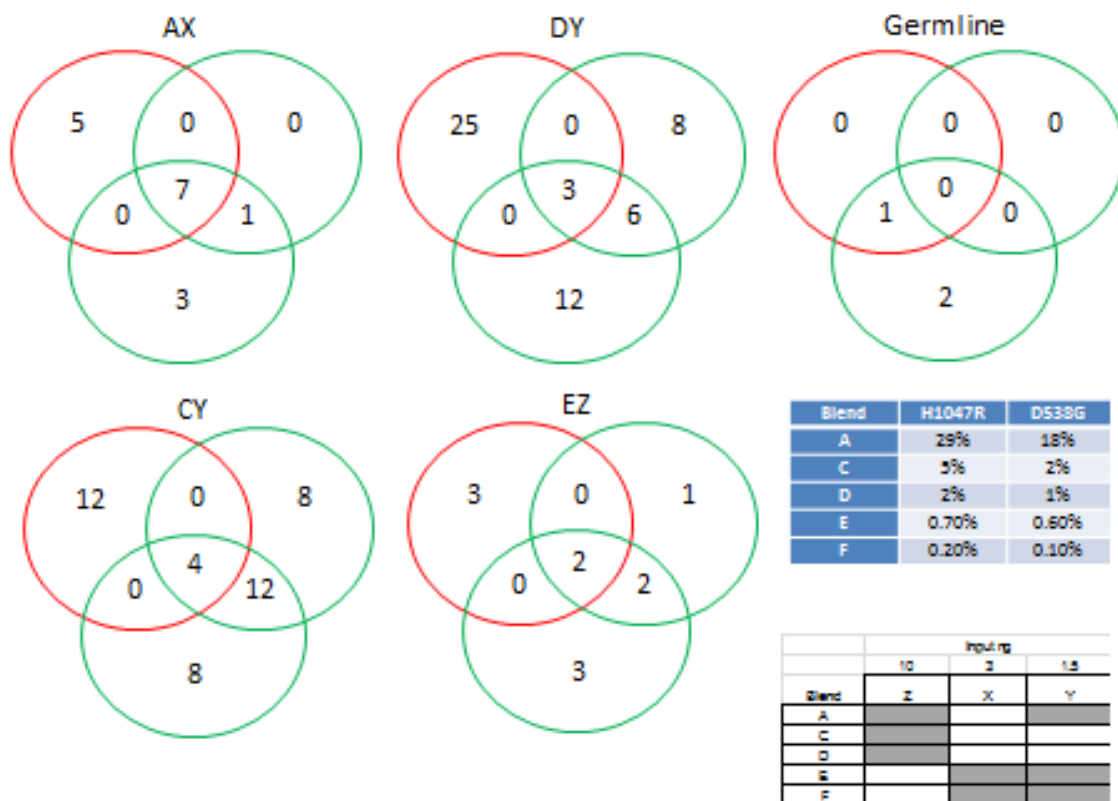
Supplementary figure 32. Observed variation in allele frequency around germline SNPs in buffy coat samples run for purity panel validation at different coverage intervals.



Supplementary figure 33. Validation of purity panel purity estimate against CLONET.



Supplementary figure 34. Observed prevalence of loss regions in purity validation set compared to prevalence in The Cancer Genome Atlas.



Supplementary figure 35. Validation of sequencing approach (see Materials and Methods). A control blend of plasma DNA with dilutions of known concentration of circulating tumor DNA was used with an amplicon-based panel and sequenced to 2000X. The Venn diagram red circles illustrate the calls made with the standard Ampliseq library preparation, the green circles those with libraries completed with the KAPA hyper prep kit to demonstrate accurate error removal with cross comparison of calls. The two green circles are the same libraries sequenced twice. Calls made with a threshold of 0.5% with pileup and iDES (see Materials and Methods) with minimum coverage of 50 and minimum alternative reads of 5. The extra calls beyond the two controls in the high purity positive control (AX) are additional subclonal *ESR1* and *TP53* mutations.

Supplementary tables

Lab ID	Screen	Day 1 (D1)									End of treatment		Days on treatment	Matched buffy
		<i>PIK3CA</i> mut 1	<i>PIK3CA</i> mut 2	Estimated total D1 AF	<i>ESR1</i> mut 1	<i>ESR1</i> mut 2	<i>ESR1</i> mut 3	<i>ESR1</i> mut 4	<i>ESR1</i> mut 5	<i>ESR1</i> total AF	EOT mut tested	Estimated total EOT AF		
34	ddPCR	E545K	E542K	0.16	0	0	0	0	0	0.00	E545K	0.14	226	
79	ddPCR	H1047R	0	0.30	D538G	Y537N	0	0	0	0.25	H1047R	0.19	59	TRUE
80	ddPCR	E545K	0	0.28	0	0	0	0	0	0.00	E545K	0.32	63	
82	ddPCR	H1047R	0	0.19	D538G	Y537N	0	0	0	0.02	H1047R	0.35	48	
152	ddPCR	H1047R	0	0.35	D538G	Y537N	Y537S	E380Q	S463P	0.05	H1047R	0.18	68	
253	ddPCR	H1047R	0	0.17	D538G	E380Q	0	0	0	0.04	H1047R	0.32	53	TRUE
392	ddPCR	0	0	0.00	D538G	E380Q	0	0	0	0.17	D538G	0.08	182	
333	ddPCR	H1047R	0	0.40	Y537S	0	0	0	0	0.03	H1047R	0.53	634	TRUE
390	ddPCR	E545K	0	0.43	0	0	0	0	0	0.00	E545K	0.59	233	
187	ddPCR	E545K	0	0.08	0	0	0	0	0	0.00	E545K	0.10	56	
61	LOH	0	0	0.23	0	0	0	0	0	0.00	LOH	0.23	57	TRUE
182	LOH	0	0	0.13	0	0	0	0	0	0.00	LOH	0.12	53	
293	LOH	0	0	0.29	0	0	0	0	0	0.00	LOH	0.27	287	TRUE
387	LOH	0	0	0.26	0	0	0	0	0	0.00	LOH	0.19	169	
404	LOH	0	0	0.22	0	0	0	0	0	0.00	LOH	0.27	168	
422	LOH	0	0	0.18	0	0	0	0	0	0.00	LOH	0.72	171	

Supplementary table 1. Sample details for patients who underwent exome sequencing of paired day 1 and end of treatment samples. Samples of sufficient purity (>10% in all but one case of 8%) were identified through either digital PCR for *PIK3CA* or *ESR1* mutations, or with targeted sequencing of SNPs using the purity panel.

Sample	Material	Median	Duplicates	On target
34 day 1	Plasma	134	41%	75%
34 EOT	Plasma	140	34%	76%
79 day 1	Plasma	116	20%	72%
79 EOT	Plasma	122	18%	77%
80 day 1	Plasma	100	24%	75%
80 EOT	Plasma	119	23%	76%
82 day 1	Plasma	91	35%	72%
82 EOT	Plasma	112	22%	76%
152 day 1	Plasma	38	68%	61%
152 EOT	Plasma	121	26%	75%
253 day 1	Plasma	104	27%	72%
253 EOT	Plasma	105	28%	72%
392 day 1	Plasma	145	41%	72%
392 EOT	Plasma	167	26%	75%
61 day 1	Plasma	179	22%	74%
61 EOT	Plasma	166	26%	69%
182 day 1	Plasma	162	25%	73%
182 EOT	Plasma	178	24%	72%
187 day 1	Plasma	139	28%	69%
187 EOT	Plasma	150	34%	65%
293 day 1	Plasma	172	18%	74%
293 EOT	Plasma	196	16%	77%
333 day 1	Plasma	178	14%	76%
333 EOT	Plasma	200	14%	77%
387 day 1	Plasma	195	15%	77%
387 EOT	Plasma	173	12%	77%
390 day 1	Plasma	181	17%	77%
390 EOT	Plasma	175	12%	75%
404 day 1	Plasma	212	15%	77%
404 EOT	Plasma	193	14%	75%
422 day 1	Plasma	179	17%	70%
422 EOT	Plasma	187	11%	73%
79BC	Buffy	58	22%	76%
253BC	Buffy	58	23%	76%
61BC	Buffy	49	6%	75%
293BC	Buffy	47	6%	76%
333BC	Buffy	47	6%	80%
108BC	Buffy	45	6%	77%
6BC	Buffy	47	6%	76%
207BC	Buffy	34	51%	72%
207T	Tumor	66	40%	77%

Supplementary table 2. Coverage and duplicates data for samples having undergone paired exome sequencing. Day 1 – Day 1 sample. EOT – End of treatment sample. BC – Buffy coat sample.

Patient	Signature.1	Signature.2	Signature.3	Signature.5	Signature.6	Signature.7	Signature.9	Signature.10	Signature.12	Signature.13	Signature.15	Signature.16	Signature.20	Signature.21	Signature.24	Signature.26	Signature.30
152 day 1	0.6391079	0	0.1685734	0	0	0	0	0	0	0	0	0	0	0.074844318	0	0	0
152 EOT	0.5418774	0	0.1545973	0	0	0	0	0	0	0	0.13740699	0.06651358	0	0	0	0	0
182 day 1	0.7945949	0	0	0	0.0991347	0	0	0.06608758	0	0	0	0	0	0	0	0	0
182 EOT	0.8661228	0	0.0892266	0	0	0	0	0	0	0	0	0	0	0	0	0	0
187 day 1	0.425692	0	0	0.3333117	0	0	0	0	0	0	0	0	0	0	0.1888072	0	0
187 EOT	0.2889863	0	0	0	0	0	0	0	0	0.17673132	0	0.11400976	0.22230187	0	0	0	0.19797078
253 day 1	0.5967391	0.0762137	0.1893982	0	0	0	0	0	0	0	0	0	0	0	0	0.07945898	0
253 EOT	0.7319089	0.2046768	0	0	0	0	0	0	0	0	0	0	0	0	0	0	0
293 day 1	0.8490427	0	0	0	0	0	0.1011275	0	0	0	0	0	0	0	0	0	0
293 EOT	0.8013355	0	0	0	0	0	0.1585412	0	0	0	0	0	0	0	0	0	0
333 day 1	0.373423	0	0	0.2408562	0	0.2958088	0	0	0	0	0	0	0	0	0	0	0
333 EOT	0.6062531	0	0	0.0737334	0	0.2942255	0	0	0	0	0	0	0	0	0	0	0
34 day 1	0.6873836	0.0764492	0	0	0	0	0	0	0.15404952	0	0	0	0	0	0	0	0
34 EOT	0.8836091	0.0684726	0	0	0	0	0	0	0	0	0	0	0	0	0	0	0
387 day 1	1	0	0	0	0	0	0	0	0	0	0	0	0	0	0	0	0
387 EOT	0.9758265	0	0	0	0	0	0	0	0	0	0	0	0	0	0	0	0
390 day 1	0.6566263	0.0769042	0	0	0	0.0820245	0	0.11327968	0	0.07116539	0	0	0	0	0	0	0
390 EOT	0.4936215	0.1781913	0	0	0	0.100286	0	0.12069709	0	0.09402304	0	0	0	0	0	0	0
392 day 1	0.5231784	0.1714332	0	0	0	0	0	0.13100183	0	0	0	0	0	0.075328039	0	0	0
392 EOT	0.792347	0.0769466	0	0	0	0	0	0.12534358	0	0	0	0	0	0	0	0	0
404 day 1	0.914459	0	0	0	0	0	0	0	0	0	0	0	0	0	0	0	0
404 EOT	0.9203781	0	0	0	0	0.0796219	0	0	0	0	0	0	0	0	0	0	0
422 day 1	0.8835858	0	0	0	0	0	0	0	0	0	0	0.11641421	0	0	0	0	0
422 EOT	0.8014821	0	0	0	0	0	0	0	0	0	0.159884	0	0	0	0	0	0
61 day 1	0.1888024	0	0.5091002	0	0	0	0.0621701	0	0	0	0.08239073	0	0	0	0	0	0
61 EOT	0.1828287	0	0.5292476	0	0	0	0	0	0	0.09921806	0	0	0	0	0	0	0
79 day 1	0.8357276	0	0	0	0	0.0870947	0.0627623	0	0	0	0	0	0	0	0	0	0
79 EOT	0.7627272	0	0	0	0	0.0787664	0.1313305	0	0	0	0	0	0	0	0	0	0
80 day 1	0.8012931	0	0	0	0	0	0	0	0	0	0	0	0	0	0	0.09725907	0
80 EOT	0.792105	0	0.0634433	0	0	0	0	0	0	0	0	0	0	0	0	0	0
82 day 1	0.6188254	0	0	0	0	0	0	0	0	0.13249308	0.11572246	0	0	0	0	0	0
82 EOT	0.6970892	0	0	0	0	0	0	0	0	0.09628119	0	0	0	0	0	0.13475991	0

Supplementary table 3. Mutational signature analysis of exome sequencing variants. Day 1– Day 1 sample. EOT – End of treatment sample.

	Patient	Chr	Position	Reference	Alternative	Change	Gene	Function	D1 AF	EOT AF
Immune pathway	61	3	121345699	C	A	nonsynonymous_SNV	FBXO40	Substrate-determining subunit of E3 ubiquitin ligase	0	0.105
	61	21	30331933	C	T	nonsynonymous_SNV	LTN1	Listerin E3 Ubiquitin Protein Ligase	0	0.078125
	253	1	158324190	C	T	nonsynonymous_SNV	CD1E	Required for the presentation of glycolipid antigens	0	0.235955
	333	5	138860775	G	A	nonsynonymous_SNV	TMEM173	Promotes the production of type I interferon (IFN-alpha and IFN-beta)	0	0.045802
	390	16	3293474	C	G	nonsynonymous_SNV	MEFV	Regulates inflammatory response in response to IFNG/IFN-gamma	0	0.029891
NOTCH family receptors	182	1	120458435	TG	T	frameshift_deletion	NOTCH2	NOTCH receptor	0.169399	0.192118
	390	19	15292441	G	A	nonsynonymous_SNV	NOTCH3	NOTCH receptor	0.591954	0.491124
	80	6	32168958	AGGTGG	A	frameshift_deletion	NOTCH4	NOTCH receptor	0.273973	0.424837
	61	1	120458305	C	A	nonsynonymous_SNV	NOTCH2	NOTCH receptor	0.037736	0
NF1	82	17	29585383	C	T	stopgain	NF1	NF1	0.247059	0.547297
	61	17	29663382	G	C	nonsynonymous_SNV	NF1	NF1	0.205556	0.29932

Supplementary table 4. Genetic aberrations in immune signalling, *NF1* and *NOTCH* pathway genes from exome sequencing. D1 – Day 1. EOT – End of treatment. Chr – Chromosome. Patient 61 had newly emergent mutations in *FBXO40* and *LTN1*, both E3 ubiquitin ligases associated with regulation of class I MHC antigen processing and presentation. Patients 333 and 390 featured emergent mutations in *TMEM173* and *MEFV* respectively, the former a promotor of interferons alpha and beta and the latter regulating the response to interferon gamma, both processes potentially relevant to the immune-mediated effects of palbociclib (16, 17) . 4/14 (28.6%) of patients with samples analyzed had an aberration in *NOTCH* family receptors and 2/14 (14.3%) mutations in *NF1*

		Day 1 (n)	End of treatment (n)	Paired (n)	Fisher's p Unpaired analysis	McNemar's p Paired analysis
>10% tumor purity	<i>RB1</i>	68	82	43	0.1	0.72
	<i>PTEN</i>	68	82	43	0.55	1
	<i>CDKN2A</i>	68	82	43	0.62	0.22
>20% tumor purity	<i>RB1</i>	37	51	17	0.3	0.25
	<i>PTEN</i>	37	51	17	0.75	NA
	<i>CDKN2A</i>	37	51	17	0.79	0.48

Supplementary table 5. Comparative statistical analyses conducted on the copy number data within samples falling into the >10% tumor purity and >20% tumor purity category. NA – unable to calculate p value.

	Mutation acquired n = 53	No mutation acquired n = 142	p value
Hormone receptor status, n(%) * n = 179			p = 0.52
ER-/PR-	16 (30.2)	32 (22.5)	
ER-/PR+	0 (0)	3 (2.1)	
ER+/PR-	14 (26.4)	37 (26.1)	
ER+/PR+	19 (35.8)	58 (40.8)	
Disease free interval ** n = 136			p = 0.61
≤24 months	6 (11.3)	21 (14.8)	
>24 months	32 (60.4)	77 (54.2)	
Menopausal status, n(%) n = 195			p = 0.80
Pre/perimenopausal	10 (18.9)	31 (21.8)	
Post-menopausal	43 (81.1)	111 (78.2)	
Sensitivity to prior endocrine treatment, n(%)			p = 1
Yes	41 (77.4)	109 (76.8)	
No	12 (22.6)	33 (23.2)	
Visceral metastases, n(%)			p = 1
Yes	33 (62.3)	89 (62.7)	
No	20 (37.7)	53 (37.3)	
Bone metastases, n(%)			p = 0.013 (q = 0.15)
Yes	48 (90.6)	103 (72.3)	
No	5 (9.4)	39 (27.5)	
Soft tissue/nodal metastases, n(%)			p = 0.89
Yes	20 (37.7)	57 (40.1)	
No	33 (62.3)	85 (59.9)	
Prior endocrine therapies, n(%)			p = 0.91
Tamoxifen only	7 (13.2)	17 (12.0)	
AI only	25 (47.2)	64 (45.1)	
AI and tamoxifen	21 (39.6)	61 (43.0)	
Prior chemotherapy, n(%)			p = 0.56
Neoadjuvant/adjuvant	22 (41.5)	56 (39.4)	
Metastatic +/- adjuvant	21 (39.6)	49 (34.5)	
None	10 (18.9)	37 (26.1)	
Prior lines of therapy for metastatic disease, n(%)			p = 0.16
0	10 (18.9)	28 (19.7)	
1	27 (50.9)	53 (37.3)	
2	15 (28.3)	48 (33.8)	
3+	1 (1.9)	13 (9.2)	
Number of disease sites, n(%)			p = 0.80
1	17 (32.1)	47 (33.1)	
2	13 (24.5)	37 (26.1)	
3+	23 (43.4)	58 (40.8)	

Supplementary table 6. Comparison of baseline clinic-pathological characteristics between patients who acquire a mutation on treatment and those who do not. P values are from Chi-squared except for ordinal variables where the Cochran-Armitage test is used. The corrected p value for the association with bone metastases is $q = 0.15$ (Bonferroni).

* 16 instances of 'not specified' were removed for the analysis.

** 59 instances of 'not applicable' were removed for the analysis

Sample	Type	Aberration	Frequency ddPCR	Purity sequencing mut	Global purity CLONET	Local purity CLONET	Single sample
17T	Tumour	<i>FGFR1</i> amp	-	None identified	no estimate	no estimate	75.0%
21P	Plasma	<i>FGFR2</i> amp	-	None identified	no estimate	no estimate	49.0%
207T	Tumour	<i>FGFR1</i> amp	-	None identified	no estimate	no estimate	76.0%
269P	Plasma	<i>FGFR2</i> amp	-	None identified	no estimate	no estimate	no estimate
316T	Tumour	<i>FGFR2</i> amp	-	None identified	43.0%	43.0%	46.0%
Sample	Type	Aberration	Frequency ddPCR	Purity sequencing	Global purity CLONET	Local purity CLONET	Single sample
1135	Plasma	None known	-	None identified	no estimate	no estimate	no estimate
2039	Plasma	None known	-	None identified	no estimate	no estimate	no estimate
1037	Plasma	None known	-	None identified	no estimate	no estimate	no estimate
1156 S	Plasma	<i>PIK3CA</i>	0.005	Not called	no estimate	11.5%	16.0%
1117 S	Plasma	<i>PIK3CA</i>	0.026	Not called	no estimate	no estimate	no estimate
1144 S	Plasma	<i>ESR1</i>	0.327 or 0.019	Not called	no estimate	29.9%	20.0%
1150 E	Plasma	<i>PIK3CA</i>	0.037	0.034	no estimate	no estimate	no estimate
1025 S	Plasma	<i>PIK3CA/ESR1</i>	0.09	<i>PIK3CA</i> 0.073, <i>ESR1</i> 0.056	no estimate	23.6%	19.0%
1086A ex1	Plasma	<i>PIK3CA</i>	0.13	0.11	no estimate	3.0%	11.0%
1153 S	Plasma	<i>PIK3CA</i>	0.171	0.143	no estimate	3.0%	10.0%
1158 S	Plasma	<i>PIK3CA</i>	0.094	0.152	no estimate	11.3%	21.0%
1016 E	Plasma	<i>ESR1</i>	0.192	0.226	40.0%	35.3%	28.0%
1118B ex1	Plasma	<i>PIK3CA</i>	0.24	0.23	44.0%	53.7%	41.0%
1147 E	Plasma	<i>TP53</i>	0.76	Not in panel	70.0%	83.3%	71.0%
1126 S	Plasma	<i>PIK3CA</i>	0.839	0.824	70.0%	82.6%	72.0%

Supplementary table 7. Validation of loss of heterozygosity method for estimating tumor content of plasma samples. Samples with known mutation allele fractions detected by digital PCR were compared to purity estimates made on sequencing data from the purity panel using CLONET and the loss of heterozygosity purity estimate.

Coverage interval	Percentile sd	Percentile mean	Percentile AF.mean	Percentile AF.sd
[20,233]	67.67	119.69	47.81	12.85
(233,459]	65.70	349.18	48.93	7.80
(459,643]	52.40	555.02	48.89	5.78
(643,796]	43.78	718.08	49.04	4.87
(796,953]	44.54	873.30	49.20	4.45
(953,1100]	40.92	1028.15	49.08	5.01
(1100,1270]	48.24	1180.86	49.02	5.37
(1270,1490]	62.85	1371.88	48.87	4.98
(1490,1870]	110.10	1665.11	49.23	4.90
(1870,5340]	494.02	2386.89	49.44	4.14

Supplementary table 8. Variation in allele fraction estimate for known heterozygous single nucleotide polymorphisms (SNPs) in the germline samples used in the purity panel validation run.